

THE TENSION FIELD CREATED BY A SPHERICAL NUCLEUS FREEZING INTO ITS LESS DENSE UNDERCOOLED MELT

G. HORVAY

General Electric Research Laboratory, Schenectady, N.Y.

(Received 18 March 1964 and in revised form 6 August 1964)

Abstract—When nickel freezes into its less dense melt, that is cooled by more than 175°C below its equilibrium freezing temperature, the solidified material exhibits—as first observed by J. L. Walker—dispersed fine-grain structure (presumably as a result of cavitation induced by huge negative pressures surrounding the growing nuclei), whereas for undercooling less than 175°C the observed structure is coarse grained. The purpose of the present analysis was to provide numerical (theoretical) estimates for the pressures, flow velocities, and time scales involved. This necessitated study of freezing as proceeding from a *finite* initial embryo. Using a “generalized orthogonalization method” of solution, the freezing process is traced out, taking the pressure dependence of freezing temperature also into account, on the basis of incompressible inviscid fluid dynamics. The solution of the governing differential equation system is represented as a sum $\sum_0^{K-1} F_k$ of [vector] functions $F_k(\xi)$ (ξ is the dimensionless radial coordinate) whose time dependence (τ is dimensionless time) is determined from orthogonality conditions (boundary layer integral equations), using in the integrand weight functions of type ξ^{km} ; $k = 0, 1, \dots, K-1$. We refer to approximations I, II, III, . . . when $K = 1, 2, 3, \dots$ ($K = 1$ corresponds to the conventional boundary layer solution of the type von Kármán–Pohlhausen–Goodman–Veynik), and to approximations II₁, II₂, II₀ when $K = 2$ and $m = 1, \frac{1}{2}, 0$. Using for $\sum F_k(\xi)$ a sequence of perturbed (in τ) decaying (in ξ) exponentials, it was found that the graph of solution II₀ is, in its asymptotic behavior ($\tau \rightarrow \infty$), indistinguishable from the well known rigorous solution of the problem where the nucleus grows from zero radius and pressure dependence of freezing temperature is ignored. However, this asymptotic era is not reached until elapse of about 10^{-7} s from start of growth, whereas the maximum inrush of fluid on to the growing nucleus (at a speed exceeding 100 m/s) occurs in the first 10^{-11} s and is accompanied by tensions of several thousand atmospheres. This first portion of the phenomenon (to 10^{-11} s) may be represented by ascending power series in $\tau^{1/2}$ in the perturbation factors, the last portion (past 10^{-7} s) by descending power series in $\tau^{1/2}$; the huge intervening portion must be bridged by numerical integration of the pertinent differential equation system. Besides corroborating the expected pressure distribution, the analysis brought forth an unexpected result. The freezing process, as now described, is, for the case of precisely zero density change, totally different from that for infinitesimal density change. The latter starts from a finite initial radius, with zero velocity, the former with infinite velocity. This discontinuity (with density change) in the solution points to the need for further studies.

NOMENCLATURE

Dimensionless equivalents of the dimensional quantities are in brackets; examples, in braces; some symbols introduced and used only in one place are not listed.

r [ξ], radial distance;
 R [\mathcal{R}], radius of freezing front;
 T [$U = \mathcal{U}(1 + \epsilon)$], temperature;
 p [\mathcal{P}], pressure;
 t [τ], time;
 σ' [\mathcal{S}'], interface surface energy (in mechanical units);

λ , heat of fusion of solid (λ' in mechanical units);
 u , liquid velocity;
 $\gamma = \rho g(\Gamma)$, weight density of liquid (solid);
 $c(C)$, specific heat of liquid (solid);
 $k(K)$, conductivity of liquid (solid),
 κ , diffusivity of liquid;
 μ , chemical potential;
 S , entropy;
 κ , Boltzmann's constant;
 $\epsilon = Y = \bar{E} - 1$, factor of density change { (2.14), (3.14) };

K, \mathcal{K} ,	conductivity ratio {(2.16)};		
\mathcal{E} ,	equation;		when this is not at time zero { $-p_m$ };
A, w, l ,	functions appearing in U {(3.6)};	c ,	at instant of zero pressure { t_c };
$\beta, \alpha, \delta, \nu, \gamma$,	λ (b, a, d, f, c, l), coefficients in asymptotic (convergent) expan- sions of $\mathcal{R}, A, w, \mathcal{U}_F, \mathcal{U}_C, l$;	C ,	pertaining to nucleus center { U_C };
Ω, ω, Ψ ,	{(4.9)};	S ,	pertaining to solid phase { p_S };
$B, \mathcal{B}, C, \mathcal{C}, D, \mathcal{D}$,	{(4.10)};	∞ ,	at $r = \infty$ { T_∞ };
\mathcal{I} ,	degree of inconsistency {(5.22)};	s.e.,	due to surface energy { $p_{s.e.}$ };
Γ ,	{(4.18)};	stag,	stagnation value { p_{stag} };
$\langle \tau^k \rangle$,	coefficient of τ^k {(4.2)}.	u ,	due to undercooling { \mathcal{U}_u };
		d ,	due to density change { \mathcal{U}_d };
		O ,	outside of interface { \mathcal{E}_O };
		I ,	inside of interface { \mathcal{E}_I };
		B ,	on boundary { \mathcal{E}_B };
Subscripts		Superscripts	
f ,	equilibrium freezing value { T_f };	a ,	absolute { T^a };
F ,	pertaining to freezing front { T_F };	\sim ,	approximate { \hat{U} };
n ,	nucleation value { R_n };	'', ...,	pertaining to various components of U {(3.6)};
0 ,	initial value { R_0 };	\wedge ,	pertaining to least inconsistent choice { $\hat{\mathcal{I}}$ }.
v ,	at instant of maximum velocity { R_v };		
M ,	at instant of maximum tension when this is at time zero { $-p_M$ };		
m ,	at instant of maximum tension		

Part I. Application of "Generalized Orthogonalization Method" to Solution of the Nucleus Growth Problem

1. INTRODUCTION

WHEN the freezing phenomenon is accompanied by density change, the dynamics of fluid motion cannot be ignored—for when the frozen phase is denser, an inrush of fluid is required to fill the void that would otherwise be created near the freezing front. This inrush of fluid is accompanied by huge negative pressures. The negative pressure is, in fact, infinite when a spherical nucleus of originally zero radius begins to grow. For this reason the greatly simplifying assumption employed in reference [1], that of zero initial radius (which permits solution of the problem in closed form), must be surrendered and replaced by the more realistic assumption that a couple of dozen liquid molecules conglomerate into a solid-like mass ("embryo") and then, suddenly, the freezing phenomenon takes over. Theories are available for the ways this "nucleation" takes place [2-4]; in fact, quantitative estimates are furnished for the number of participating molecules and the radius R_n of a

metastable nucleus (see, e.g. reference [2b], p. 260; reference [4], p. 245). The foregoing estimates are derived from molecular-kinetic considerations. But once the initial nucleus with radius R_n is established, its further growth may be studied by the methods of continuum fluid mechanics and heat transfer. The need for such an investigation was signalled by J. L. Walker [5] and his followers [6] who observed a fundamental change in the nature of freezing into an undercooled melt. Walker noted that, for undercoolings less than 175°C, nickel freezes in coarse grains (grain diameter of the order of cm); for undercoolings larger than 175°C, the solidified metal is fine grained (grain diameter of the order of 10⁻³ cm). Walker attributed this to occurrence of cavitation when the tensions about an incipient nucleus become larger than the fracture strength of the liquid. Fluid fracture strength was estimated by Fisher [7], and his method of estimate was also adopted by Irwin [8]. According to Fisher's formula—equations (61) through

(63) of reference [1]—liquid nickel should fracture when subjected to a tension of about 50 000 atm; but it was pointed out that this crude estimate may be in error (the estimate may be too high) by a factor of 10.

The analysis given in the present paper indicates that, at an undercooling of 175°C, tensions in excess of 2000 atm develop around a growing nickel nucleus, and persist for time spans of 10^{-11} s. The velocity of the intruding fluid exceeds 100 m/s for about 10^{-10} s. The huge pressure variations make it mandatory that the pressure dependence of freezing temperature be accounted for. The present analysis, following a suggestion of John W. Cahn, properly incorporates this effect. Another consideration that the huge tensions and velocities call for is the accounting for compressibility of liquid and solid. The present analysis based on incompressible fluid dynamics, will furnish the picture that *the tension field and flow field are instantaneously created throughout the fluid at time $t = 0$* ; this picture is, of course, incorrect. An even more tantalizing inconsistency to which our analysis leads is the implication that *the situation becomes graver and graver* (the tension maximum increases to infinity) *as the density change during the phase transformation decreases to zero*. This conclusion is reached by studying the behavior of, say, a sequence of samples of the given metal, all having the same properties, except for the density change (see Fig. 11). It is not clear at this point whether this crisis can be resolved by incorporation of compressibility effects, or whether further physical principles must also be invoked.

Future refinements of the theory should incorporate, as already mentioned, compressibility and viscosity effects,‡ the limiting cases of $\epsilon = -1$ (conversion of liquid into vapor) and of very small $|\epsilon|$ (this seems to present a “boundary layer” effect with respect to the

parameter ϵ), as well as a study of pressure wave interactions with other nuclei and other pressure waves that play a vital role in determining the nature of the grain structure of the metal.

The paramount questions, however, pertain to the kinetic foundations of our assumed initial condition: an embryo of critical radius R_n exists; this is carried by an energy fluctuation into a size $R_0 > R_n$. Are there other, more suitable fluctuation mechanisms that will likewise start off the process? Is use of deterministic continuum mechanics permissible in the small time and distance intervals involved (t_v and $R_v - R_0$) during which all the interesting phenomena occur, or should a probabilistic-molecular approach be adopted? The importance of such a query becomes apparent from Fig. 10(a). A $\times T_f^a$ energy fluctuation, at 70° undercooling, carries the nickel nucleus from metastable radius size R_n to initial radius size $R_0 = 1.02 R_n$. In contrast, the radius at the instant of maximum velocity, $t_v = 3 \times 10^{-12}$ s after start of freezing, has grown only to $R_v = 1.008 R_0$: the change in radius in time t_v is (except for the largest undercoolings) less than that produced by the original fluctuation.

In spite of these reservations about the physical foundations of our approach, a hydrodynamic study, based on incompressible inviscid fluid dynamics, may be regarded—as matters now stand with the freezing problem—a valuable forward step. It leads to results for metals which, when the density change is not too small, are consistent in their main features with the experimental evidence of Walker, and with Fisher's estimate of fluid fracture strength. The mathematical approach, a generalized orthogonalization procedure (alternately, it may be regarded as a generalized boundary layer method) is also of interest, *per se*.

In section 2 of the paper the governing partial differential equations of the problem (2.17–21) are established. In section 3 these are converted, by the orthogonalization method, into approximating ordinary differential equations (3.15). Section 4 presents the solution for $\tau \gg 1$ and agreement with the conventional solution (where growth from zero radius is assumed) is established. Section 5 deals with the case of $\tau \ll 1$ (start of growth). Section 6 discusses various

‡ The present theory predicts that, while freezing velocity rises (except when the density change parameter $\epsilon = 0$) to a maximum \dot{R}_v in a small time t_v ($\approx 10^{-11}$ s), the maximum tension, $-p_M$, is instantaneously established at $t = 0$. A theory incorporating compressibility should lead to the more realistic picture that $-p_M$ also requires a rise time t_M , although this may be negligibly small compared to t_v .

critical radii (nucleation radius, radius at time of maximum velocity, at time of zero pressure). The foregoing sections constitute Part I of the paper, and are concerned principally with definition of the problem, establishment of method of

solution. Part II of the paper deals, more specifically, with the nickel nucleus. In section 7 are presented numerical results based on the methods of sections 4 and 5, and numerical integration in-between. Section 8 discusses the singular case $\epsilon = 0$.

2. THE GOVERNING EQUATIONS

The governing equations for the velocity u , pressure p , and temperature T of the inviscid, incompressible liquid phase, in spherically symmetric coordinates (see (1) of reference [1]) are:

Continuity: $(r^2 u)_r = 0$

Motion: $u_r + uu_r = -p_r/\rho$ (2.1a, b, c)

Heat: $T_t + uT_r = \kappa (T_{rr} + 2T_r/r)$

These are to be solved for the boundary conditions (see (3) of reference [1]):

at $r = \infty$: $p = p_\infty$, $T = T_\infty$ (2.2b, c)

(the condition

at $r = \infty$: $u = 0$ (2.2a)

cannot be imposed, because of our restriction to incompressible fluids, but it will be found to be obeyed anyhow), and

at $r = R(t) = \text{freezing front}$: $u = -\epsilon \dot{R}$, $-\frac{c}{\lambda} T_r = \frac{1+\epsilon}{\kappa} \dot{R}$, $T = T_F \equiv T_f + \Delta T$ (2.3a, b, c)

Here k , c , $\gamma = \rho g$, $\kappa = k/\gamma c$ are conductivity, specific heat, weight density, and diffusivity of liquid phase, and K , C and

$$\Gamma = (1 + \epsilon) \gamma \quad (2.4)$$

are conductivity, specific heat, and weight density of solid phase. ϵ denotes the factor of density change. $\lambda = \text{heat of fusion of the solid in thermal units (cal/g)}$, $\lambda' = \text{heat of fusion in mechanical units (g-cm/g)}$. The formula for the freezing temperature change effected by pressure ($T^a = \text{absolute temperature}$; see Appendix) is:

$$\begin{aligned} T_F - T_f = \Delta T &= \frac{T_f^a}{\lambda'} \left[\frac{p_F - p_\infty}{\gamma} - \frac{p_S - p_\infty}{\Gamma} \right] = \frac{T_f^a}{\lambda'} \left[\left(\frac{1}{\gamma} - \frac{1}{\Gamma} \right) (p_F - p_\infty) - \frac{p_{s.e.} + p_{stag}}{\Gamma} \right] \\ &= -\frac{T_f^a}{\Gamma \lambda'} [p_{s.e.} + p_{stag} - \epsilon (p_F - p_\infty)] \quad (2.5) \end{aligned}$$

Here p_S is the pressure on the solid phase,

$$p_{s.e.} = 2\sigma'/R \quad (2.6a)$$

is the pressure on the solid phase contributed by interface surface energy (g-cm/cm^2), and

$$p_{stag} = \rho u_F^2/2 \quad (2.6a)$$

is the stagnation pressure. u_F , p_F , T_F are speed, pressure, and temperature of the fluid at the freezing front. T_f is the equilibrium freezing temperature for an ambient pressure p_∞ and planar interface.

The continuity equation (2.1a) is satisfied by

$$u(r) = R^2 u(R)/r^2 \quad (2.7a)$$

By virtue of (2.3a) we may also write

$$u(r) = -\epsilon R^2 \dot{R}/r^2 \quad (2.7b)$$

The equation of motion (2.1b) may be replaced by the integrated (Bernoulli) form (see equation (1b*) of reference [1]):

$$\frac{p(r) - p_\infty}{\rho} = -\frac{u^2}{2} - \frac{\partial}{\partial t} \int_\infty^r u \, dr \quad (2.8a)$$

which by virtue of (2.7b) becomes

$$\frac{p(r) - p_\infty}{\rho} = -\frac{1}{2} \frac{\epsilon^2 R^4 \dot{R}^2}{r^4} - \epsilon \frac{R^2 \ddot{R}}{r} - 2\epsilon \frac{R \dot{R}^2}{r} \quad (2.8b)$$

and yields for the pressure at the front

$$p_F \equiv p(R) = p_\infty - \rho \epsilon \{ R \ddot{R} + (2 + \epsilon/2) \dot{R}^2 \} \quad (2.9a)$$

From (2.6b), (2.7b) the stagnation pressure is

$$p_{\text{stag}} = \rho u_F^2/2 = \rho \epsilon^2 \dot{R}^2/2 \quad (2.9b)$$

Consequently, by (2.5):

$$-\Gamma \lambda' \Delta T/T_f^a = p_{\text{s.e.}} + p_{\text{stag}} - \epsilon(p_F - p_\infty) = \frac{2\sigma'}{R} + \rho \epsilon^2 \left(R \ddot{R} + \frac{5 + \epsilon}{2} \dot{R}^2 \right) \quad (2.10)$$

The relation (2.10) may be rewritten in the form

$$T_F - T_\infty = T_f^a \left[\frac{2\sigma'}{\Gamma \lambda'} \left(\frac{1}{R_n} - \frac{1}{R} \right) - \epsilon^2 \frac{R \ddot{R} + (5 + \epsilon) \dot{R}^2/2}{(1 + \epsilon) g \lambda'} \right] \quad (2.11)$$

In the foregoing

$$R_n = \frac{2\sigma'/\Gamma \lambda'}{1 - T_\infty^a/T_f^a} = \frac{2\sigma' c T_f^a/\lambda}{\Gamma \lambda' U_u} \quad (2.12)$$

[U_u is given by (2.16b) below] is the critical static radius (the "nucleation radius") at which, due to surface tension effect, T_F is depressed to T_∞ :

$$T_F - T_\infty = 0 \text{ when } R = R_n, \dot{R} = \ddot{R} = 0 \quad (2.13)$$

Next we consider the temperature equation (2.1c) which, by virtue of (2.7b), becomes

$$T_{rr} + \left(2 + Y \frac{R^2 \dot{R}}{\kappa r} \right) \frac{T_r}{r} - \frac{T_t}{\kappa} = 0, \quad Y \equiv \epsilon \quad (2.14a, b)$$

Occasionally (for the purpose of comparing our analysis with other methods) one may desire to neglect thermal convection, and accordingly set

$$Y = 0 \quad (2.15)$$

We non-dimensionalize our equations by writing]

$$\xi = r/R_0, \quad \mathcal{R}(\tau) = R/R_0, \quad \tau = \kappa t/R_0^2, \quad \mathcal{P} = R_0^2 g p/\kappa^2 \gamma \quad (2.16a)$$

$$U(\xi, \tau) = \frac{c}{\lambda} (T - T_\infty), \quad U_u = \frac{c T_f^a}{\lambda} \left(1 - \frac{T_\infty^a}{T_f^a} \right), \quad U_d = \frac{\epsilon^2 c T_f^a}{1 + \epsilon} \frac{\kappa^2}{R_0^2 g \lambda'} \quad (2.16b)$$

$$\mathcal{K} = K/k, \quad \mathcal{X} = Kc/kC(1 + \epsilon) \quad (2.16c)$$

for distance, radius, time, pressure; temperature; relative conductivities. Here R_0 is a suitable reference length, to be specified later, in (2.21), as the initial radius of the nucleus; U_d will be referred

to as the "density parameter", U_u as the "undercooling (parameter)". We shall use dots to denote τ derivatives of dimensionless quantities, like \mathcal{R} . Dotted R denotes t derivative. Then the "Outside equation" (2.14) becomes

$$\mathcal{E}_O \equiv U_{\xi\xi} + \left(2 + Y \frac{R^2 \dot{R}}{\xi}\right) \frac{U_\xi}{\xi} - U_\tau = 0 \quad (\xi > \mathcal{R}) \quad (2.17)$$

subject, in accordance with (2.2c), (2.11), (2.3b) to the boundary conditions

$$\xi = \infty: \quad U = 0$$

$$\xi = \mathcal{R}: \quad U = U_F \equiv U_u \left(1 - \frac{\mathcal{R}_n}{\mathcal{R}}\right) - U_d \left(\mathcal{R} \dot{\mathcal{R}} + \frac{5 + \epsilon}{2} \dot{\mathcal{R}}^2\right) \quad (2.18a, b)$$

$$\xi = \mathcal{R}: \quad \mathcal{E}_B \equiv (1 + \epsilon) \dot{\mathcal{R}} + U_\xi (\mathcal{R} + 0) - K U_\xi (\mathcal{R} - 0) = 0 \quad (2.19)$$

We refer to (2.18b) as the *dynamic temperature relation* and to (2.19) as the *freezing (or moving) boundary condition at the interface*.

Condition (2.3b) implied that the frozen nucleus is isothermal (at T_F); an equivalent assumption is that $K = \infty$. In equation (2.19) we slightly generalized the relation, admitting temperature variation also in the frozen phase. Correspondingly, we must state the conduction equation also in the frozen phase ("Inside equation")

$$\mathcal{E}_I \equiv U_{\xi\xi} + \frac{2}{\xi} U_{\xi\tau} - \frac{1}{\mathcal{K}} U_\tau = 0 \quad (\xi < \mathcal{R}) \quad (2.20)$$

The initial conditions are

$$\tau = 0: \quad \mathcal{R} = \mathcal{R}_0 \equiv 1, \quad \dot{\mathcal{R}} = 0, \quad U = 0 \quad (2.21a, b, c)$$

The pressure expression at the front (2.9a), is now written in the form

$$\frac{p^\infty - p_F}{\epsilon} = \mathcal{R} \dot{\mathcal{R}} + (2 + \epsilon/2) \dot{\mathcal{R}}^2 \quad (2.22)$$

3. GENERALIZED ORTHOGONALIZATION METHOD

Solution of a differential equation $\mathcal{E}(U) = 0$ by the conventional orthogonalization method (see, e.g. Collatz [9]) consists in seeking an approximate solution \tilde{U} of the form

$$\tilde{U} = F_0 + \sum_1^K C_k F_k(\tau, \mathbf{x}) \quad (3.1)$$

(here F_0 satisfies the inhomogeneous boundary conditions of the problem, the functions F_k ($k \geq 1$) satisfy homogeneous boundary conditions; τ, \mathbf{x} are abbreviations for the independent variables $\tau_1, \tau_2, \dots; x_1, x_2, \dots$) and determining the coefficients C_k from the *conditions of orthogonality of error* $\mathcal{E}(\tilde{U})$ to conveniently chosen functions g_k :

$$k = 1, 2, \dots, K: \quad \mathcal{E}(\tilde{U}) \perp g_k, \quad \text{i.e.} \quad \int_{\tau, \mathbf{x}} \mathcal{E}(\tilde{U}) g_k(\tau, \mathbf{x}) \, d\mathbf{x} \, d\tau = 0 \quad (3.2)$$

In particular, when the g_k are chosen as the F_k , then the method is referred to as Galerkin's method. Furthermore, if \tilde{U} and its derivatives up to the orders appearing in \mathcal{E} are continuous, then $\mathcal{E}(\tilde{U})$ is also continuous; if, moreover, the integrand vanishes near infinite boundaries in an adequate manner and the g_k constitute a complete set of functions, then $\mathcal{E}(\tilde{U}) \rightarrow 0$ as $K \rightarrow \infty$. Hence \tilde{U} tends, as $K \rightarrow \infty$, to a solution of $\mathcal{E}(U) = 0$.

A generalization of the conventional orthogonalization method consists in the following. We adopt as starting point the approximate solution

$$\tilde{U} = \sum_1^K F_k \{ \tau, \mathbf{x}, w_j(\tau) \} \quad (3.3)$$

i.e. instead of numerical coefficients C_k we now seek to determine *functions* $w_j(\tau)$ (which, moreover, need not appear as linear factors appended to the F_k). And in place of (3.2) we now write

$$k = 0, 1, \dots, K: \quad \int_{\mathbf{x}} \mathcal{E}(\tilde{U}) g_k(\tau, \mathbf{x}) d\mathbf{x} = 0 \quad (3.4)$$

i.e. we omit the τ integration. Then the orthogonalization conditions (3.4) reduce to $K + 1$ ordinary differential equations for the functions w_j if τ is a single variable τ , and to partial differential equations for the functions w_j if τ represents an aggregate of variables τ_1, τ_2, \dots .

In our problem, equations (2.17, 20, 19), we have the single τ coordinate τ , and the single \mathbf{x} coordinate ξ . We choose for functions g_k the two sets

$$\left. \begin{aligned} \xi \geq \mathcal{R}: \quad g_0 = 1, g_k = (\xi - \mathcal{R})^k \\ \xi \leq \mathcal{R}: \quad h_0 = 1, h_j = \xi^j \end{aligned} \right\} \quad (3.5a, b)$$

while we write (omitting the tilde from the \tilde{U})

$$\xi \geq \mathcal{R}: \quad U(\tau) = U_F \{ A' \exp[-(\xi - \mathcal{R})/w'] + A'' \exp[-(\xi - \mathcal{R})/w''] \\ + A''' \exp[-(\xi - \mathcal{R})/w'''] + \dots \} \quad A'(\tau) + A''(\tau) + A'''(\tau) + \dots = 1 \quad (3.6a)$$

$$\xi \leq \mathcal{R}: \quad U(\tau) = U_C + (U_F - U_C) (\xi/\mathcal{R})^{2+1/l} \quad (3.6b)$$

i.e. we assume that $U(\tau)$ decays exponentially from the value (2.18b) at \mathcal{R} , to 0 at $\xi = \infty$, in the liquid phase, characterized by *decay distances* $w'(\tau), w''(\tau), \dots$ and *coupling functions* $A^{(k)}(\tau)$; while $U(\tau)$ rises from $U_C(\tau)$ at the sphere center to $U_F(\tau)$ at the interface as a power of ξ/\mathcal{R} , with variable exponent $2 + 1/l(\tau)$. We shall refer to (3.6a), when terminated with $A^{(k)} [\exp - (\xi - \mathcal{R})/w^{(k)}]$ as the $A^{(k)}$ (or briefly, k th) approximation. Clearly, our assumed expressions (3.6a, b) automatically satisfy the boundary conditions (2.18a, b) in the somewhat stricter form:

$$\xi = \infty: \quad \xi^2 U = \xi^2 U_\xi = 0, \quad \xi = \mathcal{R}: \quad U = U_F \quad (3.1a, b)$$

while the freezing condition (2.19) must still be imposed.

The particular choice (3.6b) is suggested by the observation that the rigorous solution $U(\tau)$ of the problem where a unit temperature jump $U_F - U_C = \mathbf{1}(\tau)$ [$\mathbf{1}(\tau) =$ Heaviside function] is imposed at time $\tau = 0$ on a sphere surface \mathcal{R} creates at small times a surface gradient

$$\tau \ll 1: \quad \partial U / \partial \xi |_{\mathcal{R}-0} = 1/\sqrt{(\pi\tau)} \quad (3.8)$$

see Carslaw and Jaeger [10], p. 348, equation (6). For the $U_F - U_C = \mathbf{1}(\tau)$ boundary condition our expression (3.6b) likewise gives an infinite surface gradient at time 0 if (3.11c), (5.11) is assumed, and so does (3.6a) for $\partial U / \partial \xi |_{\mathcal{R}+0}$ if (3.11b), (5.11) is assumed.

Integrating the outside equation (3.4) by parts, we obtain

$$\left. \begin{aligned} 0 &= \int_{\mathcal{R}}^{\infty} \mathcal{E}_O g_k \xi^2 d\xi = \int_{\mathcal{R}}^{\infty} \{ (\xi^2 U_\xi)_\xi + Y \mathcal{R}^2 \dot{\mathcal{R}} U_\xi - U_\tau \xi^2 \} g_k d\xi \\ &= \{ [\xi^2 U_\xi + Y \mathcal{R}^2 \dot{\mathcal{R}} U] g_k \}_{\mathcal{R}}^{\infty} - \int_{\mathcal{R}}^{\infty} \{ \xi^2 U_\xi + Y \mathcal{R}^2 \dot{\mathcal{R}} U \} g_{k\xi} d\xi \\ &\quad - [U \xi^2 \dot{\mathcal{R}} g_k]_{\xi=\mathcal{R}} - (d/d\tau) \int_{\mathcal{R}}^{\infty} U g_k \xi^2 d\xi + \int_{\mathcal{R}}^{\infty} U g_{k\tau} \xi^2 d\xi \end{aligned} \right\} \quad (3.9)$$

i.e. on observing (3.7a) and noting that $g_k(\mathcal{R}) = \delta_{k0}$ ($= 1$ for $k = 0$, and $= 0$ otherwise; k is non-negative, but need not be an integer)

$$\begin{aligned} (d/d\tau) \int_{\mathcal{R}} U g_k \xi^2 d\xi &= -\mathcal{R}^2 [U_\xi(\mathcal{R} + 0) + (1 + Y)\dot{\mathcal{R}} U_F] \delta_{k0} \\ &\quad - \int_{\mathcal{R}} [\{\xi^2 U_\xi + Y\mathcal{R}^2 \dot{\mathcal{R}} U\} g_{k\xi} - \xi^2 U g_{k\tau}] d\xi \end{aligned} \quad (3.10a)$$

while from the inside equation, noting that $h_j(\mathcal{R}) = \mathcal{R}^j$, $h_{j\tau} = 0$, we find similarly

$$(d/d\tau) \int_0^{\mathcal{R}} U h_j \xi^2 d\xi = \mathcal{R}^{2+j} [\mathcal{K} U_\xi(\mathcal{R} - 0) + \dot{\mathcal{R}} U_F] - \mathcal{K} \int_0^{\mathcal{R}} \xi^2 U_\xi h_{j\xi} d\xi \quad (3.10b)$$

In conjunction with the dynamic temperature relation (2.18b) and the freezing condition $\mathcal{E}_B = 0$, now reading

$$(1 + \epsilon)\dot{\mathcal{R}} - \left(\frac{A'}{w'} + \frac{A''}{w''} + \frac{A'''}{w'''} + \dots \right) U_F + \frac{2l + 1}{l} \mathcal{K} \frac{U_C - U_F}{\mathcal{R}} = 0 \quad (3.10c)$$

equations (3.10a, b), using $2K + 1$ equations (3.10a) (e.g. $k = 0, 1, 2, \dots, 2K$; or, $k = 0, \frac{1}{2}, 1, \dots, K$) and two equations (3.10b) ($j = 0, 1$), constitute $5 + 2K$ differential equations for the $5 + 2K$ unknowns \mathcal{R} , U_F , U_C , w' , l ; w'' , w''' , \dots ; A' , A'' , A''' , \dots , subject to the initial conditions

$$\tau = 0: \quad \mathcal{R} = 1, \quad \dot{\mathcal{R}} = U_F = U_C = 0 \quad (3.11a)$$

$$w' = w'' = w''' = \dots = 0, \quad l = 0 \quad (3.11b, c)$$

$$A'' = a_0'', A''' = a_0''', \dots; \quad A' = a_0' = 1 - a_0'' - a_0''' - \dots \quad (3.11d)$$

where a_0'', a_0''', \dots are suitable constants. Henceforth we shall omit the single primes associated with the A' and w' terms.

The $k = 0, j = 0$ members of (3.10a, b) may be referred to as the *primitive boundary layer approximation*; for these are the equations one is led to if, according to the precept of von Kármán-Pohlhausen for hydrodynamical problems (see, e.g. Schlichting [11]) or Veynik [12] and Goodman [13] for heat conduction problems, one multiplies the governing partial differential equations $\mathcal{E}_O = 0$, $\mathcal{E}_I = 0$ by the volume element $4\pi\xi^2 d\xi$ and integrates by parts. The $k = j = 0$ equations relate the change in enthalpy/ 4π outside and inside the nucleus, $(\int_{\mathcal{R}} U \xi^2 d\xi)^*$ and $(\int_0^{\mathcal{R}} U \xi^2 d\xi)^*$,

to the heat poured into the respective regions at the boundary. The $k > 0, j > 0$ equations are recognized as boundary layer equations, utilizing weight functions g_k, h_j .

For the choice (3.5), (3.6), (3.7), the equations (3.10a, b) become, on carrying out the indicated integrations and dividing the (3.10a) equations by $k!$, the (3.10b) equations by \mathcal{R}^{j+1} :

$$\begin{aligned} &\left. \begin{aligned} \frac{d}{d\tau} \left\{ U_F [\mathcal{R}^{2k} \{A w^{k+1} + A'' w''^{k+1} + \dots\} + 2(k+1)\mathcal{R} \{A w^{k+2} + A'' w''^{k+2} + \dots\} \right. \\ &\quad \left. + (k+1)(k+2)\{A w^{k+3} + A'' w''^{k+3} + \dots\} \right\} \\ &= \delta_{k0} U_F \mathcal{R}^2 \left[\frac{A}{w} + \frac{A''}{w''} + \dots - (1 + Y)\dot{\mathcal{R}} \right] + (1 - \delta_{k0}) U_F [\mathcal{R}^{2k} \{A w^{k-1} \\ &\quad + A'' w''^{k-1} + \dots\} + 2k\mathcal{R} \{A w^k + A'' w''^k + \dots\} + k(k+1)\{A w^{k+1} + A'' w''^{k+1} + \dots\}] \\ &\quad - (1 - \delta_{k0}) U_F \dot{\mathcal{R}} [(1 + Y)\mathcal{R}^{2k} \{A w^k + A'' w''^k + \dots\} + 2k\mathcal{R} \{A w^{k+1} + A'' w''^{k+1} + \dots\} \\ &\quad + k(k+1)\{A w^{k+2} + A'' w''^{k+2} + \dots\}] \end{aligned} \right\} \quad (3.13a) \end{aligned}$$

$$\frac{1}{\mathcal{R}^{j+1}} \frac{d}{d\tau} \left\{ \mathcal{R}^{j+3} \left[\frac{(2l+1)(j+3)}{1+l(j+5)} U_C + \frac{1}{1+l(j+5)} U_F \right] \right\} \\ = \mathcal{R} \dot{\mathcal{R}} U_F + \frac{(3l+1)(2l+1)}{l\{1+l(j+3)\}} \mathcal{X}(U_F - U_C) \quad (3.13b)$$

Performing the indicated differentiations, using the notation

$$\mathcal{U}/U = \mathcal{U}_m/U_m \equiv 1/(1 + \epsilon), \quad \mathcal{E} \equiv 1 + Y \quad (3.14)$$

($m = \text{any subscript}$), and restating also the equation $\mathcal{R} \mathcal{E}_B = 0$, one finds the equations, valid for $j \geq 0, k \geq 0$:

$$\frac{1}{j+3} \frac{2l+1}{1+l(j+5)} \mathcal{R}^2 \dot{\mathcal{U}}_C + \frac{1}{1+l(j+5)} \mathcal{R}^2 \dot{\mathcal{U}}_F + (\mathcal{U}_C - \mathcal{U}_F) \left[\frac{2l+1}{1+l(j+5)} \mathcal{R} \dot{\mathcal{R}} \right. \\ \left. - \frac{\mathcal{R} \dot{\mathcal{R}}}{\{1+l(j+5)\}^2} + \frac{(3l+1)(2l+1)}{l\{1+l(j+3)\}} \mathcal{X} \right] = 0 \quad (3.15^j)$$

$$\mathcal{R} \ddot{\mathcal{R}} + \left(2 + \frac{1}{l} \right) \mathcal{R}(\mathcal{U}_C - \mathcal{U}_F) - \left(\frac{A}{w} + \frac{A''}{w''} + \dots \right) \mathcal{R} \mathcal{U}_F = 0 \quad (3.15_B)$$

$$\left. \begin{aligned} & \{ (A \mathcal{U}_F)^* w^{k+1} \} [\mathcal{R}^2 + 2(k+1) \mathcal{R} w + (k+1)(k+2) w^2] + \{ \}'' [\}'' + \dots \\ & + \{ A \mathcal{U}_F w_k \} [(k+1) \dot{w} \{ \mathcal{R}^2 + 2(k+2) \mathcal{R} w + (k+2)(k+3) w^2 \} \\ & + \mathcal{R} \{ \mathcal{E} \mathcal{R}^2 + 2(k+1) \mathcal{R} w + (k+1)(k+2) w^2 \} - \mathcal{R}^2/w - 2k \mathcal{R} - k(k+1) w] \\ & + \{ \}'' [\}'' + \dots = 0 \end{aligned} \right\} (3.15_k^j)$$

Expressions like $\{ \}'' [\}''$ mean: repeat the preceding $\{ \} [\}$ expression, but replace therein A, w by A'', w'' , etc.

We shall regard (3.15⁰) as the equation governing the variation of $\mathcal{U}_C(\tau)$, (3.15¹) as the equation governing $l(\tau)$, (3.15_B) as the equation governing $\mathcal{U}_F(\tau)$, (4.3a) as the equation governing $\mathcal{R}(\tau)$; (3.15₀⁰), (3.15₀^{2k}), (3.15₀^{4k}) as the equations governing $w(\tau), w''(\tau), w'''(\tau)$, respectively, and (3.15₀^k), (3.15₀^{2k}) as the equations governing the coupling coefficients $A''(\tau), A'''(\tau)$. The latter (3.15₀) scheme refers to the third approximation III_k; III₁ [k in (3.5a) progresses in units of $\frac{1}{2}$] denotes the third approximation, based on (3.15₀^{0, 1, 2}). In first approximation, I , only (3.15₀⁰) of (3.15₀^k) will be utilized.

We shall be most concerned with the second approximations II₁, II_{1/2} based on (3.15₀^{0, 1, 2}) and (3.15₀^{0, 1/2, 1}), respectively, and particularly with the approximation II₀ which one obtains as one passes, in equations (3.15₀^{0, k, 2k}) to $k = 0$.

For most purposes (i.e. for calculating Figs. 10) we shall need the solution only for small times (as represented by ascending power series in $\tau^{1/2}$), and for large times (as represented by descending power series in $\tau^{1/2}$), and these solutions can be determined in the II₀ approximation very conveniently from II_k by passage to $k = 0$ in the solution itself. However, when we are concerned with behavior of the system for all times (i.e. including the range $\tau \sim 1$), then we must integrate the pertinent differential equations numerically from the small time solution forward to the large time solution or from the large time solution backward to the small time solution, as in Figs. 6 through 8. The outside equations II₀ are obtained from (3.15₀^k) in the same fashion as (4.17c) in the next section is obtained from (4.11), utilizing the relations (4.14). Since the equations are lengthy and we shall not use them in the sequel, we do not write them out; we merely refer to them as (3.16₀^{0, ' , ''}). When we regard $l(\tau)$ as the known function (4.7)—we rewrite this relation now as

$$l = \mathcal{K}/4l, \quad l(0) = 0 \quad (3.17a)$$

and denote furthermore

$$z = \dot{\mathcal{R}} = (\mathcal{R})^* \quad (3.17b)$$

then (3.17a, b), the dynamic temperature relation (4.3a), the outside equations (3.16_o'), the inside equation (3.15_i'), and the moving boundary condition (3.15_B) constitute eight first-order non-linear equations—not containing time explicitly—in the eight unknowns $l, \mathcal{R}, z, w, \mathcal{U}_F, A\mathcal{U}_F, \mathcal{U}_C, w''$.

4. SOLUTION FOR $\tau \gg 1$

The pressure effect on freezing temperature rapidly disappears as the nucleus expands; therefore, one expects the radius to grow as $\tau^{1/2}$ near $\tau \rightarrow \infty$, i.e. as if there were no initial freezing point depression, and the initial radius were zero. More specifically, we assume a time dependence near infinity

$$\left. \begin{aligned} \mathcal{R} &= 2\beta_\infty \tau^{1/2} [1 + \beta_{1/2} \tau^{-1/2} + \beta_1 \tau^{-1} + \dots], & w &= 2\delta_\infty \tau^{1/2} [1 + \delta_{1/2} \tau^{-1/2} + \dots], \\ w'' &= 2\delta''_\infty \tau^{1/2} [1 + \delta''_{1/2} \tau^{-1/2} + \dots], & w''' &= 2\delta'''_\infty \tau^{1/2} [1 + \delta'''_{1/2} \tau^{-1/2} + \dots], \\ \mathcal{U}_F &= \nu_0 + \nu_{1/2} \tau^{-1/2} + \nu_1 \tau^{-1} + \dots, & \mathcal{U}_C &= \gamma_0 + \gamma_{1/2} \tau^{-1/2} + \gamma_1 \tau^{-1} + \dots, \\ l &= 2\lambda_\infty \tau^{-1/2} [1 + \lambda_{1/2} \tau^{-1/2} + \dots], & A &= a_0 + a_{1/2} \tau^{-1/2} + a_1 \tau^{-1} + \dots, \\ A'' &= a''_0 + a''_{1/2} \tau^{-1/2} + \dots, & A''' &= a'''_0 + a'''_{1/2} \tau^{-1/2} + \dots, \\ a_0 + a''_0 + a'''_0 + \dots &= 1, & a_{1/2} + a''_{1/2} + a'''_{1/2} + \dots &= 0, & a_1 + a'_1 + a'''_1 + \dots &= 0, \dots \end{aligned} \right\} (4.1)$$

Placing (4.1) into (3.15), one obtains for $j = 0, 1; B$; and arbitrary k :

$$\begin{aligned} &2\beta_\infty^2 \tau^0 \left\langle (\gamma_0 - \nu_0) \left\{ \frac{2}{5} + \frac{\mathcal{K}}{\beta_\infty^2} \right\} \right\rangle + 2\beta_\infty^2 \tau^{-1/2} \left\langle (\gamma_0 - \nu_0) \{ \} + \gamma_{1/2} \left\{ \frac{4}{15} + \frac{\mathcal{K}}{\beta_\infty^2} \right\} - \nu_{1/2} \left\{ \frac{3}{5} + \frac{\mathcal{K}}{\beta_\infty^2} \right\} \right\rangle \\ &+ 2\beta_\infty^2 \tau^{-1} \left\langle (\gamma_0 - \nu_0) \{ \} + \gamma_{1/2} \left\{ \frac{2}{15} \beta_{1/2} + \frac{1/50}{\lambda_\infty} + \frac{\mathcal{K}}{4\lambda_\infty \beta_\infty^2} \right\} - \nu_{1/2} \left\{ \frac{4}{5} \beta_{1/2} + \frac{1/50}{\lambda_\infty} + \frac{\mathcal{K}}{4\lambda_\infty \beta_\infty^2} \right\} \right\rangle \\ &+ \gamma_1 \left\{ \frac{2}{15} + \frac{\mathcal{K}}{\beta_\infty^2} \right\} - \nu_1 \left\{ \frac{4}{5} + \frac{\mathcal{K}}{\beta_\infty^2} \right\} \right\rangle + \dots = 0 \quad (4.2a) \end{aligned}$$

$$\begin{aligned} &2\beta_\infty^2 \tau^0 \left\langle (\gamma_0 - \nu_0) \left\{ \frac{1}{3} + \frac{3}{4} \frac{\mathcal{K}}{\beta_\infty^2} \right\} \right\rangle + 2\beta_\infty^2 \tau^{-1/2} \left\langle (\gamma_0 - \nu_0) \{ \} + \gamma_{1/2} \left\{ \frac{1}{4} + \frac{3}{4} \frac{\mathcal{K}}{\beta_\infty^2} \right\} \right. \\ &\quad \left. - \nu_{1/2} \left\{ \frac{1}{2} + \frac{3}{4} \frac{\mathcal{K}}{\beta_\infty^2} \right\} \right\rangle + \dots = 0 \quad (4.2b) \end{aligned}$$

$$\begin{aligned} &-\beta_\infty \tau^0 \left\langle -2\beta_\infty + \nu_0 \left\{ \frac{\alpha_0}{\delta_\infty} + \frac{\alpha''_0}{\delta''_\infty} \right\} + 2 \frac{\mathcal{K}}{\beta} (\nu_0 - \gamma_0) \right\rangle - \beta_\infty \tau^{-1/2} \left\langle -2\beta_\infty \beta_{1/2} + \nu_0 \right. \\ &\quad \times \left\{ \left[\frac{\alpha_0}{\delta_\infty} (\beta_{1/2} - \delta_{1/2}) + \frac{\alpha_{1/2}}{\delta_\infty} \right] + []'' \right\} + \nu_{1/2} \left\{ \frac{\alpha_0}{\delta_\infty} + \frac{\alpha''_0}{\delta''_\infty} \right\} + \frac{2\mathcal{K}}{\beta_\infty} [(\nu_0 - \gamma_0) \{ \} + \\ &\quad \left. + (\nu_{1/2} - \gamma_{1/2}) \right\rangle + \dots = 0 \quad (4.2B) \end{aligned}$$

$$\left. \begin{aligned}
 & 2^{k+2} \nu_0 \tau^{(k+1)/2} \left\langle [a_0 \delta_\infty^k] \left[\mathcal{E} \beta_\infty^3 + 3(k+1) \beta_\infty^2 \delta_\infty + 3(k+1)(k+2) \beta_\infty \delta_\infty^2 \right. \right. \\
 & \quad \left. \left. + (k+1)(k+2)(k+3) \delta_\infty^3 - \frac{\beta_\infty^2}{2\delta_\infty} - k\beta_\infty - \frac{k(k+1)}{2} \delta_\infty \right] + [I'' [I''] \right\rangle \\
 & + 2^{k+2} \nu_0 \tau^{k/2} \left\langle [a_0 \delta_\infty^k] \left[\mathcal{E} \beta_\infty^3 \{2\beta_{1/2} + k\delta_{1/2}\} + (k+1) \beta_\infty^2 \delta_\infty \{4\beta_{1/2} \right. \right. \\
 & \quad \left. \left. + (3k+2)\delta_{1/2}\} + (k+1)(k+2) \beta_\infty \delta_\infty^2 \{2\beta_{1/2} + (3k+4)\delta_{1/2}\} \right. \right. \\
 & \quad \left. \left. + (k+1)(k+2)^2(k+3) \delta_\infty^3 \delta_{1/2} - \frac{\beta_\infty^2}{2\delta_\infty} \{2\beta_{1/2} + (k-1)\delta_{1/2}\} - k\beta_\infty \{\beta_{1/2} \right. \right. \\
 & \quad \left. \left. + k\delta_{1/2}\} - \frac{k(k+1)^2}{2} \delta_\infty \delta_{1/2} \right] + [I'' [I''] + [(a_{1/2} + a_0 \nu_{1/2}/\nu_0) \delta_\infty^k] \left[\mathcal{E} \beta_\infty^3 \right. \right. \\
 & \quad \left. \left. + (3k+2) \beta_\infty^2 \delta_\infty + (k+1)(3k+4) \beta_\infty \delta_\infty^2 + (k+1)(k+2)^2 \delta_\infty^3 \right. \right. \\
 & \quad \left. \left. - \frac{\beta_\infty^2}{2\delta_\infty} - k\beta_\infty - \frac{k(k+1)}{2} \delta_\infty \right] + [I'' [I'']] \right\rangle + \dots = 0
 \end{aligned} \right\} (4.2_b)$$

We stated in (4.2) the equations as they appear in the Π_k approximation. (In the third approximation we have to retain also $\{ \}''' [I''']$ type expressions and a_0''/δ_∞'' terms.) Moreover, in the light of (4.5), below, we did not write out in (4.2_I, 2_B) all the $(\nu_0 - \gamma_0)$ coefficients, but indicated them mostly by $\{ \}$.

Because of (2.18b), which we now rewrite in the form

$$\left. \begin{aligned}
 \mathcal{U}_F(\tau) &= \mathcal{U}_u \left(1 - \frac{\mathcal{R}_n}{\mathcal{R}} \right) - \mathcal{U}_d \left(\mathcal{R} \ddot{\mathcal{R}} + \frac{5 + \epsilon}{2} \dot{\mathcal{R}}^2 \right) \\
 \dot{\mathcal{U}}_F(\tau) &= \mathcal{U}_u \mathcal{R}_n \dot{\mathcal{R}} / \mathcal{R}^2 - \mathcal{U}_d [(6 + \epsilon) \dot{\mathcal{R}} \ddot{\mathcal{R}} + \mathcal{R} \ddot{\mathcal{R}}]
 \end{aligned} \right\} (4.3a, b)$$

there exists a further relation between the coefficients β_k and the coefficients ν_k . Inserting (4.1) into (4.3a) there results

$$\nu_0 = \mathcal{U}_u, \quad \nu_{1/2} = -\mathcal{U}_u \mathcal{R}_n / 2\beta_\infty, \quad \nu_1 = \frac{1}{2} \mathcal{U}_u \mathcal{R}_n \frac{\beta_{1/2}}{\beta_\infty} - \frac{3 + \epsilon}{2} \mathcal{U}_d \beta_\infty^2, \dots \quad (4.4)$$

The condition $\langle \tau^0 \rangle = 0$ in (4.2_I, 2_I) [we denote the coefficient of τ^j by $\langle \tau^j \rangle$] leads, in the light of the first expression in (4.4), to

$$\gamma_0 = \nu_0 = \mathcal{U}_u \quad (4.5)$$

while the two equations $\langle \tau^{-1/2} \rangle = 0$ lead to a contradiction in the ratio $\gamma_{1/2}/\nu_{1/2}$. The reason for this is that the λ parameters have not yet entered the scene [they first appear at the stage $\langle \tau^{-1} \rangle = 0$], and so we have two equations in one unknown, $\gamma_{1/2}/\nu_{1/2}$. There are two ways to eliminate this difficulty. One is to write $l(\tau)$ in the form

$$l(\tau) = \lambda_0 + \lambda_{1/2} \tau^{-1/2} + \lambda_1 \tau^{-1} + \dots \quad (4.6)$$

Then λ_0 properly enters at an earlier stage, and no difficulty arises in solving the two (4.2_I) equations $\langle \tau^{-1/2} \rangle = 0$ for $\gamma_{1/2}/\nu_{1/2}$ and λ_0 . The second is to *assume* the expression of $l(\tau)$ and correspondingly discard (4.2_I). We shall adopt this second alternative both for the sake of simplicity, and because

the small time solution of section 5 will be seen to run into difficulty when both equations (3.15_r) are retained. Accordingly, we set

$$l(\tau) = 2\lambda_\infty \tau^{1/2} \equiv l_{1/2} \tau^{1/2}, \quad l_{1/2} = (\mathcal{K}/2)^{1/2} \quad (4.7)$$

where $l_{1/2}$ is the expression (5.16a) derived in the next section for small times.

The condition $\langle \tau^0 \rangle = 0$ in (4.2_B) gives

$$\beta_\infty = \frac{1}{2} \mathcal{U}_u \left(\frac{\alpha_0}{\delta_\infty} + \frac{\alpha_0''}{\delta_\infty''} + \frac{\alpha_0'''}{\delta_\infty'''} + \dots \right), \quad \frac{\Omega}{\mathcal{U}_u} = \frac{\Psi}{2\delta_\infty^2} \quad (4.8a, b)$$

In (4.8b) and (4.10) we adopted the notation

$$\Omega = \beta_\infty / \delta_\infty, \quad \omega'' = \delta_\infty'' / \delta_\infty, \quad \omega''' = \delta_\infty''' / \delta_\infty, \quad \Psi = \alpha_0 + \frac{\alpha_0''}{\omega''} + \frac{\alpha_0'''}{\omega'''} + \dots \quad (4.9)$$

Henceforth we shall write ω instead of ω'' .

Denoting furthermore

$$\left. \begin{aligned} B_k &= \mathcal{E} \Omega^3 + 3(k+1) \Omega^2 + 3(k+1)(k+2) \Omega + (k+1)(k+2)(k+3) \\ B_k'' &= \mathcal{E} \Omega^2 + 3(k+1) \Omega^2 \omega + 3(k+1)(k+2) \Omega \omega^2 + (k+1)(k+2)(k+3) \omega^3 \\ B_k''' &= \mathcal{E} \Omega^3 + 3(k+1) \Omega^2 \omega''' + 3(k+1)(k+2) \Omega \omega'''^2 + (k+1)(k+2)(k+3) \omega'''^3 \\ \mathcal{B}_k &= \Omega^3 + 2k \Omega^2 + k(k+1) \Omega, \quad \mathcal{B}_k'' = \Omega^3 + 2k \Omega^2 \omega + k(k+1) \Omega \omega^2 \end{aligned} \right\} \quad (4.10a)$$

$$B = B_0, \quad B'' = B_0'', \quad \mathcal{B} = \mathcal{B}_0, \quad \mathcal{B}'' = \mathcal{B}_0'' \quad (4.10b)$$

$$\left. \begin{aligned} C &= 3 \Omega^2 + 9 \Omega + 11 & C'' &= 3 \Omega^2 \omega + 9 \Omega \omega^2 + 11 \omega^3 \\ D &= 3 \Omega + 6 & D'' &= 3 \Omega \omega^2 + 6 \omega^3 \\ \mathcal{C} &= 2 \Omega^2 + \Omega & \mathcal{C}'' &= 2 \Omega^2 + \Omega \omega \\ \mathcal{D} &= \Omega & \mathcal{D}'' &= \Omega \omega \end{aligned} \right\} \quad (4.10c)$$

we may write the $\langle \tau^{(1+k)/2} \rangle = 0$ equations (4.2_k) in the form

$$\begin{aligned} \alpha_0 B_k + \omega^k \alpha_0'' B_k'' + \omega''^k \alpha_0''' B_k''' + \dots \\ = (\Psi \mathcal{U}_u)^{-1} [\alpha_0 \mathcal{B}_k + \omega^{k-1} \alpha_0'' \mathcal{B}_k'' + \omega''^{k-1} \alpha_0''' \mathcal{B}_k''' + \dots] \end{aligned} \quad (4.11k)$$

In particular, for $k = 0$

$$\alpha_0 B + \alpha_0'' B'' + \alpha_0''' B''' + \dots = \Omega^3 / \mathcal{U}_u \quad (4.11_0)$$

The first task, in the III_k approximation, is to solve (4.11₀, $\frac{1}{2}$, 1, $\frac{3}{2}$, 2) for Ω , ω , α_0'' , ω'' , α_0''' (note that $\alpha_0 = 1 - \alpha_0'' - \alpha_0'''$) for given undercooling $U_u = \mathcal{E} \mathcal{U}_u$. In the II₀ approximation we must solve (4.20^o, ', '''), below, for Ω , ω , α_0'' . If we have a first guess $\bar{\Omega}$, $\bar{\omega}$, $\bar{\alpha}_0''$, ... available for the quantities Ω , ω , α_0'' , ... we may write

$$\Omega = \bar{\Omega} + \delta_\Omega, \quad \omega = \bar{\omega} + \delta_\omega, \quad \alpha_0'' = \bar{\alpha}_0'' + \delta_\alpha'', \dots \quad (4.12)$$

and solve for the small corrections δ_Ω , δ_ω , δ_α'' , ... iteratively, from linearized equations.

Once the foregoing quantities are available, one can calculate β_∞ on the basis of (4.8) from the formula

$$\beta_\infty = \frac{\Omega \sqrt{2}}{[\Omega \Psi \mathcal{U}_u]^{1/2}} \quad (4.13)$$

δ_∞ from (4.8b), δ_∞'' from ω'' etc.

For the purpose of determining the Π_0 approximation, we expand the terms of (4.2^k) in powers of k . Noting that

$$\omega^k = 1 + \frac{k}{1!} \ln \omega + \frac{k^2}{2!} \ln^2 \omega + \frac{k^3}{3!} \ln^3 \omega + \dots [\ln^2 \omega \equiv (\ln \omega)^2] \tag{4.14}$$

we obtain expressions of the following sort:

$$\langle \tau^{(k+1)/2} \rangle = 0: \quad f_0(x_1, y_1, z_1) + kf_1 + k^2f_2 + k^3f_3 = R_0 + kR_1 + k^2R_2 + k^3R_3 \tag{4.15a}$$

$$\langle \tau^{k/2} \rangle = 0: \quad g_0(x_2, y_2, z_2) + kg_1 + k^2g_2 + k^3g_3 = S_0 + kS_1 + k^2S_2 + k^3S_3 \tag{4.15b}$$

.....

where

$$x_1, y_1, z_1 = \delta_\infty, \delta''_\infty, a''_0; \quad x_2, y_2, z_2 = \delta_{1/2}, \delta'_{1/2}, a'_{1/2}; \dots \tag{4.16}$$

(the R_k are independent of $x_i, y_i, z_i, i \geq 1$; the S_k are independent of $x_i, y_i, z_i, i \geq 2$ etc.), and all higher k terms are lumped into f_3, R_3, g_3, \dots . The equations (4.15a), written out in detail for $k = 0, m, 2m$ are

$$\left. \begin{aligned} f_0 &= R_0 \\ f_0 + mf_1 + m^2f_2 + m^3f_3 &= R_0 + mR_1 + m^2R_2 + m^3R_3 \\ f_0 + 2mf_1 + 4m^2f_2 + 8m^3f_3 &= R_0 + 2mR_1 + 4m^2R_2 + 8m^3R_3 \end{aligned} \right\} \tag{4.17a}$$

By rearrangement one obtains

$$f_0 = R_0, \quad f_1 - 2mf_3 = R_1 - 2m^2R_3, \quad f_2 + 3mf_3 = R_2 + 3mR_3 \tag{4.17b}$$

For $m \rightarrow 0$ these reduce to

$$f_0 = R_0, \quad f_1 = R_1, \quad f_2 = R_2 \tag{4.17c}$$

The three equations (4.2^{0, k, 2k}) are replaced, for $k \rightarrow 0$, in this fashion by

$$\tau^{1/2} ({}^\circ\Gamma_{1/2} + {}^\circ\Gamma''_{1/2}) + \tau^0 ({}^\circ\Gamma_0 + {}^\circ\Gamma''_0) + \tau^{-1/2} ({}^\circ\Gamma_{-1/2} + {}^\circ\Gamma''_{-1/2}) + \dots = 0 \tag{4.18^{\circ}}$$

$$\begin{aligned} \tau^{1/2} ({}^\circ\Gamma_{1/2} + {}^\circ\Gamma_{1/2} \ln \delta_\infty + {}^\circ\Gamma''_{1/2} + {}^\circ\Gamma''_{1/2} \ln \delta''_\infty) \\ + \tau^0 ({}^\circ\Gamma_0 + {}^\circ\Gamma_0 \ln \delta_\infty + {}^\circ\Gamma''_0 + {}^\circ\Gamma''_0 \ln \delta''_\infty) + \dots = 0 \end{aligned} \tag{4.18'}$$

$$\begin{aligned} \tau^{1/2} ({}^\circ\Gamma_{1/2} + {}^\circ\Gamma_{1/2} \ln \delta_\infty + \frac{1}{2} {}^\circ\Gamma_{1/2} \ln^2 \delta_\infty + {}^\circ\Gamma''_{1/2} \\ + {}^\circ\Gamma''_{1/2} \ln \delta''_\infty + \frac{1}{2} {}^\circ\Gamma''_{1/2} \ln^2 \delta''_\infty) + \tau^0 () + \dots = 0 \end{aligned} \tag{4.18''}$$

Omitting for more convenient writing, the subscript ∞ of β_∞ and δ_∞ , the expressions of the Γ are as follows (the Γ'' have the same expressions, with α_k and δ_l being replaced by α''_k, δ''_l):

$$\left. \begin{aligned} {}^\circ\Gamma_{1/2} &= a_0 \{E \beta^3 + 3 \beta^2 \delta + 6 \beta \delta^2 + 6 \delta^3 - \beta^2/2\delta\} \\ {}^\circ\Gamma_{1/2} &= a_0 \{3 \beta^2 \delta + 9 \beta \delta^2 + 11 \delta^3 - \beta - \frac{1}{2} \delta\} \\ {}^\circ\Gamma_{1/2} &= a_0 \{3 \beta \delta^2 + 6 \delta^3 - \frac{1}{2} \delta\} \end{aligned} \right\} \tag{4.19}$$

$$\begin{aligned}
 {}^{\circ}\Gamma_0 &= \alpha_0 \left\{ 2 \mathcal{E} \beta^3 \delta_{1/2} + 2 \beta^2 \delta (2 \beta_{1/2} + \delta_{1/2}) + 4 \beta \delta^2 (\beta_{1/2} + 2 \delta_{1/2}) \right. \\
 &\quad \left. + 12 \delta^3 \delta_{1/2} - (\beta^2/2\delta) (2 \beta_{1/2} - \delta_{1/2}) \right\} + (\alpha_{1/2} + \alpha_0 \nu_{1/2}/\nu_0) \\
 &\quad \times \left\{ \mathcal{E} \beta^3 + 2 \beta^2 \delta + 4 \beta \delta^2 + 4 \delta^3 - \beta^2/2 \delta \right\} \\
 {}^{\prime}\Gamma_0 &= \alpha_0 \left\{ \mathcal{E} \beta^3 \delta_{1/2} + \beta^2 \delta (4 \beta_{1/2} + 5 \delta_{1/2}) + 6 \beta \delta^2 (\beta_{1/2} + 3 \delta_{1/2}) + 28 \delta^3 \delta_{1/2} \right. \\
 &\quad \left. - (\beta^3/2\delta) \delta_{1/2} - \beta \beta_{1/2} - \frac{1}{2} \delta \delta_{1/2} \right\} + (\alpha_{1/2} + \alpha_0 \nu_{1/2}/\nu_0) \\
 &\quad \times \left\{ 3 \beta^2 \delta + 7 \beta \delta^2 + 8 \delta^3 - \beta - \frac{1}{2} \delta \right\} \\
 {}^{\prime\prime}\Gamma_0 &= \alpha \left\{ 3 \beta^2 \delta \delta_{1/2} + \beta \delta^2 (2 \beta_{1/2} + 13 \delta_{1/2}) + 23 \delta^3 \delta_{1/2} - \beta \delta_{1/2} - \delta \delta_{1/2} \right\} \\
 &\quad + (\alpha_{1/2} + \alpha_0 \nu_{1/2}/\nu_0) \left\{ 3 \beta \delta^2 + 5 \delta^3 - \frac{1}{2} \delta \right\}
 \end{aligned} \tag{4.19_0}$$

Similarly, in terms of the notation (4.10), the equations (4.11) become replaced by

$$\alpha_0 B + \alpha_0'' B'' = \mathcal{B} \mathcal{U}_u \tag{4.20^{\circ}}$$

$$\alpha_0 C + \alpha_0'' \{C'' + B'' \ln \omega\} = (\Psi \mathcal{U}_u)^{-1} [\alpha_0 \mathcal{C} + \alpha_0'' (\mathcal{C}'' + \omega^{-1} \mathcal{B}'' \ln \omega)] \tag{4.20'}$$

$$\begin{aligned}
 \alpha_0 D + \alpha_0'' \{D'' + C'' \ln \omega + \frac{1}{2} B'' \ln^2 \omega\} &= (\Psi \mathcal{U}_u)^{-1} \\
 &\times [\alpha_0 \mathcal{D} + \alpha_0'' (\mathcal{D}'' + \mathcal{C}'' \ln \omega + \frac{1}{2} \omega^{-1} \mathcal{B}'' \ln^2 \omega)] \tag{4.20''}
 \end{aligned}$$

The rigorous value of the parameter β_{∞} is available in the literature. In the absence of pressure and density effects (i.e. for $\mathcal{E} = 1$ etc.), it is given by the ‘‘Rigorous’’ curve in Fig. 1(a). {The curve is the $\mathcal{A} = 1$ curve in Fig. 3 of reference [14], and the $\epsilon = 0$ curve in Fig. 2 of reference [1]. The present β_{∞} , U_u symbols are denoted in these references by $\Omega^{1/2}$, U_f and β , $(T_f - T_{\infty})/\theta$. The curve is plotted also in a number of the references cited in reference [14].} In Fig. 1(a) we furthermore plot β_{∞} as obtained by the present method in the I, II₁, II_{1/2}, II₀ approximations [using the approach indicated in (4.12)]; in Fig. 1(b) we plot the parameter Ω ; in Figs 1(c) and (d) we plot the parameters α_0 , α_0'' and ω , respectively. In addition, we show a plot in Fig. 1(a) of β_{∞} in the A'' approximation where, using (4.11_{0, 1}), A'' was assigned the *fixed* (independent of \mathcal{U}_u) value

$$A'' = \frac{3}{4} = 1 - A \tag{4.21}$$

It will be noted from (4.11₀) that as $\mathcal{U}_u \rightarrow 0$, also $\Omega \rightarrow 0$, while as $\mathcal{E} \mathcal{U}_u \rightarrow 1$, $\Omega \rightarrow \infty$. For $\mathcal{U}_u \ll 1$ (and for \mathcal{E} not necessarily 1) the rigorous β_{∞} behaves [as is readily verified from reference [1], formula (31)] as

$$\beta_{\infty} = (\mathcal{U}_u/2)^{1/2} = 0.707 \mathcal{U}_u^{1/2} \tag{4.22a}$$

while (4.11₀) furnishes, on anticipating that $\mathcal{U}_u \ll 1$ implies

$$\Omega \ll 1 \tag{4.23a}$$

the relation

$$\mathcal{U}_u \ll 1: \quad \Omega = (6 \alpha_0 \mathcal{U}_u)^{1/3} \tag{4.24a, 25a}$$

From this and (4.13) it follows that in the first approximation ($\alpha_0 \equiv 1$)

$$\beta_{\infty} = (3/4)^{1/6} \mathcal{U}_u^{2/3} = 0.953 \mathcal{U}_u^{2/3} \tag{4.24b}$$

In the II₁ approximation, anticipating, for $\mathcal{U}_u \ll 1$, also

$$\omega^3 \ll 1, \quad \alpha_0^2/\alpha_0''^2 \ll 1 \tag{4.23b, c}$$

(4.11₂) reduces to

$$10 = \Omega/\Psi \mathcal{U}_u \tag{4.25b}$$

$$= \Omega \omega/\alpha_0'' \mathcal{U}_u \tag{4.25c}$$

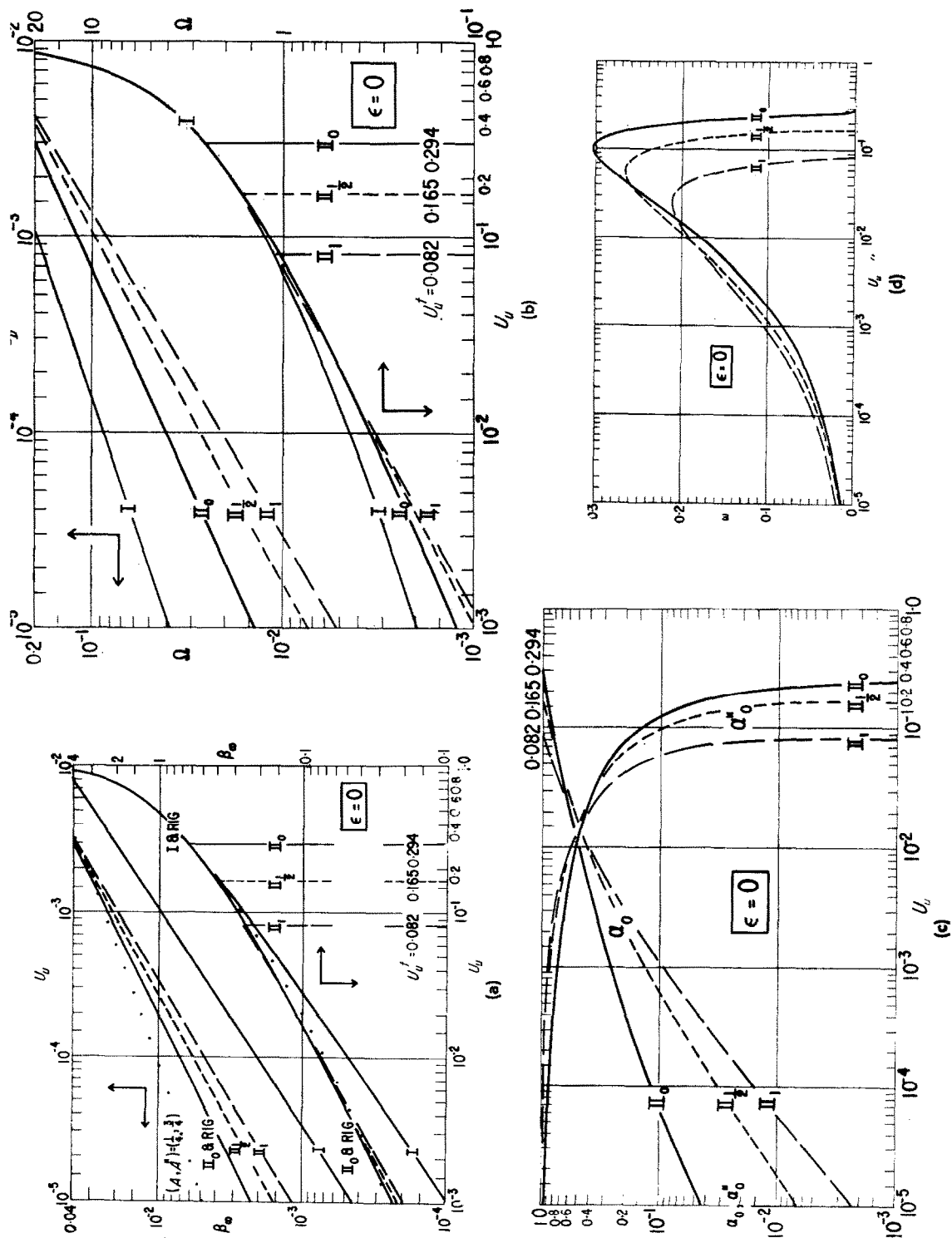


FIG. 1. Solidification parameter β_∞ and parameters Ω , α , ω of the large time solution for the case of zero density change.

while (4.11₁) becomes

$$12 = (\Omega/\Psi\mathcal{U}_u)[1 + \omega^2\alpha_0''/\alpha_0] \quad (4.25d)$$

By virtue of (4.25b) this gives

$$\omega = (\alpha_0/5)^{1/2} \quad (4.25e)$$

Inserting (4.25e, 24a) into (4.25c) and noting (4.13), one finds

$$\alpha_0 = 20.3 \mathcal{U}_u^{4/5}, \quad \Omega = 4.95 \mathcal{U}_u^{3/5}, \quad \beta = \Omega/\sqrt{(20)} = 1.12 \mathcal{U}_u^{3/5} \quad (4.25f, g, h)$$

In the II_‡ approximation, (4.11₁, 11_‡, 25a) lead similarly to

$$12 = \Omega/\Psi\mathcal{U}_u = \Omega\omega/\alpha_0''\mathcal{U}_u, \quad 17.5 = (\Omega/\Psi\mathcal{U}_u)[1 + \omega^{3/2}\alpha_0''/\alpha_0] \quad (4.26a, b)$$

$$\omega = (11\alpha_0/24)^{2/3}, \quad \alpha_0 = 11.11 \mathcal{U}_u^{2/3}, \quad \Omega = 4.05 \mathcal{U}_u^{5/9} \quad (4.26c, d, e)$$

$$\beta = \Omega/\sqrt{(24)} = 0.827 \mathcal{U}_u^{5/9} \quad (4.26f)$$

while in the II_{1/n} approximation (4.11_{1/n}, 11_{2/n}, 25a) give

$$(n+1)(3n+2)/n = \Omega/\Psi\mathcal{U}_u = \Omega\omega/\alpha_0''\mathcal{U}_u \quad (4.27a)$$

$$(2n+1)(3n+1)/n = (\Omega/\Psi\mathcal{U}_u)[1 + \omega^{(n+1)/n}\alpha_0''/\alpha_0] \quad (4.27b)$$

$$\omega = \left[\frac{3n^2 - 1}{(n+1)(3n+2)} \alpha_0 \right]^{n/(n+1)} = \left[\frac{(3n^2 - 1)(n+1)^2(3n+2)^2}{6n^3} \mathcal{U}_u^2 \right]^{n/(4n+1)} \quad (4.27c)$$

$$\alpha_0 = \left[\frac{(n+1)^{2n+1} (3n+2)^{2n+1}}{(6^{1/3}n)^{n+1} (3n^2 - 1)^n} \right]^{3/(4n+1)} \mathcal{U}_u^{(2n+2)/(4n+1)} \quad (4.27d)$$

$$\beta = \Omega \left[\frac{n}{2(n+1)(3n+2)} \right]^{1/2} = \left[\frac{3n}{2(3n^2 - 1)} \right]^{n/(4n+1)} \left[\frac{(n+1)(3n+2)}{2n} \right]^{(1/2)/(4n+1)} \mathcal{U}_u^{(2n+1)/(4n+1)} \quad (4.27e)$$

If one regards α_0 as a fixed (independent of \mathcal{U}_u) constant, as in (4.21), then (4.25b, d) are replaced by

$$12 = \Omega/\Psi\mathcal{U}_u \quad (4.28a)$$

and this, in conjunction with (4.13, 24a) yields

$$\beta = \Omega/\sqrt{24} = \frac{1}{2}(\alpha_0\mathcal{U}_u/\sqrt{6})^{1/3} \quad (4.28b)$$

One notes from (4.24b) that, in first approximation, β_∞ rises at small undercoolings as $\mathcal{U}_u^{2/3}$, in contrast to the rigorous rise $\mathcal{U}_u^{1/2}$, equation (4.22a), whereas in second approximation, keeping α_0 as a *fixed* (independent of \mathcal{U}_u) constant, it rises [see (4.28b)] as $\mathcal{U}_u^{1/3}$. On the other hand, permitting variation of α_0 , the II₁ approximation (4.25h) furnishes an exponent 3/5, the II_‡ approximation (4.26f) furnishes 5/9, and the general II_{1/n} approximation (4.27e) furnishes the exponent $(2n+1)/(4n+1)$. Thus, the smaller $k = 1/n$, the closer we get to the rigorous asymptotic behavior $\mathcal{U}_u^{1/3}$; but the smaller (inferior) the multiplying numerical coefficient becomes. Thus, the asymptotic formula (4.26f) of II_‡ is superior to the asymptotic formula (4.25h) of II₁ only for $\mathcal{U}_u < 10^{-3}$, whereas taking also the nonasymptotic behavior into account, Fig. 1(a) reveals that II_‡ is persistently better than II₁; likewise II₀ is persistently better than II_‡; the one-term asymptotic formulas (4.27) are seen to become less and less adequate as $n = 1/k$ increases.

At the high end of the spectrum the approximations II₁, II_‡, II₀ are seen to be valid up to $\mathcal{U}_u^\dagger = 0.082, 0.165, 0.29373$, respectively; at these \mathcal{U}_u values, α_0'' passes through a zero. (Symbols \mathcal{U}_u^\dagger

and U_u^\dagger are used to denote the undercooling appropriate to $\alpha_0'' = 0$. The dagger is appended also to the corresponding Ω , ω , β_∞ values.) We have not explored what happens to the II approximations beyond \mathcal{U}_u^\dagger . However, we note that in the II₀ approximation the equations (4.20), at \mathcal{U}_u^\dagger , become

$$\left. \begin{aligned} \mathcal{E}\Omega^3 + 3\Omega^2 + 6\Omega + 6 &= \Omega^3/\mathcal{U}_u \\ 3\Omega^2 + 9\Omega + 11 &= \frac{\Omega/\mathcal{U}_u}{1 + \alpha_0''/\omega} \left[2\Omega + 1 + \frac{\alpha_0''}{\omega} \Omega^2 \ln \omega \right] \\ 3\Omega + 6 &= \frac{\Omega/\mathcal{U}_u}{1 + \alpha_0''/\omega} \left[1 + \frac{1}{2} \frac{\alpha_0''}{\omega} \Omega^2 \ln^2 \omega \right] \end{aligned} \right\} \quad (4.29^\circ, ', '')$$

It is seen that these equations are satisfied by

$$\alpha_0'' = \omega = \omega^{-1}\alpha_0'' = \omega^{-1}\alpha_0'' \ln \omega = 0 \quad (4.30a)$$

$$\frac{1}{2} \omega^{-1}\alpha_0'' \ln^2 \omega = \frac{\Omega(3 - 1/\mathcal{U}_u) + 6}{\Omega^3/\mathcal{U}_u} \quad (4.30b)$$

In other words, ω also passes through a zero at \mathcal{U}_u^\dagger (and beyond \mathcal{U}_u^\dagger it, presumably, becomes complex). The zero of ω is weaker than the zero of α_0'' , so that $\omega^{-1}\alpha_0'' \ln^2 \omega$ remains a finite number. Solution of (4.29^o, ') yields, for $\mathcal{E} = 1$, the pair of values

$$\mathcal{U}_u^\dagger = 0.29373, \quad \Omega^\dagger = 2.58585 \quad (4.31a)$$

and the corresponding β_∞ is obtained from (4.13) in the form

$$\text{I, II}_0: \quad \beta_\infty^\dagger = (\mathcal{U}_u^\dagger \Omega^\dagger / 2)^{1/2} = 0.61626 \quad (4.31b)$$

For comparison we also mention that for $\mathcal{U}_u = 0.29373$ one finds the rigorous value

$$\text{Rig:} \quad \beta_\infty = 0.6150 \quad (4.31c)$$

Thus, the II₀ and I approximations agree at \mathcal{U}_u^\dagger , and differ from the rigorous solution, in regard to the value of β_∞ , by 0.2 per cent. Since II₀ and I furnish values, which for $\mathcal{U}_u < \mathcal{U}_u^\dagger$ and $\mathcal{U}_u > \mathcal{U}_u^\dagger$, respectively, are indistinguishable on the graph paper from the rigorous solution, we have not concerned ourselves with an examination of the behavior of II₀ in the range $\mathcal{U}_u^\dagger < \mathcal{U}_u < 1$. Rather, we have decided to adopt II₀ as the approximate solution appropriate for $0 < \mathcal{U}_u \leq \mathcal{U}_u^\dagger$, and I as the solution appropriate for $\mathcal{U}_u^\dagger \lesssim \mathcal{U}_u < 1$.

For U_u close to 1 (more specifically, for $\Omega \gg 1$) the I approximation furnishes, on the basis of (4.29^o, 13), the estimate

$$\left. \begin{aligned} \Omega(1 + \epsilon) &= \frac{3U_u}{1 - U_u} \left(1 + \frac{2}{\Omega} + \frac{2}{\Omega^2} \right) \\ \beta_\infty &= \left[\frac{\Omega U_u}{2(1 + \epsilon)} \right]^{1/2} \simeq \frac{U_u}{1 + \epsilon} \sqrt{\left(\frac{3/2}{1 - U_u} \right)} \end{aligned} \right\} \quad (4.32)$$

In Table I are tabulated, for $\epsilon = 0.2, 0.1, 0, -0.1$, values of $\beta_\infty, \Omega, \alpha_0'', \omega$ vs \mathcal{U}_u in the II₀ approximation when $\mathcal{U}_u \leq \mathcal{U}_u^\dagger$, and values of β_∞, Ω vs U_u in the I approximation when $0.1 \leq U_u < 1.0$.

In what has preceded we have determined all the leading coefficients in (4.1); this involved determination of the solution of the non-linear algebraic (or transcendental) equations (4.11) [or (4.20)], as illustrated in Fig. 1. *All further coefficients of (4.1) are determined from successive linear equations [listed in (4.2_I, 2_B) and (4.2_O) or (4.18)], not more than 5 at a time.* [We regard the β coefficients as determined by the ν coefficients through (4.4).] Thus, in the II₁ approximation we solve for $\gamma_{1/2}$ in

Table 1. Fundamental parameters

Method	ϵ	$\Pi_0: \mathcal{U}_u$ I: U_u	β	Ω	ω	α_0''
Π_0	+ 0.2	10^{-5}	0.0 ² 222161	0.0138039	0.0133877	0.956769
		$10^{-9/2}$	0.0 ² 403373	0.0240356	0.0217249	0.928582
		10^{-4}	0.0 ² 729633	0.0415367	0.0347011	0.885537
		$10^{-7/2}$	0.0131356	0.0711414	0.0543233	0.823712
		10^{-3}	0.0235582	0.120856	0.0830068	0.740846
		$10^{-5/2}$	0.0422736	0.204696	0.123403	0.636521
		10^{-2}	0.0766249	0.349979	0.177931	0.509782
		$10^{-3/2}$	0.142818	0.619653	0.246316	0.353563
		0.08	0.246561	1.04398	0.297776	0.193276
		0.10	0.284036	1.20059	0.332780	0.149367
		0.12	0.320204	1.35364	0.330704	0.112838
		0.15	0.373180	1.58088	0.284523	0.0694170
		0.20	0.463809	1.96276	0.218861	0.0229372
		0.25	0.550686	2.35828	0.0990553	0.0 ² 315913
		0.32196	0.69297	2.9830	0	0
		I		0.1	0.220276	1.16452
	0.2		0.381733	1.74864		
	0.38635		0.69297	2.9830		
	0.4		0.717969	3.09287		
	0.6		1.16158	5.39711		
	0.8		1.98604	11.8330		
Π_0	+ 0.1	10^{-5}	0.0 ² 222161	0.0138039	0.0133877	0.956769
		$10^{-9/2}$	0.0 ² 403373	0.0240356	0.0217249	0.928582
		10^{-4}	0.0 ² 729631	0.0415366	0.0347012	0.885537
		$10^{-7/2}$	0.0131355	0.0711406	0.0543238	0.823713
		10^{-3}	0.0235575	0.120852	0.0830089	0.740848
		$10^{-5/2}$	0.0422698	0.204672	0.123412	0.636522
		10^{-2}	0.0766032	0.349853	0.177966	0.509755
		$10^{-3/2}$	0.142683	0.618917	0.246427	0.353296
		0.08	0.245890	1.04042	0.297684	0.191937
		0.10	0.283021	1.19517	0.302256	0.147462
		0.12	0.318762	1.31584	0.299373	0.110373
		0.15	0.370925	1.56834	0.280879	0.0662796
		0.20	0.456634	1.93778	0.206161	0.0197506
		0.25	0.543725	2.31231	0.0707413	0.0 ² 173772
		0.30638	0.64987	2.7569	0	0
		I		0.1	0.234884	1.21375
	0.2		0.408128	1.83725		
	0.33702		0.61987	2.7569		
	0.4		0.771090	3.27019		
	0.6		1.25319	5.75848		
	0.8		2.15355	12.7539		
Π_0	0	10^{-5}	0.0 ² 222161	0.0138039	0.0133877	0.956769
		$10^{-9/2}$	0.0 ² 403372	0.0240356	0.0217249	0.928582
		10^{-4}	0.0 ² 729628	0.0415364	0.0347013	0.885537
		$10^{-7/2}$	0.0131354	0.0711397	0.0543243	0.823714
		10^{-3}	0.0235568	0.120847	0.0830110	0.740849
		$10^{-5/2}$	0.0422660	0.204649	0.123421	0.636523
		10^{-2}	0.0765816	0.349728	0.178001	0.509728
		$10^{-3/2}$	0.142548	0.618184	0.246539	0.353031
		0.08	0.245226	1.03690	0.297593	0.190609

Table 1—continued

Method	ϵ	$\Pi_0: \mathcal{U}_u$ I: U_u	β	Ω	ω	a_0''
Π_0	0	0.10	0.282020	1.18984	0.301730	0.145579
		0.12	0.317345	1.33822	0.298027	0.107947
		0.15	0.368721	1.55612	0.277153	0.0632290
		0.20	0.452595	1.91368	0.192958	0.0168341
		0.25	0.537104	2.26849	0.0445722	0.0 ⁸ 809378
		0.28	0.590286	2.48410	0.0 ⁴ 83140	0.0 ⁶ 158509
		0.29373	0.61626	2.58585	0	0
I		0.1	0.252069	1.27078		
		0.2	0.439311	1.92994		
		0.29373	0.61626	2.58585		
		0.4	0.834244	3.47982		
		0.6	1.36262	6.18912		
		0.8	2.35431	13.8570		
Π_0	- 0.1	10 ⁻⁵	0.0 ² 222161	0.0138039	0.0133877	0.956769
		10 ^{-9/2}	0.0 ² 403372	0.0240355	0.0217249	0.928582
		10 ⁻⁴	0.0 ² 729626	0.0415362	0.0347014	0.885537
		10 ^{-7/2}	0.0131352	0.0711389	0.0543247	0.823714
		10 ⁻³	0.0235561	0.120843	0.0830131	0.740851
		10 ^{-5/2}	0.0422622	0.204625	0.123430	0.636524
		10 ⁻²	0.0765600	0.349602	0.178037	0.509701
		10 ^{-3/2}	0.142414	0.617454	0.246651	0.352767
		0.08	0.244569	1.03343	0.297503	0.189292
		0.10	0.281032	1.18460	0.301201	0.143717
		0.12	0.315953	1.33074	0.296665	0.105559
		0.15	0.366567	1.54422	0.273342	0.0602634
		0.20	0.448683	1.89041	0.179250	0.0141811
		0.25	0.530826	2.22669	0.0227865	0.0 ² 288175
		0.28310	0.58888	2.4499	0	0
		I		0.1	0.272629	1.33788
0.2	0.476800			2.04604		
0.25479	0.58888			2.4499		
0.4	0.910696			3.73215		
0.6	1.49576			6.71188		
0.8	2.59938			15.2028		

terms of $\nu_{1/2}$ from $\langle \tau^{-1/2} \rangle = 0$ of (4.2₇⁰); then from $\langle \tau^{-1/2} \rangle = 0$ of (4.2_B), $\langle \tau^0 \rangle = 0$ of (4.2₀⁰), $\langle \tau^{1/2} \rangle = 0$ of (4.2₀¹), $\langle \tau^1 \rangle = 0$ of (4.2₀²) we solve for $\nu_{1/2}$, $\alpha_{1/2}$, $\delta_{1/2}$, $\delta'_{1/2}$; and so on. We shall give in Section 7 the numerical values of these coefficients for nickel ($\epsilon = 0.06$) for $U_u = 0.025, 0.25$ in the Π_0 and I approximations.

5. SOLUTION FOR $\tau \ll 1$

We assume momentarily that $A^{(k)}$ in (3.6) have constant prescribed values

$$A = a_0, A'' = a''_0 = 1 - a_0, A''' = A'''' = \dots = 0 \tag{5.1}$$

Then, in the light of the initial conditions (3.11) and noting (3.8), we seek solution of (3.15) for $\tau \ll 1$ in the form

$$\left. \begin{aligned} \mathcal{R} &= 1 + b_{n_1} \tau^{n_1} + b_{n_2} \tau^{n_2} + \dots, \quad w = d_{r_1} \tau^{r_1} + d_{r_2} \tau^{r_2} + \dots, \quad w'' + d_{r_1}'' \tau^{r_1} + \dots \\ \mathcal{U}_C &= c_{p_1} \tau^{p_1} + c_{p_2} \tau^{p_2} + \dots, \quad \mathcal{U}_F = f_{s_1} \tau^{s_1} + f_{s_2} \tau^{s_2} + \dots, \quad l = l_{1/2} \tau^{1/2} + \dots \end{aligned} \right\} \quad (5.2)$$

Noting also (4.3) we stipulate

$$2 \leq n_1 < n_2 < \dots, \quad 0 < r_1 < r_2 < \dots, \quad 0 < p_1 < \dots, \quad 0 < s_1 < \dots \quad (5.3a, b, c, d)$$

[The condition $n_1 \geq 2$ arises from the requirement $\mathcal{U}_F(0) \neq \infty$.] Introducing these expansions into (3.15), the vanishing of the lowest τ powers in (3.15) [$\tau^{r_1+s_1-1}$ and $\tau^{s_1-r_1}$ in (3.15_O), τ^{p_1-1} and $\tau^{s_1-1/2}$ in (3.15_I), $\tau^{s_1-r_1}$ and τ^{n_1-1} in (3.15_B)] implies, respectively,

$$2r_1 - 1 = 0, \quad p_1 - \frac{1}{2} = s_1, \quad s_1 = r_1 + n_1 - 1 \quad (5.4)$$

[If r_1 were zero, then the first line in (3.15_O) would furnish τ^{s_1-1} terms, the others would furnish higher terms, and the coefficient of τ^{s_1-1} could not be made to vanish. Thus we cannot admit $0 \leq r_1$ as a possibility, but must insist on the stricter relation (5.3b).]

From (5.3, 4) it now follows that

$$r_1 = \frac{1}{2}, \quad p_1 - \frac{1}{2} = s_1 = n_1 - \frac{1}{2} \geq \frac{3}{2} \quad (5.5a)$$

$$\dot{\mathcal{U}}_C(0) = 0, \quad \dot{\mathcal{U}}_F(0) = 0 \quad (5.5b, c)$$

and from (4.3b) also that

$$\ddot{\mathcal{R}}(0) = 0 \quad (5.5d)$$

The value of R_0 has been left, so far, unspecified. If we choose

$$R_0 = R_n, \quad \text{i.e.} \quad \mathcal{R}_n = \mathcal{R}_0 = 1 \quad (5.6a)$$

then by (4.3a)

$$\dot{\mathcal{R}}(0) = 0 \quad (5.6b)$$

This implies that

$$n_1 > 2 \quad (5.6c)$$

On differentiating (3.15_O) we next find

$$\ddot{\mathcal{U}}_F(0) = 0, \quad s_1 > 2 \quad (5.7a)$$

and from (4.3b)

$$\ddot{\mathcal{R}}(0) = 0, \quad n_1 > 4 \quad (5.7b)$$

Similarly, one finds that all derivatives of $\mathcal{U}_F, \mathcal{R}$ vanish at $\tau = 0$. It follows that \mathcal{R}_n is a radius of neutral equilibrium of the nucleus. Once it is of this size it cannot grow or shrink without external disturbance. So we are prompted to choose for initial radius

$$R_0 > R_n, \quad \text{i.e.} \quad \mathcal{R}_n < \mathcal{R}_0 = 1 \quad (5.8)$$

Condition (5.8) implies that in (5.2) we must set

$$n_1 = 2 \quad (5.9a)$$

in order that we may satisfy (4.3a) at $\tau \rightarrow 0$ by choosing

$$b_2 = \frac{\mathcal{U}_u}{\mathcal{U}_d} \frac{\mathcal{R}_0 - \mathcal{R}_n}{2\mathcal{R}_0^3} = \frac{1}{2} \frac{\mathcal{U}_u}{\mathcal{U}_d} (1 - \mathcal{R}_n) \quad (5.9b)$$

From (5.5a) we correspondingly obtain

$$p_1 - \frac{1}{2} = s_1 = \frac{3}{2} \quad (5.10a)$$

and from (4.3b)

$$n_2 = \frac{7}{3} \quad (5.10b)$$

These considerations lead for $\tau \ll 1$ to the choice

$$\begin{aligned} \mathcal{R} &= 1 + b_2 \tau^2 + b_{7/2} \tau^{7/2} + b_4 \tau^4 + \dots, \quad w = d_{1/2} \tau^{1/2} + d_1 \tau + \dots, \quad w' = d'_{1/2} \tau^{1/2} + d'_1 \tau + \dots \\ \mathcal{U}_F &= f_{3/2} \tau^{3/2} + f_2 \tau^2 + \dots, \quad \mathcal{U}_C = c_2 \tau^2 + c_{5/2} \tau^{5/2} + \dots, \quad l = l_{1/2} \tau^{1/2} + l_1 \tau + \dots \\ A &= a_0 + a_{1/2} \tau^{1/2} + \dots, \quad A'' = a''_0 + a''_{1/2} \tau^{1/2} + \dots, \quad a_0 + a''_0 = 1, \quad a_{1/2} + a''_{1/2} = 0, \dots \end{aligned} \quad (5.11)$$

(We restrict ourselves to the second approximation.) The placement of (5.11) into (3.15) leads to the equations

$$\begin{aligned} \tau \left\langle \frac{2}{3} c_2 - f_{3/2} \left[\frac{\mathcal{K}}{l_{1/2}} - 2l_{1/2} \right] \right\rangle + \tau^{3/2} \left\langle \frac{5}{6} c_{5/2} + (c_2 - f_2) \left[\frac{\mathcal{K}}{l_{1/2}} - \frac{5}{2} l_{1/2} \right] \right. \\ \left. - f_{3/2} \left[\mathcal{K} \left(2 - \frac{l_1}{l_{1/2}^2} \right) - \frac{5}{2} l_1 + \frac{3.5}{2} l_{1/2}^2 \right] \right\rangle + \tau^2 \left\langle c_3 + (c_{5/2} - f_{5/2}) \left[\frac{\mathcal{K}}{l_{1/2}} - 3l_{1/2} \right] \right. \\ \left. + (c_2 - f_2) \left[\mathcal{K} \left(2 - \frac{l_1}{l_{1/2}^2} \right) - 3l_1 + 15l_{1/2}^2 \right] - f_{3/2} \left[\mathcal{K} \left(-\frac{l_{3/2}}{l_{1/2}^2} + \frac{l_1^2}{l_{1/2}^3} \right) \right. \right. \\ \left. \left. - 3l_{3/2} + 30l_1 l_{1/2} - 75l_{1/2}^3 \right] \right\rangle + \dots = 0 \quad (5.12a) \end{aligned}$$

$$\begin{aligned} \tau \left\langle \frac{1}{2} c_2 - f_{3/2} \left[\frac{\mathcal{K}}{l_{1/2}} - 2l_{1/2} \right] \right\rangle + \tau^{3/2} \left\langle \frac{5}{6} c_{5/2} + (c_2 - f_2) \left[\frac{\mathcal{K}}{l_{1/2}} - \frac{5}{2} l_{1/2} \right] - f_{3/2} \left[\mathcal{K} \left(1 - \frac{l_1}{l_{1/2}^2} \right) \right. \right. \\ \left. \left. - \frac{5}{2} l_1 + 15l_{1/2}^2 \right] \right\rangle + \dots = 0 \quad (5.12b) \end{aligned}$$

$$\begin{aligned} \tau \left\langle 2b_2 - f_{3/2} \left[\frac{K}{l_{1/2}} + \frac{a_0}{d_{1/2}} + \frac{a''_0}{d'_{1/2}} \right] \right\rangle + \tau^{3/2} \left\langle K \left[\frac{c_2 - f_2}{l_{1/2}} - f_{3/2} \left(2 - \frac{l_1}{l_{1/2}^2} \right) \right] \right. \\ \left. - \left\{ \frac{f_2 a_0 + f_{3/2} a_{1/2}}{d_{1/2}} \right\} - \{ \}'' + f_{3/2} \left[a_0 \frac{d_1}{d_{1/2}^2} + a''_0 \frac{d'_1}{d'_{1/2}^2} \right] \right\rangle + \tau^2 \left\langle K \left[\frac{c_{5/2} - f_{5/2}}{l_{1/2}} \right. \right. \\ \left. \left. + (c_2 - f_2) \left(2 - \frac{l_1}{l_{1/2}^2} \right) + f_{3/2} \left(\frac{l_{3/2}}{l_{1/2}^2} - \frac{l_1^2}{l_{1/2}^3} \right) \right] - \left\{ \frac{f_{5/2} a_0 + f_2 a_{1/2} + f_{3/2} a_1}{l_1} \right\} - \{ \}'' \right. \\ \left. + (f_2 a_0 + f_{3/2} a_{1/2}) \left(\frac{d_1}{d_{1/2}^2} \right) + ()'' ()'' + (f_{3/2} a_0) \left(\frac{d_{3/2}}{d_{1/2}^2} - \frac{d_1^2}{d_{1/2}^3} \right) + ()'' ()'' \right\rangle + \dots = 0 \quad (5.12B) \end{aligned}$$

$$\begin{aligned}
& f_{3/2} \tau^{(k+2)/2} \left\langle [a_0 d_{1/2}^k] \left[\frac{k+4}{2} d_{1/2} - \frac{1}{d_{1/2}} \right] + []'' []'' \right\rangle + f_{3/2} \tau^{(k+3)/2} \left\langle [a_0 d_{1/2}^k] \right. \\
& \left. \left[(k+1)(k+5) d_{1/2}^2 + \frac{(k+1)(k+5)}{2} d_1 + (1-k) \frac{d_1}{d_{1/2}^2} - 2k \right] + []'' []'' + [(a_{1/2} + a_0 f_2/f_{3/2}) d_{1/2}^k] \right. \\
& \left. \left[\frac{k+5}{2} d_{1/2} - \frac{1}{d_{1/2}} \right] + []'' []'' \right\rangle + f_{3/2} \tau^{(k+4)/2} \left\langle [a_0 d_{1/2}^k] [(k+1)(k+2)(k+6) d_1 d_{1/2} \right. \\
& + \frac{1}{2} (k+1)(k+2)(k+6) d_{1/2}^3 + \frac{1}{2} (k+1)(k+6) d_{3/2} \\
& + \frac{1}{4} k(k+1)(k+6) \frac{d_1^2}{d_{1/2}} + (1-k) \frac{d_{3/2}}{d_{1/2}^2} - (1-k)(2-k) \frac{d_1^2}{d_{1/2}^3} \\
& - 2k^2 \frac{d_1}{d_{1/2}} - k(k+1) d_{1/2}] + []'' []'' + [(a_{1/2} + a_0 f_2/f_{3/2}) d_{1/2}^k] \left[(k+1)(k+6) d_{1/2}^2 \right. \\
& + \frac{1}{2} (k+1)(k+6) d_1 + (1-k) \frac{d_1}{d_{1/2}^2} - 2k \left. \right] + []'' []'' + \left[\left(a_1 + a_{1/2} \frac{f_2}{f_{3/2}} + a_0 \frac{f_{5/2}}{f_{3/2}} \right) d_{1/2}^k \right] \\
& \left. \left[\frac{k+6}{2} d_{1/2} - \frac{1}{d_{1/2}} \right] + []'' []'' \right\rangle + \dots = 0 \quad (5.12^k)
\end{aligned}$$

Expressions (5.11) can be solution of (3.15) only when each $\langle \tau^k \rangle$ in (5.12) vanishes. Because b_2 is a fixed quantity (5.9b), and since the f_k , b_k coefficients are related by virtue of (5.11), (4.3) by

$$f_{3/2} = -\frac{3}{4} \mathcal{U}_d b_{7/2}, \quad f_2 = \mathcal{U}_u \mathcal{R}_n b_2 - 12 [b_4 + (1 + \epsilon/6) b_2^2] \mathcal{U}_d,$$

$$f_{5/2} = -\frac{6}{4} \mathcal{U}_d b_{9/2}, \quad f_3 = -20 \mathcal{U}_d b_5, \dots \quad (5.13)$$

the coefficients b_k may be regarded as known quantities, and the equations (5.12_I), (5.12_B), (5.12_O); $j = 0, 1$; $k = 0, m, 2m$ constitute six sets of equations in the six sets of unknowns $c_n, l_n, f_n, d_n, a_n'', d_n''$.

From (5.12_B) we find, noting (5.9b, 16a) and Fig. 2 that the leading coefficient of the \mathcal{U}_F series

$$f_{3/2} = 2b_2 \left\{ \frac{\bar{K}}{l_{1/2}} + \frac{a_0}{d_{1/2}} + \frac{a_0''}{d_{1/2}'} \right\} \quad (5.14a)$$

is a positive quantity. In the I, II₀ approximations it has, by (5.16a, 19, 25) the value

$$\left. \begin{aligned}
\text{I: } & f_{3/2} = 2b_2 / \{ (\sqrt{2}) + \bar{K} \sqrt{(2/\mathcal{K})} \} \\
\text{II}_0: & f_{3/2} = 2b_2 / \{ \frac{3}{2} + \bar{K} \sqrt{(2/\mathcal{K})} \}
\end{aligned} \right\} \quad (5.14b)$$

The vanishing of $\langle \tau \rangle$ in (5.12_I, 1) implies

$$c_2 = 0 \quad (5.15)$$

$$l_{1/2} = \sqrt{(\mathcal{K}/2)} \quad (5.16a)$$

On taking the difference of the $\langle \tau^{3/2} \rangle$ expressions in (5.12_I, 1) we next obtain

$$\frac{5}{24} c_{5/2} = -\frac{1}{4} f_{3/2} \mathcal{K} < 0$$

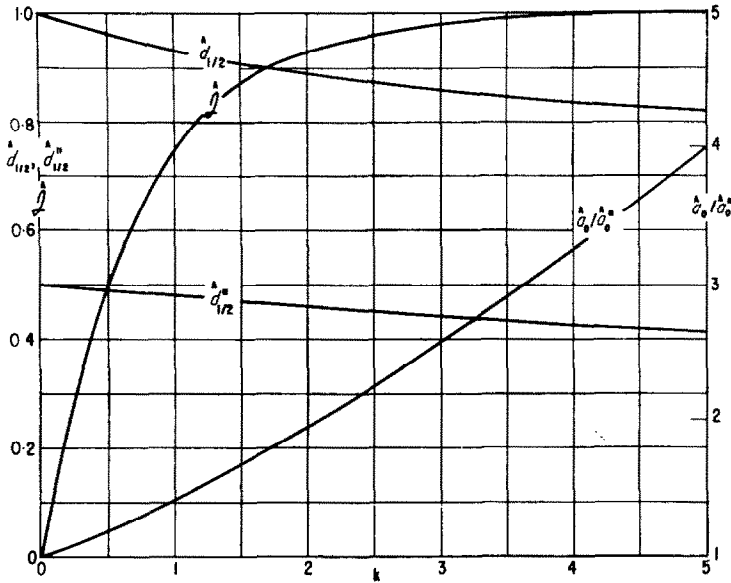


FIG. 2. The degree of inconsistency, \mathcal{S} , of the ascending power series solution Π_k .

i.e. we find that, according to the present model, the nucleus center temperature begins to decrease as the surface temperature starts to increase, in violation of the second law of thermodynamics. For this reason we are prompted to assume that $l(\tau)$ is a completely determined function

$$l(\tau) = l_{1/2} \tau^{1/2}, \quad l_{1/2} = \sqrt{\mathcal{K}/2}, \quad l_1 = l_{3/2} = \dots \equiv 0 \tag{5.16b}$$

This permits us to discard (5.12₁'), and we obtain from the relation (5.12₀') that

$$\frac{c_{5/2}}{f_{3/2}} = \frac{99}{10} \mathcal{K} - \frac{3}{10} \sqrt{2\mathcal{K}} \frac{f_2}{f_{3/2}} \tag{5.17a}$$

where, in the light of (5.28, 29), $c_{5/2}$ is seen to be a positive quantity. In the I, Π_0 approximations its value is

$$\left. \begin{aligned} \text{I:} \quad \frac{c_{5/2}}{f_{3/2}} &= 9.9 \mathcal{K} + \frac{1/3 + 3/5 R}{10/9 + R/\sqrt{\mathcal{K}}} \sqrt{\mathcal{K}} \\ \text{II}_0: \quad \frac{c_{5/2}}{f_{3/2}} &= 9.9 \mathcal{K} + \frac{0.302512 + 3R/5}{1.065632 + R/\sqrt{\mathcal{K}}} \sqrt{\mathcal{K}} \end{aligned} \right\} \tag{5.17b}$$

The time dependence (5.16b) of $l(\tau)$ leads to the surface gradient

$$\partial U / \partial \xi |_{\mathcal{R}=0} = (2 + \sqrt{2/\mathcal{K}} \tau) (U_F - U_C) \tag{5.18}$$

of the temperature (3.6b), which is consistent with the infinite gradient (3.8) at $\tau \rightarrow 0$, and also with the expected behavior ($\rightarrow 0$) at $\tau \gg 1$. Equations (3.6b), (5.16, 17) constitute a significant improvement over former approaches that regarded the frozen nucleus as isothermal.

The equations $\langle \tau^{1+k/2} \rangle = 0$ of (5.12₀) create a greater dilemma. If we restrict ourselves to the first

approximation, $A = 1$, $A'' = A''' = \dots = 0$, and correspondingly retain only (12_0^0) , then $\langle \tau \rangle = 0$ furnishes

$$a_0 = 1: \quad d_{1/2} = 1/\sqrt{2} \tag{5.19}$$

But if we permit both A and A'' terms to appear and, accordingly, retain the three equations $(12_0^0, k, 2k)$, then it is found that the lead-off terms in these equations

$$\langle \tau \rangle = 0, \quad \langle \tau^{1+k/2} \rangle = 0, \quad \langle \tau^{1+k} \rangle = 0 \tag{5.20^0, ', ''}$$

respectively, are inconsistent; they cannot be solved for $d_{1/2}, d''_{1/2}, a''_0$. [The implication of this is: at small times (3.15₀) cannot be solved in the form of (5.11), by restricting oneself to expansions in half powers of τ ; logarithmic terms or perhaps other types of fractional powers should also be included; this question has not been explored.]

One may define a measure of the inconsistency. We may vary d and d'' in the three expressions (5.20^{0, ', ''}) [we omit the subscript $\frac{1}{2}$ of $d_{1/2}, d''_{1/2}$ in (5.21–27) for the sake of more convenient writing; the ratios ρ^0, ρ', ρ'' are not to be confused with the symbol ρ of density]:

$$\left. \begin{aligned} -\frac{a_0}{a''_0} &= \frac{d''(2 - 1/d''^2)}{d(2 - 1/d^2)} \equiv -\rho^0 \\ -\frac{a_0}{a''_0} &= \frac{d''^{1+k}(2 + k/2 - 1/d''^2)}{d^{1+k}(2 + k/2 - 1/d^2)} \equiv -\rho' \\ -\frac{a_0}{a''_0} &= \frac{d''^{1+2k}(2 + k - 1/d''^2)}{d^{1+2k}(2 + k - 1/d^2)} \equiv -\rho'' \end{aligned} \right\} \tag{5.21^0, ', ''}$$

and determine \hat{d}, \hat{d}'' from the requirement

$$\mathcal{J}(d, d'') = \left| \frac{\rho^0 - \rho'}{\rho^0} \right| = \text{minimum} \tag{5.22}$$

We regard this choice \hat{d}, \hat{d}'' (and the corresponding ratio $\hat{a}_0/\hat{a}''_0 \equiv \hat{\rho}^0$) of d, d'' (and a_0/a''_0) as the *least inconsistent choice* for the given k , and define the minimum degree of inconsistency as

$$\hat{\mathcal{J}} \equiv \mathcal{J}(\hat{d}, \hat{d}'') = [1 - \rho'/\rho^0]_{\min} \tag{5.23}$$

Clearly, in order that the ratio \hat{a}_0/\hat{a}''_0 be positive, it is necessary that \hat{d}, \hat{d}'' straddle the value $1/\sqrt{2}$. The value greater than $1/\sqrt{2}$ will be labeled \hat{d} , the value smaller than $1/\sqrt{2}$ will be labeled \hat{d}'' , in accordance with our convention in (3.6a) and elsewhere to let w (and thus d) be associated with the dominating temperature term. One finds that \mathcal{J} is minimized by

$$\left. \begin{aligned} \hat{d}^2 &= \frac{5 + \frac{1}{2}k + (9 + k + k^2/4)^{1/2}}{2(4 + k)}, \quad \hat{d}''^2 = \frac{5 + \frac{1}{2}k - (9 + k + k^2/4)^{1/2}}{2(4 + k)} \\ \hat{d} &= 1 - \frac{k}{12} + \frac{34k^2}{12^3} + \dots, \quad \hat{d}'' = \frac{1}{2} \left(1 - \frac{k}{24} + \frac{k^2/2}{12^3} + \dots \right) \end{aligned} \right\} \tag{5.24}$$

and that

$$\frac{\hat{a}_0}{1 - \hat{a}_0} = \frac{\hat{a}_0}{\hat{a}''_0} = 1 + \frac{3k}{8} + \frac{74k^2}{12^3} + \dots, \quad \hat{\mathcal{J}} = 1.4432k - 1.1351k^2 + \dots$$

For $k = 0$ these relations specialize to

$$\hat{d} = 1, \quad \hat{d}'' = \frac{1}{2}, \quad \hat{a}_0 = \hat{a}''_0 = \frac{1}{2}, \quad \hat{\mathcal{J}} = 0 \tag{5.25}$$

In Fig. 2 we plot $\hat{d}_{1/2}$, $\hat{d}_{1/2}''$, \hat{a}_0/\hat{a}_0'' and \mathcal{J} vs k . It is seen that as $k \rightarrow 0$ the inconsistency disappears. This then indicates that, in contrast with the general case of Π_k , an ascending power series solution in $\tau^{1/2}$, nevertheless, does exist for the special case of Π_0 .

Once the solution (5.25) of the equation $\langle \tau \rangle = 0$ of (5.12₀) is available, determination of the higher coefficients d_n , d_n'' , a_n'' of the Π_0 solution proceeds by the method of (4.15–17). Accordingly, (5.12₀) must be replaced by

$$\left. \begin{aligned} \tau \langle {}^\circ C_1 + {}^\circ C_1' \rangle + \tau^{3/2} \langle {}^\circ C_{3/2} + {}^\circ C_{3/2}' \rangle + \tau^2 \langle {}^\circ C_2 + {}^\circ C_2' \rangle + \dots = 0 \\ \tau \langle {}' C_1 + {}^\circ C_1 \ln d + {}' C_1' + {}^\circ C_1' \ln d'' \rangle + \tau^{3/2} \langle {}' C_{3/2} + {}^\circ C_{3/2} \ln d + {}' C_{3/2}' \\ \quad + {}^\circ C_{3/2}' \ln d'' \rangle + \dots = 0 \\ \tau \langle {}'' C_1 + {}' C_1 \ln d + \frac{1}{2} {}^\circ C_1 \ln^2 d + {}'' C_1' + {}' C_1' \ln d'' + \frac{1}{2} {}^\circ C_1' \ln^2 d'' \rangle \\ \quad + \tau^{3/2} \langle {}'' C_{3/2} + {}' C_{3/2} \ln d + \frac{1}{2} {}^\circ C_{3/2} \ln^2 d + {}'' C_{3/2}' + {}' C_{3/2}' \ln d'' \\ \quad + \frac{1}{2} {}^\circ C_{3/2}' \ln^2 d'' \rangle + \dots = 0 \end{aligned} \right\} \quad (5.26^{\circ}, ', '')$$

$$\left. \begin{aligned} {}^\circ C_1 = a_0 \left\{ 2d - \frac{1}{d} \right\}, \quad {}' C_1 = \frac{1}{2} da_0, \quad {}'' C_1 = 0 \\ {}^\circ C_{3/2} = a_0 \left\{ \frac{5}{2} d_1 + 5d^2 + \frac{d_1}{d^2} \right\} + (a_{1/2} + a_0 f_2/f_{3/2}) \left\{ \frac{5}{2} d - \frac{1}{d} \right\} \\ {}' C_{3/2} = a_0 \left\{ 3d_1 + 6d^2 - \frac{d_1}{d^2} - 2 \right\} + (a_{1/2} + a_0 f_2/f_{3/2}) \frac{d}{2}, \quad {}'' C_{3/2} = a_0 \left\{ \frac{1}{2} d_1 + d^2 \right\} \end{aligned} \right\} \quad (5.27)$$

$$\begin{aligned} {}^\circ C_2 = a_0 \left\{ 3d_{3/2} + 12d_1d + 6d^3 + \frac{d_{3/2}}{d^2} - 2\frac{d_1^2}{d^3} \right\} + (a_{1/2} + a_0 f_2/f_{3/2}) \left\{ 3d_1 + 6d^2 + \frac{d_1}{d^2} \right\} \\ + \left(a_1 + a_{1/2} \frac{f_2}{f_{3/2}} + a_0 \frac{f_{5/2}}{f_{3/2}} \right) \left\{ 3d - \frac{1}{d} \right\} \end{aligned}$$

$$\begin{aligned} {}' C_2 = a_0 \left\{ \frac{7}{2} d_{3/2} + 20d_1d + 10d^3 + \frac{3}{2} \frac{d_1^2}{d} - \frac{d_{3/2}}{d^2} + 3\frac{d_1^2}{d^3} - d \right\} \\ + (a_{1/2} + a_0 f_2/f_{3/2}) \left\{ \frac{7}{2} d_1 + 7d^2 - \frac{d_1}{d^2} - 2 \right\} + \left(a_1 + a_{1/2} \frac{f_2}{f_{3/2}} + a_0 \frac{f_{5/2}}{f_{3/2}} \right) \frac{d}{2} \end{aligned}$$

$${}'' C_2 = a_0 \left\{ \frac{1}{2} d_{3/2} + 9d_1d + \frac{9}{2} d^3 + \frac{7}{4} \frac{d_1^2}{d} - \frac{d_{3/2}}{d^2} - 2\frac{d_1}{d} - d \right\} + (a_{1/2} + a_0 f_2/f_{3/2}) \left\{ \frac{1}{2} d_1 + d^2 \right\}$$

As was pointed out earlier, in connection with (5.20), the equations $\langle \tau^1 \rangle = 0$ of (5.26) are inconsistent; their solution (5.25) in the limit $k \rightarrow 0$ must be determined in the fashion of (5.21–24). But once (5.25) is available and is introduced into the C_n , $n \geq 3/2$, the remaining equations $\langle \tau_n \rangle = 0$, $n \geq 3/2$ are found to be consistent. The parameters $a_{1/2}'$, d_1 , d_1'' ; a_1'' , $d_{3/2}$, $d_{3/2}''$; . . . are determined from $\langle \tau^{3/2} \rangle = 0$, $\langle \tau^2 \rangle = 0$, . . . as expressions in $f_2/f_{3/2}$, $f_{5/2}/f_{3/2}$, . . .; the latter quantities are then determined from (5.12_B). In this fashion one finds

$$\begin{aligned}
 \text{I: } \quad d_1 &= -\frac{5}{9} - \frac{\sqrt{2} f_2}{18 f_{3/2}}, \quad \frac{f_2}{f_{3/2}} = -\frac{1}{\sqrt{2}} \frac{10/9 + 2K}{10/9 + K/\sqrt{\mathcal{K}}} \\
 d_{3/2} &= \frac{497}{810} \sqrt{2} + \frac{76}{405} \frac{f_2}{f_{3/2}} + \frac{49}{810} \sqrt{2} \frac{f_2^2}{f_{3/2}^2} - \frac{\sqrt{2} f_{5/2}}{10 f_{3/2}} \\
 \frac{f_{5/2}}{f_{3/2}} &= \frac{\frac{247}{405} + \frac{99}{10} K(\sqrt{\mathcal{K}}) - \sqrt{2} \left(\frac{199}{405} + \frac{13}{10} K \right) \frac{f_2}{f_{3/2}} - \frac{1}{405} \frac{f_2^2}{f_{3/2}^2}}{6/5 + K/\sqrt{\mathcal{K}}}
 \end{aligned} \quad (5.28)$$

$$\begin{aligned}
 \text{II}_0: \quad d_1 &= \frac{-[128 + 226 \ln 2 + 176 \ln^2 2] - [12 + 4 \ln 2 - 21 \ln^2 2] f_2/f_{3/2}}{60 + 91 \ln 2 + 40.5 \ln^2 2} \\
 &= -2.5734689 - 0.0328557 \frac{f_2}{f_{3/2}} \\
 d_1'' &= \frac{-[22 + 65.5 \ln 2 + 38.25 \ln^2 2] + [12 + 28 \ln 2 + 15 \ln^2 2] f_2/f_{3/2}}{60 + 91 \ln 2 + 40.5 \ln^2 2} \\
 &= -0.60180744 + 0.27091582 \frac{f_2}{f_{3/2}} \\
 -a_{1/2} &= a_{1/2}'' = -1.4819755 + 0.5324351 \frac{f_2}{f_{3/2}}, \quad \frac{f_2}{f_{3/2}} = -\frac{1}{\sqrt{2}} \frac{1.008373 + 2K}{1.065632 + K/\sqrt{\mathcal{K}}} \\
 d_{3/2} &= 15.167308 - 3.748830 \frac{f_2}{f_{3/2}} + 0.997599 \frac{f_2^2}{f_{3/2}^2} + 0.0886061 \frac{f_{5/2}}{f_{3/2}} \\
 d_{3/2}'' &= 5.144726 - 2.509527 \frac{f_2}{f_{3/2}} + 0.504992 \frac{f_2^2}{f_{3/2}^2} + 0.273480 \frac{f_{5/2}}{f_{3/2}} \\
 -a_1 &= a_1'' = 9.042587 - 6.074998 \frac{f_2}{f_{3/2}} + 1.522209 \frac{f_2^2}{f_{3/2}^2} + 0.753757 \frac{f_{5/2}}{f_{3/2}} \\
 \frac{f_{5/2}}{f_{3/2}} &= \frac{2.704046 + 9.9 K(\sqrt{\mathcal{K}}) - (1.536703 + 1.838478 K) f_2/f_{3/2} + 0.197916 f_2^2/f_{3/2}^2}{1.175561 + K/\sqrt{\mathcal{K}}}
 \end{aligned} \quad (5.29)$$

The formula

$$\frac{c_3}{f_{3/2}} = -\frac{75}{4} \sqrt{2\mathcal{K}^3} + \frac{19}{2} \mathcal{K} \frac{f_2}{f_{3/2}} - \left(\sqrt{\frac{\mathcal{K}}{2}} \right) \frac{f_{5/2} - c_{5/2}}{f_{3/2}} \quad (5.30)$$

holds for both I and II; in fact, for all approximations.

For the special case

$$K = \mathcal{K} = 1 \quad (5.31)$$

we obtain

$$\begin{aligned}
 \text{I: } \quad d_{1/2} &= 0.707107, \quad d_1 = -0.473684, \quad d_{3/2} = -0.080042, \quad f_{3/2} = 0.707107b_2, \\
 f_2/f_{3/2} &= -1.042052, \quad f_{5/2}/f_{3/2} = 5.975951, \quad c_{5/2}/f_{3/2} = 10.34210, \\
 c_{3/2}/f_{3/2} &= -33.3287
 \end{aligned} \quad (5.32a)$$

$$\left. \begin{aligned} \text{II}_0: \quad a_0 = a''_0 = \frac{1}{2}, \quad -a_{1/2} = a''_{1/2} = -2.030291, \quad -a_1 = a''_1 = 22.556996, \\ d_{1/2} = 1, \quad d''_{1/2} = \frac{1}{2}, \quad d_1 = -2.539633, \quad d''_1 = -0.880804, \quad d_{3/2} = 20.749393, \\ d''_{3/2} = 10.312385, \quad f_{3/2} = 0.686291 b_2, \quad f_2/f_{3/2} = -1.029826, \\ f_{5/2}/f_{3/2} = 7.487628, \quad c_{5/2}/f_{3/2} = 10.33692, \quad c_3/f_{3/2} = -34.2851 \end{aligned} \right\} \quad (5.32b)$$

and by (5.13)

$$\text{I:} \quad b_{7/2} = -0.0808122 \frac{b_2}{\mathcal{U}_d}, \quad \frac{b_4}{b_2} = \frac{\mathcal{U}_u \mathcal{R}_n + 0.736842}{12 \mathcal{U}_d} - \left(1 + \frac{\epsilon}{6}\right) b_2, \quad b_{9/2} = -0.268294 \frac{b_2}{\mathcal{U}_d} \quad (5.33a)$$

$$\text{II}_0: \quad b_{7/2} = -0.0784333 \frac{b_2}{\mathcal{U}_d}, \quad \frac{b_4}{b_2} = \frac{\mathcal{U}_u \mathcal{R}_n + 0.706761}{12 \mathcal{U}_d} - \left(1 + \frac{\epsilon}{6}\right) b_2, \quad b_{9/2} = -0.326266 \frac{b_2}{\mathcal{U}_d} \quad (5.33b)$$

We could, if we wanted, adopt an approximate solution to the general II_k problem at small times, using the least incompatible values represented in Fig. 2, and then determining the rest of the d_n , d''_n , a_n coefficients from the higher equations $\langle \tau^m \rangle = 0$ in (5.12 $_0^k$). However, in the light of the availability of the accurately determined, simpler, and—by Fig. 1—much better II_0 solution, there is no incentive to carry out such computations. All our work, henceforth, will be based on the I and II_0 solutions.

The closeness of the I and II_0 expressions (5.32a, b) and (5.33a, b) of f_n and b_n suggests that the ascending solutions I, II_0 are probably very good representations of the true solution.

We list below the pertinent expressions also in the “simplified” I approximation when the additional approximation is made that the nucleus is isothermal:

$$U_C = U_F \quad (5.34)$$

Then the inside equations (2.20), (3.15 $_I$), (5.12 $_I$) are to be omitted; in (2.19), (3.15 $_B$), (5.12 $_B$) the \mathcal{K} terms (which represent the U_C effect) are to be omitted, and (5.32a), (5.33a) are to be replaced by

$$\left. \begin{aligned} d_{1/2} = 1/\sqrt{2}, \quad d_1 = -\frac{1}{2}, \quad d_{3/2} = 11(\sqrt{2})/24 \\ f_{3/2} = (\sqrt{2}) b_2, \quad f_2/f_{3/2} = -1/\sqrt{2}, \quad f_{5/2}/f_{3/2} = 11/12 \\ b_{7/2} = -\frac{4\sqrt{2}}{35} \frac{b_2}{\mathcal{U}_d}, \quad \frac{b_4}{b_2} = \frac{\mathcal{U}_u \mathcal{R}_n + 1}{12 \mathcal{U}_d} - \left(1 + \frac{\epsilon}{2}\right) b_2, \quad b_{9/2} = -\frac{11\sqrt{2}}{189} \frac{b_2}{\mathcal{U}_d} \end{aligned} \right\} \quad (5.35)$$

6. CRITICAL RADII

We have introduced previously—in (2.13)—a critical radius, the nucleation radius \mathcal{R}_n which, according to (5.8), delineates the initial nuclei sizes for which growth will or will not occur. Another critical nucleus radius

$$\mathcal{R}_v = 1 + b_2 \tau_v^2 + b_{7/2} \tau_v^{7/2} + b_4 \tau_v^4 + \dots \quad (6.1)$$

characterizes the growing nucleus at the instant τ_v at which the inflow velocity (for $\epsilon > 0$, outflow velocity for $\epsilon < 0$) is a maximum. By (2.7) the inflow velocity is largest at the freezing front, where its value

$$-u_F = \epsilon \dot{R} \quad (6.2a)$$

reaches a maximum at time τ_v for which

$$\ddot{\mathcal{R}} = 2 b_2 + \frac{35}{4} b_{7/2} \tau^{3/2} + 12 b_4 \tau^2 + \frac{63}{4} \tau^{5/2} + \dots = 0 \quad (6.2b)$$

Since according to (5.9b, 13, 14)

$$-\frac{8}{35} \frac{b_2}{b_{7/2}} = \left\{ K\sqrt{(2/\mathcal{K})} + \frac{a_0}{d_{1/2}} + \frac{a_0''}{d_{1/2}''} + \dots \right\} \mathcal{U}_a = m^{3/2} \mathcal{U}_a \quad (6.3a)$$

$$m^{3/2} = \left. \begin{array}{l} (\sqrt{2}) + K\sqrt{(2/\mathcal{K})}, \quad \text{I} \\ \frac{3}{2} + K\sqrt{(2/\mathcal{K})}, \quad \text{II}_0 \end{array} \right\} \quad (6.3b)$$

the solution of (6.2b) leads to

$$\tau_v = \left[-\frac{4/35}{b_{7/2}} \left(2 b_2 + 12 b_4 \tau_v^2 + \frac{63}{4} b_{9/2} \tau_v^{5/2} + \dots \right) \right]^{2/3} = m' \mathcal{U}_a^{2/3} \quad (6.4a)$$

$$m' = m \left\{ 1 + 6 \frac{b_4}{b_2} \tau_v^2 + \frac{63}{8} \frac{b_{9/2}}{b_2} \tau_v^{5/2} + \dots \right\}^{2/3}$$

$$\simeq \begin{cases} m \left[1 + 3 \frac{b_4}{b_2} \tau_v^2 \right]^{2/3}, & \text{for } 6 b_4 \tau_v^2 / b_2 = \text{smallest term} \\ m \left[1 + 6 \frac{b_4}{b_2} \tau_v^2 + \frac{63}{16} \frac{b_{9/2}}{b_2} \tau_v^{5/2} \right]^{2/3}, & \text{for } \frac{63}{8} \left| \frac{b_{9/2}}{b_2} \right| \tau_v^{5/2} = \text{smallest term} \end{cases} \quad (6.4b, 6.4c)$$

The (6.4b) expression of m' is based on the observation that the smallest term in the $\{ \}^{2/3}$ expression is, in most of our range of interest, the $6b_4\tau_v/b_2$ term; and in a semiconvergent expansion it is found most expeditious (cf. Lanczos, p. 5 of reference [15]) to carry the expansion up to the term preceding the smallest term, and add on the smallest term with half weight. The expression $m\mathcal{U}_a^{2/3}$ is a first estimate for τ_v ; it may be improved by multiplying this by the correction factor $\{ \}^{2/3}$ into which the foregoing first estimate is first inserted. Roughly, we can say, when $K = \mathcal{K} = 1$, that

$$\tau_v = 2' \mathcal{U}_a^{2/3} \quad (2' = \text{a trifle larger than } 2) \dagger \quad (6.4d)$$

Further critical radii \mathcal{R}_M [or \mathcal{R}_m ; see (6.7, 8)] and \mathcal{R}_c relate to the condition of maximum negative pressure and zero pressure at the front, respectively. The pressure in the liquid may be written, by (2.8b, 22), in the form

$$p = p_\infty - \epsilon \frac{\mathcal{R}}{\xi} \left[\mathcal{R} \ddot{\mathcal{R}} + \left(2 + \frac{\epsilon}{2} \frac{\mathcal{R}^3}{\xi^3} \right) \mathcal{R}^2 \right] \quad (6.5a)$$

At the front $\xi = \mathcal{R}$, using (5.11), this becomes

$$p_F = p_\infty - 2\epsilon b_2 \left[1 + \frac{35}{8} \frac{b_{7/2}}{b_2} \tau^{3/2} + \left\{ (5 + \epsilon) b_2 + 6 \frac{b_4}{b_2} \right\} \tau^2 + \dots \right] \quad (6.5b)$$

Calculated curves for \mathcal{R} , $\dot{\mathcal{R}}$, $\ddot{\mathcal{R}}$, in the case of nickel, are shown in Figs. 4-9. \mathcal{R} starts out with a large positive value at $\tau = 0$, passes through a zero at τ_v ; then, depending on the imposed undercooling U_u , it may (or may not) fluctuate about 0; finally it approaches zero through negative values.

† Quite a bit larger than 2 for large undercoolings.

Ensuing possibilities for p_F are sketched, for the case $\epsilon > 0$ (to which we will, henceforth, restrict ourselves), in Fig. 3. Curve *a* illustrates the case of *exceedingly large undercooling*, when in (6.5a)

$$(2 + \epsilon/2)\dot{\mathcal{R}}_v^2 \geq \ddot{\mathcal{R}}(0) [\dot{\mathcal{R}}_v \equiv \dot{\mathcal{R}}(\tau_v)] \tag{6.6a}$$

In this case the tension at the front, $-p_F$, increases up to $-p_m$, at t_m , shortly before t_v , and then it decays slowly to $-p_\infty = -1$ atm, passing through the zero value at some large time t_c . Curve *b* illustrates that case of *large undercooling* where the maximum, $-p_m$, of $-p_F$ near t_v does not quite reach the initial maximum $-p_M$. [Subscripts *m* and *M* are used to refer to the maximum tension condition in accordance with (6.6a), (6.6b); since τ_m nearly coincides with τ_v the simpler estimates

$$\tau_m \simeq \tau_v, -p_m \simeq -p_v = -p_\infty + 2\epsilon(1 + \epsilon/4)\dot{\mathcal{R}}_v^2 \tag{6.7}$$

may be adopted for this case.] When

$$(2 + \epsilon/2)\dot{\mathcal{R}}_v^2 < \ddot{\mathcal{R}}(0) \tag{6.6b}$$

then the initial tension is the maximum. In this case, therefore

$$\tau_M = 0, -p_M = 2\epsilon b_2 - p_\infty = \frac{1 + \epsilon R_0 - R_n R_0^2 g \lambda' T_f - T_\infty}{\epsilon R_0} - p_\infty \tag{6.8}$$

In contrast to (6.7), this result is true, as are also (6.14) and (5.9b), in all approximations (I, II, etc.)!! Conditions (6.6a, b) may be stated also in the form

$$\left. \begin{aligned} (1 + \epsilon/4)b_2\tau_v^2 \left[1 + \frac{7b_{7/2}}{2b_2}\tau_v^{3/2} + 4\frac{b_4}{b_2}\tau_v^2 + \dots \right] &\geq \frac{1}{4} \\ (1 + \epsilon/4)b_2\tau_v^2 [] &< \frac{1}{4} \end{aligned} \right\} \tag{6.9a, b}$$

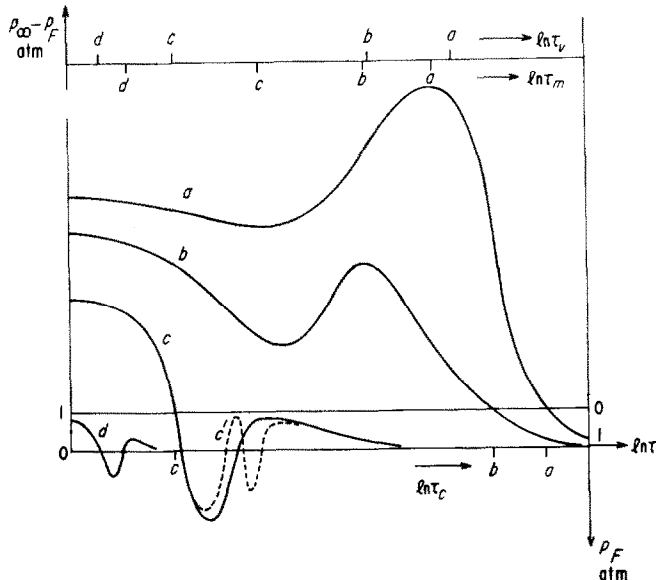


FIG. 3. Qualitative behavior of the front pressure with time for various degrees of undercooling: $(T_f - T_\infty)_a > (T_f - T_\infty)_b > (T_f - T_\infty)_c > (T_f - T_\infty)_d$.

Clearly, for $\epsilon > 0$, the maximum negative pressure always occurs at the front, $\xi/\mathcal{R} = 1$. [For $\epsilon < 0$, in the case (6.6a), the maximum positive pressure may occur slightly ahead of the front. Formulas (6.7, 8) also hold for $\epsilon < 0$.] It is noted, by (6.8b), (2.16a), that p_M is negative only when

$$U_u (1 - \mathcal{R}_n) > p_\infty U_d / \epsilon = \frac{\epsilon}{1 + \epsilon} \frac{c T_f^a}{\lambda} \frac{p_\infty}{\gamma \lambda'} \left(\mathcal{R}_n = \frac{R_n}{R_0} \right) \quad (6.10)$$

In other words, there is a least initial radius, R_0^* , which must be exceeded (at a given undercooling) in order that p_M be negative. Curve c in Fig. 3 illustrates the case of *moderate undercooling* where $R_0 > R_0^*$; it is noted that for this case τ_c , the time at which the front pressure crosses zero, is barely larger than τ_v . Curve c' illustrates the case where \mathcal{R} has several fluctuations about zero. [For quantitative illustrations, see Figs 8(a), (c) and Fig. 9(c).]

Depending on the location ξ in the liquid, the zero pressure condition for $\epsilon > 0$ is reached at various times (it is never reached for $\epsilon < 0$); it is reached last at the front. Curve d in Fig. 3 illustrates the case of *small undercooling*, where the condition (6.10) is disobeyed; here there is no τ_c .

From the ascending series expression (6.5b) we find that

$$\tau_c = m \mathcal{U}_d^{2/3} \left[1 - \frac{p_\infty}{2\epsilon b_2} + \left\{ (5 + \epsilon) b_2 + 6 \frac{b_4}{b_2} \right\} \tau_c^2 + \dots \right]^{2/3} \quad (6.11a)$$

is the time at which the front pressure passes through zero. The corresponding radius is

$$\mathcal{R}_c = 1 + b_2 \tau_c^2 + b_{7/2} \tau_c^{7/2} + b_4 \tau_c^4 + \dots \quad (6.11b)$$

This formula applies to cases of moderate undercooling, like Fig. 3 curve c or Fig. 9(b), curve $T_f - T_\infty = 17.5^\circ$; for large undercooling the descending series formula (4.1) of \mathcal{R} must be used. It leads to the expression for p_F :

$$p_F = p_\infty - \epsilon \beta_\infty^2 \tau^{-1} \left[1 + \frac{\epsilon}{2} - \beta_{1/2} \tau^{-1/2} - (2 + \epsilon) \beta_1 \tau^{-1} + \dots \right] \quad (6.12)$$

From this, one obtains

$$\tau_c = \frac{(1 + \epsilon/2) \beta_\infty^2}{p_\infty / \epsilon + \beta_\infty^2 \tau_c^{-3/2} [\beta_{1/2} + (2 + \epsilon) \beta_1 \tau_c^{-1/2} + \dots]} \quad (6.13a)$$

$$\simeq \frac{(1 + \epsilon/2) \epsilon \beta_\infty^2 / p_\infty}{1 + \epsilon \beta_\infty^2 \beta_{1/2} \tau_c^{-3/2} / 2 p_\infty} \simeq (1 + \epsilon/2) \epsilon \beta_\infty^2 / p_\infty \quad (6.13b, c)$$

$$\mathcal{R}_c = 2 \beta_\infty \tau_c^{1/2} [1 + \beta_{1/2} \tau_c^{-1/2} + \dots] \quad (6.13d)$$

Formula (6.13c) was stated previously, in a slightly different form, in equation (50b) of reference [1].

The extent ξ_M , at time $\tau = 0$, of the negative pressure region is given by

$$r_M / R_0 = \xi_M = \epsilon \mathcal{R}(0) / p_\infty = 2 \epsilon b_2 / p_\infty = 1 - p_M / p_\infty \quad (6.14)$$

At the interface \mathcal{R} the liquid pressure p_F discontinuously increases to the solid pressure value

$$p_S = p_F + p_{\text{stag}} + p_{\text{s.e.}} = p_F + \frac{\epsilon^2}{2} \mathcal{R}^2 + 2 \frac{\mathcal{R}'}{\mathcal{R}} \quad (6.15a)$$

$$\mathcal{R}' = \sigma' R_0 g / \kappa^2 \gamma \quad (6.15b)$$

At time $\tau = 0$ this is

$$p_S(0) = p_M + 2 \mathcal{R}' \quad (6.16a)$$

and may be a very large negative quantity, approaching (6.8b) in magnitude if μ_M dominates; alternately it may be a very large positive quantity if $2\sigma'$ dominates; at time τ_v it will have acquired the value

$$\mu_S(\tau_v) = \mu_\infty - 2\epsilon R_v^2 + 2\sigma' / R_v \quad (6.16b)$$

[cf. (6.7b)], which is usually positive. Then, with passage of time, μ_S subsides to μ_∞ .

REFERENCES

1. G. HORVAY, Freezing into an undercooled melt accompanied by density change, Proc. 4th Natl. Congr. of Applied Mechanics, ASME, 1315 (1962).
2. (a) D. TURNBULL and J. H. HOLLOWOM, Nucleation, in *Progress in Metal Physics*, Vol. 4, p. 333. Pergamon Press, London (1953).
(b) D. TURNBULL, Phase changes, in *Solid State Physics*, Vol. 3, p. 225. Academic Press, New York (1956).
3. A. H. COTTRELL, *Theoretical Structural Metallurgy*. St. Martin's Press, London (1955).
4. B. CHALMERS, *Physical Metallurgy*. John Wiley, New York (1959).
5. (a) J. L. WALKER, The influence of large amounts of undercooling on the grain size of nickel, in *Physical Chemistry of Process Metallurgy*, Vol. 2, p. 845. Interscience, New York (1961).
(b) J. L. WALKER, Principles of solidification, in *Transactions Vacuum Metallurgy Conference*. American Vacuum Society (1963).
6. (a) G. A. COLLIGAN and B. J. BAYLES, Dendrite growth velocity in undercooled nickel melts, *Acta Met.* 10, 895 (1962).
(b) D. P. STUHR, A study of energy-induced nucleation in supercooled bismuth, RPI, Troy, N.Y., master's thesis (1962).
(c) M. E. GLICKSMAN, Dynamic effects arising from high-speed crystal growth, Oral presentation AIME Meeting, Cleveland (October, 1963).
7. J. C. FISHER, Fracture of liquids, *J. Appl. Phys.* 19, 1062 (1948).
8. G. R. IRWIN, Fracture, in *Encyclopedia of Physics*, Vol. VI (Elasticity and Plasticity). Springer, Berlin (1958).
9. L. COLLATZ, *The Numerical Treatment of Differential Equations*. Springer, Berlin (1960).
10. H. S. CARSLAW and J. C. JAEGER, *Conduction of Heat in Solids*. Oxford University Press, London (1959).
11. H. SCHLICHTING, *Boundary Layer Theory*. McGraw-Hill, New York (1960).
12. A. I. VEYNIK, *Priblizhennii Raschet Processov Teploprovodnosti*. G.E.I., Moscow (1959).
13. T. R. GOODMAN, The heat balance integral and its application to problems involving a change of phase, *Trans. Amer. Soc. Mech. Engrs* 80, 335 (1958).
14. G. HORVAY and J. W. CAHN, Dendritic and spheroidal growth, *Acta Met.* 9, 695 (1961).
15. C. LANZOS, *Linear Differential Operators*. D. Van Nostrand, New York (1961).

APPENDIX. CAHN'S FORMULA FOR THE DEPRESSION OF FREEZING TEMPERATURE DUE TO PRESSURE

At the melting point, T_f (corresponding to ambient pressure p_∞), the chemical potentials μ_L and μ_S of liquid and solid phases must equal, and so must $\mu_L + d\mu_L$ and $\mu_S + d\mu_S$ at $T_F = T_f + dT$. But

$$d\mu_L = \frac{\partial\mu_L}{\partial T} dT + \frac{\partial\mu_L}{\partial p} dp = -S_L dT + \frac{dp_L}{\gamma}, \quad d\mu_S = -S_S dT + \frac{dp_S}{\Gamma} \quad (A1)$$

(S = entropy). It follows that

$$(S_L - S_S) dT = \frac{dp_L}{\gamma} - \frac{dp_S}{\Gamma} \quad (A2a)$$

from which

$$T_F - T_f = dT = \frac{T_f^\infty}{\lambda'} \left(\frac{p_F - p_\infty}{\gamma} - \frac{p_S - p_\infty}{\Gamma} \right) \quad (A2b)$$

i.e. (2.5) holds.

Part II. Growth of the Nickel Nucleus

7. INTEGRATION OF THE GOVERNING EQUATIONS

In this section we apply the analysis of Part I to the nickel nucleus. We shall use the property values (g stands for gram weight), cf. (54) of reference [1]:

$$\left. \begin{aligned} \epsilon &= 0.06, & T_f &= 1455^\circ\text{C} = 1728^\circ\text{K}, & p_\infty &= 1033 \text{ g/cm}^2 = 1 \text{ atm} \\ K &= k = 0.165 \text{ cal/cm}\cdot\text{sec}\cdot\text{C}^\circ, & \Gamma &= 1.06\gamma = 8.92 \text{ g/cm}^3 \\ C &= 0.105 \text{ cal/g}\cdot\text{C}^\circ, & c &= 0.106 \text{ cal/g}\cdot\text{C}^\circ, & \kappa &= k/\gamma c = 0.185 \text{ cm}^2/\text{sec} \\ \lambda &= 74 \text{ cal/g}, & \lambda' &= 3.16 \times 10^8 \text{ g}\cdot\text{cm/g}, & \sigma' &= 0.360 \text{ g}\cdot\text{cm/cm}^2 (= 255 \text{ erg/cm}^2) \\ \kappa &= \text{Boltzmann's constant} = 1.41 \times 10^{-19} \text{ g}\cdot\text{cm/d}\ddot{\text{a}}\text{g} (= 1.38 \times 10^{-16} \text{ erg/deg}) \end{aligned} \right\} \quad (7.1a)$$

By (2.16c)

$$\mathcal{K} = \mathcal{K}' = 1 \quad (7.1b)$$

[More frankly stated, the somewhat uncertain values of k , c near T_f were so selected that (7.1b) hold.] As undercooling temperature we first select

$$T_f - T_\infty = 17.5 \text{ degC} \quad (7.2a)$$

Accordingly, by (2.16b)

$$U_u = \frac{0.106 \times 1728}{74} \times \frac{17.5}{1728} = 2.47 \times 0.01013 = 0.025 \quad (7.2b)$$

is the dimensionless undercooling. The nucleation radius (2.13) is

$$R_n = \frac{2 \times 0.26 \times 2.47}{8.92 \times 3.16 \times 10^8} \frac{1}{U_u} = \frac{4.55 \times 10^{-8}}{U_u} = 1.82 \times 10^{-6} \text{ cm} \quad (7.2c)$$

For initial nucleus radius we choose

$$R_0 = 2^{1/3} R_n = 2.293 \times 10^{-6} \text{ cm}, \quad \mathcal{R}_n = R_n/R_0 = 0.794 \quad (7.2d)$$

This exceeds the least R_0 value for which tension may arise [see (6.10)],

$$R_0^* = \left[1 - \frac{\epsilon}{1 + \frac{\epsilon p_\infty c T_f^a / \lambda'}{U_u}} \right]^{-1} R_n = \left[1 - \frac{0.06 \times 1033}{8.92 \times 3.16 \times 10^8} \times \frac{2.47}{0.025} \right]^{-1} R_n = 1.000217 R_n \quad (7.2e)$$

by a considerable margin.

The density parameter (2.16b) in the temperature is

$$U_a = \frac{0.06^2}{1.06} \times 2.47 \times \left(\frac{0.185}{2.293 \times 10^{-6}} \right)^2 \times \frac{1}{981 \times 3.16 \times 10^6} = 0.0176 \quad (7.2f)$$

and the scale factors for distance, time, velocity, acceleration, temperature, and pressure are

$$\left. \begin{aligned} r/\xi &= R_0 = 2.29 \times 10^{-6} \text{ cm}, & t/\tau &= R_0^2/\kappa = 2.83 \times 10^{-11} \text{ sec} \\ \dot{R}/\dot{\mathcal{R}} &= \kappa/R_0 = 8.08 \times 10^4 \text{ cm/s}, & \ddot{R}/\ddot{\mathcal{R}} &= \kappa^2/R_0^3 = 2.86 \times 10^{15} \text{ cm/s}^2 \\ (T - T_\infty)/U &= \lambda/c = 698^\circ\text{C}, & p/\rho &= (\kappa/R_0)^2 \gamma/g = 5.60 \times 10^7 \text{ g/cm}^2 = 5.42 \times 10^4 \text{ atm} \end{aligned} \right\} \quad (7.3)$$

Note that temperatures U and \mathcal{U} are related [see (3.14)] by

$$U = 1.06\mathcal{U} \quad (\mathcal{U}_u = 0.0235849, \mathcal{U}_a = 0.01660377) \quad (7.4a)$$

and that the dimensionless atmospheric pressure is

$$p_\infty = 1033/5.60 \times 10^7 = 1.84 \times 10^{-5} \quad (7.4b)$$

while the dimensionless surface tension σ' of formula (6.15b) is given by

$$\sigma' = \frac{0.260}{5.60 \times 10^7 \times 2.293 \times 10^{-6}} = 2.03 \times 10^{-3} \quad (7.4c)$$

One must keep in mind an important restriction on our analysis: the phenomena described by a continuum analysis must not involve such small quantities (in space, time, mass) that quantum phenomena would also come into play. The distance and time scales

$$R_0 = 2.3 \times 10^{-6} \text{ cm}, \quad R_0^2/\kappa = 2.8 \times 10^{-11} \text{ s}$$

are indeed much larger than the radius 0.5×10^{-8} cm of the first Bohr orbit, or the travel time 10^{-16} s of an electron in the first Bohr orbit. When we switch, in (7.7), to an undercooling of 175°C (the largest undercooling we shall be concerned with), R_0 and R_0^2/κ will be replaced by 2.3×10^{-7} cm and 2.8×10^{-13} s; these quantities are still a safe margin away from the atomic scale.

After these preliminaries we may proceed to the calculation of the parameters b_k etc., and β_k etc., of the ascending (5.11) and descending (4.1) solutions. We find, by (5.9b), that

$$\text{I, II}_0: \quad b_2 = \frac{1}{2} \frac{U_u}{U_a} (1 - \mathcal{R}_n) = \frac{1}{2} \frac{0.025}{0.0176} \times 0.206 = 0.1463068 \quad (7.5a, 6a)$$

Hence, by (5.19, 25)

$$\text{I: } a_0 = 1, \quad d_{1/2} = 1/\sqrt{2}; \quad \text{II}_0: \quad a_0 = a_0'' = \frac{1}{2}, \quad d_{1/2} = 1, \quad d_{1/2}' = \frac{1}{2} \quad (7.5b, 6b)$$

and by (5.32, 33)

$$\begin{aligned} \text{I: } \quad & b_{7/2} = -0.712090, \quad b_4 = 0.533198, \quad b_{9/2} = -2.36412 \\ & d_1 = -0.473684, \quad d_{3/2} = -0.080042 \\ & f_{3/2} = 0.1034545, \quad f_2 = -0.1078050, \quad f_{5/2} = 0.618239 \\ & c_{5/2} = 1.069937, \quad c_3 = -3.44800 \end{aligned} \quad (7.5c)$$

$$\begin{aligned} \text{II}_0: \quad & b_{7/2} = -0.691128, \quad b_4 = 0.511109, \quad b_{9/2} = -2.87494 \\ & -a_{1/2} = a_{1/2}'' = -2.030291, \quad -a_1 = a_1'' = 22.55700 \\ & d_1 = -2.539633, \quad d_{3/2} = 20.74939, \quad d_1' = -0.880804, \quad d_{3/2}' = 10.31238 \\ & f_{3/2} = 0.1004090, \quad f_2 = -0.103404, \quad f_{5/2} = 0.751825 \\ & c_{5/2} = 1.03792, \quad c_3 = -3.44253 \end{aligned} \quad (7.6c)$$

are the leading coefficients in the ascending expansions of \mathcal{R} , A , A'' , w , w'' , \mathcal{U}_F , \mathcal{U}_C in the I and II_0 approximations. As in Table 1, and noting (5.5, 9), we next determine the basic parameters

$$\begin{aligned} \text{I}_0: \quad & a_0 = 1, \quad \beta_\infty = 0.08725369, \quad \Omega = 0.6455999, \quad \delta_\infty = \beta_\infty/\Omega = 0.1351513, \\ & \nu_0 = \gamma_0 = 0.0235849 \end{aligned} \quad (7.5d)$$

$$\text{II}_0: \quad a_0 = 1 - a'_0 = 0.6032083, \quad \beta_\infty = 0.1212497, \quad \Omega = 0.5321140, \quad \omega = 0.2280827$$

$$\delta_\infty = \beta_\infty/\Omega = 0.2278641, \quad \delta'_\infty = \omega\delta_\infty = 0.05197186, \quad \gamma_0 = \nu_0 = 0.0235849 \quad (7.6d)$$

for the asymptotic expansions (4.1). This takes care of (4.20) or, equivalently, of the $\langle \tau^{1/2} \rangle = 0$ equations of (4.18). The $\langle \tau^0 \rangle = 0$ equation of (4.18^o) in case of I, and of equations (4.18^o, ', '') in case of II₀, in conjunction with the $\langle \tau^{-1/2} \rangle = 0$ equations of (4.2_J^o, 2_B) and the relations (4.4) then lead to

$$\text{I:} \quad \beta_{1/2} = -6.438463, \quad \delta_{1/2} = -4.514249, \quad \nu_{1/2} = -0.1073101, \quad \gamma_{1/2} = -0.1075819 \quad (7.5e)$$

$$\text{II}_0: \quad \beta_{1/2} = 30.6502, \quad -a_{1/2} = a''_{1/2} = -64.8562, \quad \delta_{1/2} = -68.7592,$$

$$\delta''_{1/2} = -106.705, \quad \nu_{1/2} = -0.0772225, \quad \gamma_{1/2} = -0.0775994 \quad (7.6e)$$

For $T_f - T_\infty = 175$ degC undercooling, $R_0 = 2^{1/3}R_n$, one finds similarly the basic parameters

$$R_n = 1.82 \times 10^{-7} \text{ cm}, \quad U_d = 1.76, \quad \mathcal{R}_n = 0.794, \quad \mathcal{U}_u = 0.235849, \quad \mathcal{U}_d = 1.660377$$

$$b_2 = 0.01463068, \quad \mu_\infty = 1.84 \times 10^{-7}, \quad \delta' = 2.03 \times 10^{-4} \quad (7.7a)$$

and the scale factors

$$R/\xi = R_0 = 2.293 \times 10^{-7} \text{ cm}, \quad t/\tau = 2.83 \times 10^{-13} \text{ s}, \quad \dot{R}/\dot{\mathcal{R}} = 8.08 \times 10^5 \text{ cm/s},$$

$$\ddot{R}/\ddot{\mathcal{R}} = 2.86 \times 10^{18} \text{ cm/s}^2, \quad (T - T_\infty)/U = 698 \text{ degC}, \quad p/\mu_\infty = 5.42 \times 10^6 \text{ atm} \quad (7.7b)$$

The coefficients (7.5b, 6b) remain unchanged. The other coefficients become

$$\text{I:} \quad b_{7/2} = -0.000712090, \quad b_4 = 0.000462378, \quad b_{9/2} = -0.00236412,$$

$$d_1 = -0.473684, \quad d_{3/2} = -0.080042, \quad f_{3/2} = 0.01034545, \quad f_2 = -0.01078050,$$

$$f_{5/2} = 0.06182390, \quad c_{5/2} = 0.1069937, \quad c_3 = -0.344800, \quad (7.8a)$$

$$a_0 = 1, \quad \beta_\infty = 0.5087406, \quad \Omega = 2.194768, \quad \delta_\infty = 0.2317970, \quad \nu_0 = \gamma_0 = 0.2358490,$$

$$\beta_{1/2} = -1.326735, \quad \delta_{1/2} = -0.722970, \quad \nu_{1/2} = -0.1840467, \quad \gamma_{1/2} = -0.1988997 \quad (7.8b)$$

$$\text{II}_0: \quad b_{7/2} = -0.000691128, \quad b_4 = 0.000440290, \quad b_{9/2} = -0.00287494,$$

$$-a_{1/2} = a''_{1/2} = 2.030291, \quad -a_1 = a'_1 = 22.55700, \quad d_1 = -2.539633,$$

$$d_{3/2} = 20.74939, \quad d'_1 = -0.880804, \quad d''_{3/2} = 10.31238, \quad f_{3/2} = 0.01004090,$$

$$f_2 = -0.0103404, \quad f_{5/2} = 0.0751825, \quad c_{5/2} = 0.103792, \quad c_3 = -0.344253 \quad (7.9a)$$

$$1 - a'_0 = a_0 = 0.996257039, \quad \beta_\infty = 0.5163892, \quad \Omega = 2.190297, \quad \omega = 0.1035666,$$

$$\delta_\infty = 0.2357622, \quad \delta'_\infty = 0.02441709, \quad \gamma_0 = \nu_0 = 0.2358490, \quad \beta_{1/2} = -1.05641$$

$$-a_{1/2} = a''_{1/2} = 0.136379, \quad \delta_{1/2} = -0.390083, \quad \delta''_{1/2} = 23.0660,$$

$$\nu_{1/2} = -0.181321, \quad \gamma_{1/2} = -0.196368 \quad (7.9b)$$

For $\mathcal{R}_n = 2^{-1/3}$ and $U_u = 0.25, 0.025$ we plot in Figs. 4 and 5, by method II₀, and in Figs. 6, 7 and 8 by method I, the variation with time τ of the auxiliary parameters A, w, w' and of the principal variables of the problem, $\mathcal{R} - 1, \mathcal{R}, \mathcal{R}, \mathcal{U}_F, \mathcal{U}_C$. For small times ($\tau = 10^{-6}$ to $\tau \simeq 0.1$) the solution ascending in $\tau^{1/2}$ was used (coefficient of last retained term, e.g. $b_{7/2}$ or b_4 , is marked on the curves in Figs. 4 and 5), for large times ($\tau = 10^6$ to $\tau \simeq 10^2$) the solution descending in $\tau^{1/2}$ was used (coefficient of last retained term, e.g. $\beta_{1/2}$, is marked on the curves in Figs. 4 and 5).

The intervening portion must be bridged by numerical integration. However, as the dimensional summary figure of the four calculations, Fig. 9 indicates, the I and II₀ solutions are indistinguishable, at $U_u = 0.25$, in their small time and large time behaviors (presumably also in-between);

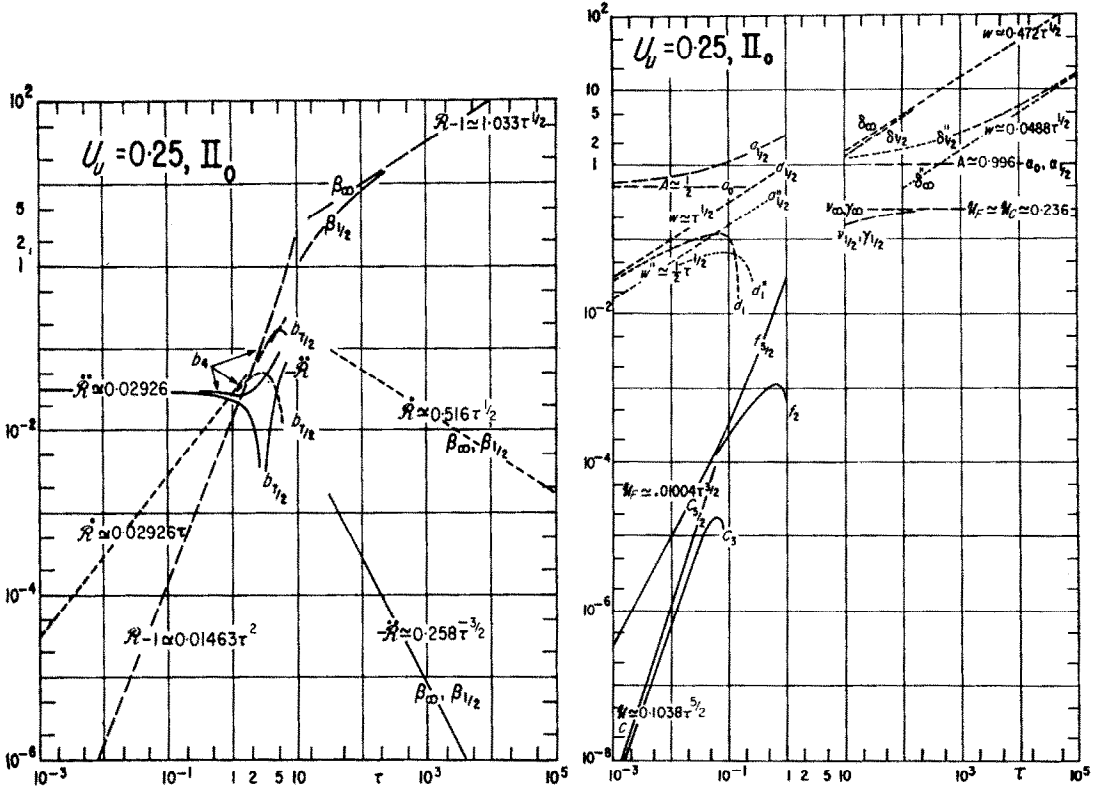


FIG. 4. Ascending and descending power series solutions (in $\tau^{1/2}$), terminated with the term that labels the curve. The asymptotic behavior is marked on the curves. Nickel, for $R_n = 0.794$, $T_f - T_\infty = 175$ degC, method Π_0 solution.

while at $U_u = 0.025$, I and Π_0 are indistinguishable in their small time behavior, and not importantly different in their large time behavior. For this reason a bridging of the small and large time regimes was undertaken only for the I calculations; even these calculations, programmed for an IBM 7094 computer, constituted a considerable financial effort. The equations (3.17a, b), (4.3a), (3.15^o, 15^o), (15_B) may be restated, for the case (7.1b), in the somewhat more convenient notation

$$z = \mathcal{R}, \quad u = \mathcal{U}_F, \quad v = \mathcal{U}_C \tag{7.10}$$

as follows:

$$l = \frac{1}{4l^2}, \quad \dot{\mathcal{R}} = z, \quad \dot{z} = \frac{1}{\mathcal{R}\mathcal{U}_d} \left\{ -u + \mathcal{U}_u \frac{\mathcal{R} - \mathcal{R}_n}{\mathcal{R}} \right\} - \frac{5 + \epsilon z^2}{2\mathcal{R}} \tag{7.11a, b, c}$$

$$\begin{aligned} wu \left[\mathcal{R}^2 + 4\mathcal{R}w + 6w^2 + \frac{(\mathcal{R}^2 + 2\mathcal{R}w + 2w^2)\mathcal{R}/w}{5 + 1/l + \mathcal{R}/w} \right] &= \frac{(\mathcal{R}^2 + 2\mathcal{R}w + 2w^2)w}{5 + 1/l + \mathcal{R}/w} \\ &\times \left[u \left(\frac{z}{w} - \frac{1}{4l^2} \right) + \frac{1}{\mathcal{U}_d} \left(u - \mathcal{U}_u \frac{\mathcal{R} - \mathcal{R}_n}{\mathcal{R}} \right) + \frac{3 + \epsilon}{2} z^2 + \frac{v}{4l^2} + 3(v - u) \right. \\ &\times \left. \left[\frac{2l + 1}{l} \frac{z}{\mathcal{R}} - \frac{1/4l^2}{5l + 1} + \frac{(2l + 1)(5l + 1)}{l^2 \mathcal{R}^2} \right] \right] + u \left[-z \{ \mathcal{E}\mathcal{R}^2 + 2\mathcal{R}w + 2w^2 \} + \frac{\mathcal{R}}{w} \right] \tag{7.11d} \end{aligned}$$

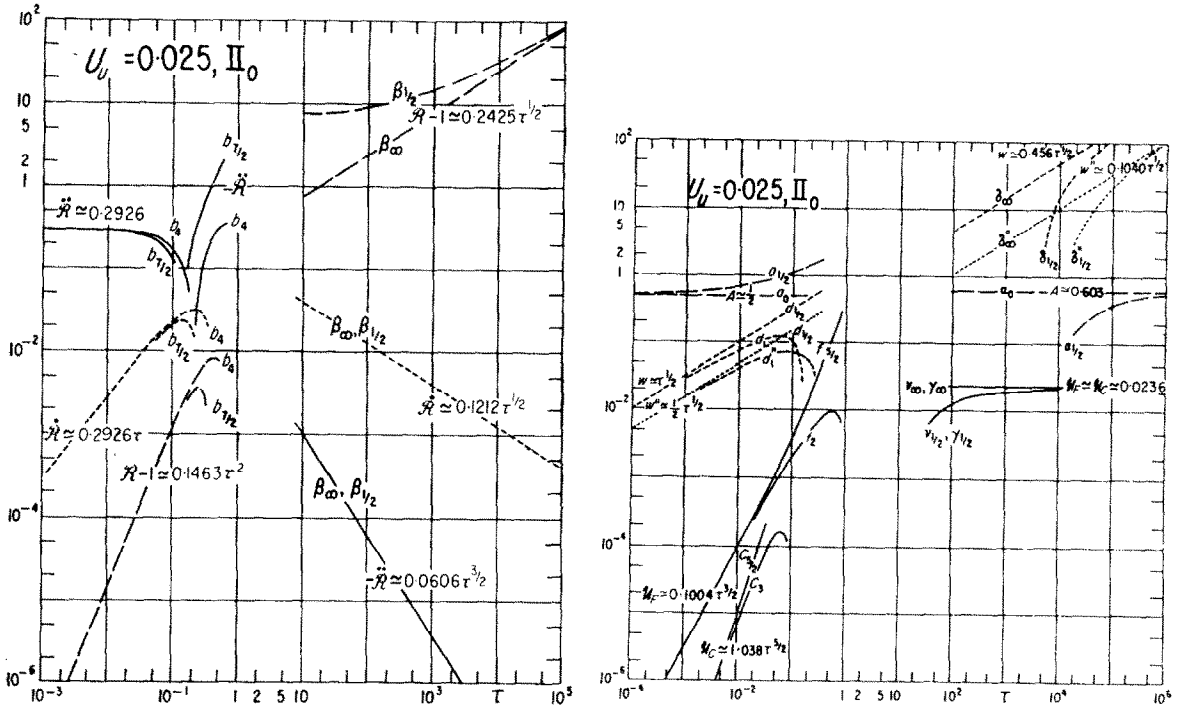


FIG. 5. Ascending and descending power series solutions (in $\tau^{1/2}$), terminated with the term that labels the curve. The asymptotic behavior is marked on the curves. Nickel, for $\mathcal{R}_n = 0.794$, $T_f - T_\infty = 17.5$ degC, method II₀ solution.

$$\begin{aligned} \dot{v} = & \frac{3l/(2l+1)}{5+1/l+\mathcal{R}/w} \left[u \left(\frac{z}{w} - \frac{1}{4l^3} - \frac{\mathcal{R}w}{w^2} \right) + \frac{1}{\mathcal{U}_a} \left(u - \mathcal{U}_u \frac{\mathcal{R} - \mathcal{R}_n}{\mathcal{R}} \right) + \frac{3+\epsilon}{2} z^2 + \frac{v}{4l^3} \right] \\ & + 3 \frac{2+1/l+\mathcal{R}/w}{5+1/l+\mathcal{R}/w} (u-v) \left\{ \frac{z}{\mathcal{R}} - \frac{1/l}{(2l+1)(5l+1)} + \frac{5l+1}{12\mathcal{R}^2} \right\} \end{aligned} \quad (7.11e)$$

$$(2+1/l+\mathcal{R}/w)u = \mathcal{R}z + (2+1/l)v \quad (7.11f)$$

The integration was carried out by means of the FACE program developed by N. S. Mathias and D. N. Ewart. This is a very crude but convenient integration scheme devised for very large equation systems: the integration is based on the slopes of the pertinent functions at the beginning of the integration step ("Euler's method"); no iterations are involved. As initial values the data furnished by the power series representation at $\tau = 10^{-6}$ were used. The integration step was 10^{-9} from $\tau = 10^{-6}$ to 10^{-5} , 10^{-8} from 10^{-5} to 10^{-4} , 10^{-7} in the next decade, and so on. We shall briefly refer to this as a 0.001 step computation ($0.001 = 10^{-9}/10^{-6} = 10^{-8}/10^{-5} = \dots$). Thus, 80 000 integration steps were performed between $\tau = 10^{-6}$ and 10^2 in each of the computations A, C, D, E, F. In computation B, 0.01 steps were used. F refers to the computation at $U_u = 0.25$; A, B, C, D, E to the computations at $U_u = 0.025$. In computation C, we used equations (7.11) of method I up to $\tau = 0.3691$ (here \mathcal{U}_C catches up with \mathcal{U}_F); from here on we continued with *simplified method I* computations. The latter expression is used to refer to the assumption (5.34) of isothermal nucleus. Computations D, E refer to cases where simplified equations were used right from the beginning. In computations A, B, C, D, F we used initial values accurate to about six significant digits (except for l which was chosen with eight-digit accuracy); the critical item was \mathcal{U}_C of which only two coeffi-

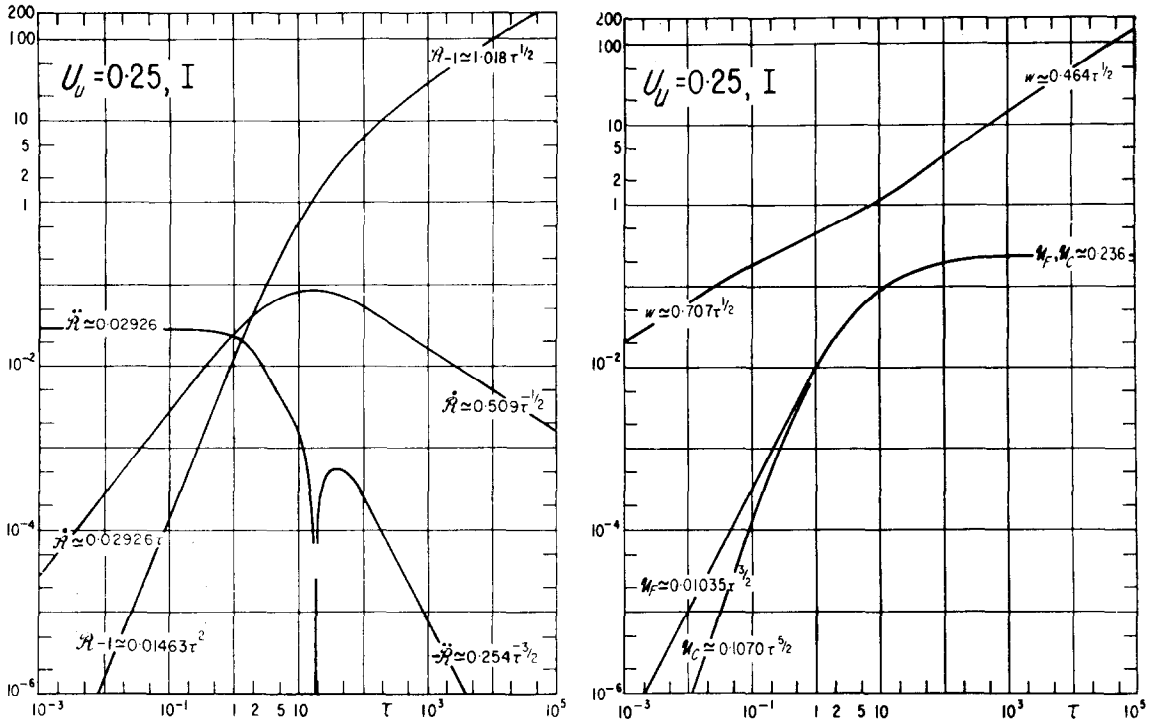


FIG. 6. In the range $\tau = 10^{-6}$ to 10^{+3} , a numerically integrated solution connects ascending and descending power series expansions. The asymptotic behavior is marked on the curves. Nickel, for $\mathcal{R}_n = 0.794$, $T_f - T_\infty = 175$ degC, method I solution.

cients, $c_{5/2}$, c_3 were available. In computation *E* we repeated *D*, using initial values accurate to eight digits, determined in accordance with (5.35). In Table 2 we compare values furnished by *A*, *B*, *C*, *D*, *E* at $\tau = 10^{-6}$, 0.1, 10 and 30.01 (*B* is given at 30.1; results at 30.0 were not printed out). It is noted that the *l* equation (7.11a) is independent of all others, and its solution is $l = \sqrt{(\tau/2)}$. Thus, the deviation of the calculated $l(0.1) = (\sqrt{5})/10 \approx 0.22360609$, $l(10) = (\sqrt{5}) \approx 2.2360562$ by *A*, *D*, *E*, *F* (0.22366221, 2.2366221 by *B*) from the rigorous eight-digit value $(\sqrt{5}) = 2.2360680$ is an indication of the discretization and roundoff errors accumulated during the integration process: the last three retained digits of the independently determined function $l(\tau)$ (the last four digits for calculation *B*) are meaningless. In fact, we may ascribe the error in $l(\tau)$ as largely due to discretization: since $l(\tau)$ is monotonically increasing, its last digit is discarded after every 20 000 integrations (because the decimal point moves to the right): this eliminates a major share of the roundoff error. This conclusion is supported by the observation that a change from the 0.01 step *B* scheme to the 0.001 step *A* scheme decreases the error by a factor of about 10. Thus we must assume that the interrelated quantities \mathcal{R} , \mathcal{U}_F are also in error in their last two or three digits at the time τ_v is reached. Past τ_v , \mathcal{R} and \mathcal{U}_F no longer increase monotonically, and thus we may expect a precipitous increase in their roundoff error.

Figure 6 is based on computation *F* in the interval $\tau = 10^{-6}$ to 10^3 . Figure 7 is based on computation *A* to $\tau = 0.3691$ and on *D* from thereon; in Fig. 8 the computations *A* and *E* are compared.

‡ The entries at $\tau = 10^{-6}$ are the input values.

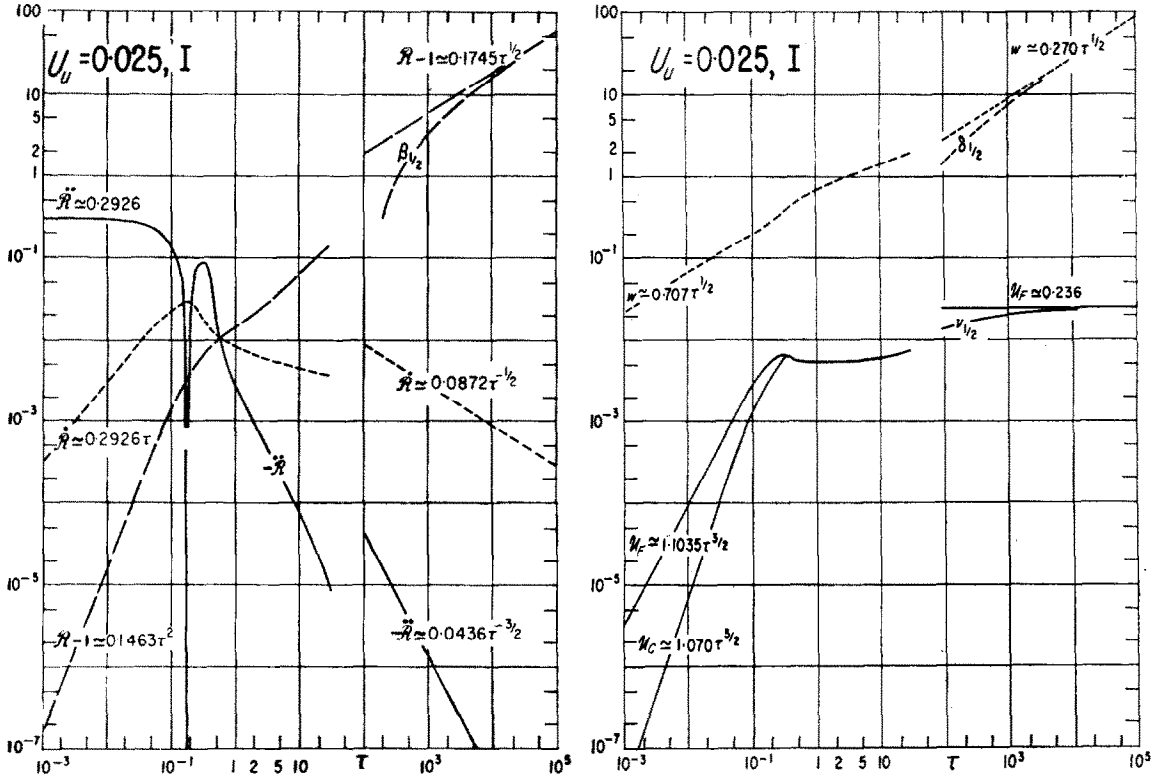


FIG. 7. In the range $\tau = 10^{-6}$ to $\tau = 30$, a numerically integrated solution continues the ascending power series solution. The descending power series solution is also shown. Nickel, for $R_n = 0.794$, $T_f - T_\infty = 17.5$ degC; method I solution to $\tau = 0.3691$ (crossing of W_C and W_F), and simplified method I (assumption of isothermal nucleus) from thereon.

The breakdown of the computations around $\tau = 40$ is due to the fact that in the expression (7.11c) of the acceleration

$$R\dot{z} = \frac{W_u}{W_d} \left(1 - \frac{R_n}{R} \right) - \frac{u}{W_d} - \frac{5 + \epsilon}{2} \frac{z^2}{R} \tag{7.12}$$

the last three digits, as explained above, are meaningless, while the first five significant digits cancel out in the subtraction. We illustrate this point by writing the above expression term by term for A , E , F , at $\tau = 30.01$, and for F also at $\tau = 1000$:

$A:$	$0.43245288 - 0.43241861 - 0.00003960 = -0.0000533$	}	(7.13)
$E:$	$0.42487816 - 0.42485318 - 0.00003438 = -0.0000940$		
$F:$	$0.10745757 - 0.09270495 - 0.01640874 = -0.00165612$		
$F:$	$0.13831634 - 0.13789611 - 0.00067059 = -0.00025036$		

Thus, at $U_u = 0.25$, to which F pertains, we have enough retained accuracy to continue the calculations past $\tau = 30$ up to $\tau = 1000$,[†] at $U_u = 0.025$ all eight digits lose significance by the time

[†] By the time we reach $\tau = 10^3$ only the first two retained digits remain significant: $R - 1$, \dot{R} , \ddot{R} , W_F are 29.2, 0.0163, -0.04828, 0.229 by forward numerical integration, 29.8, 0.0161, -0.04805, 0.230 by two-term descending power series formula.

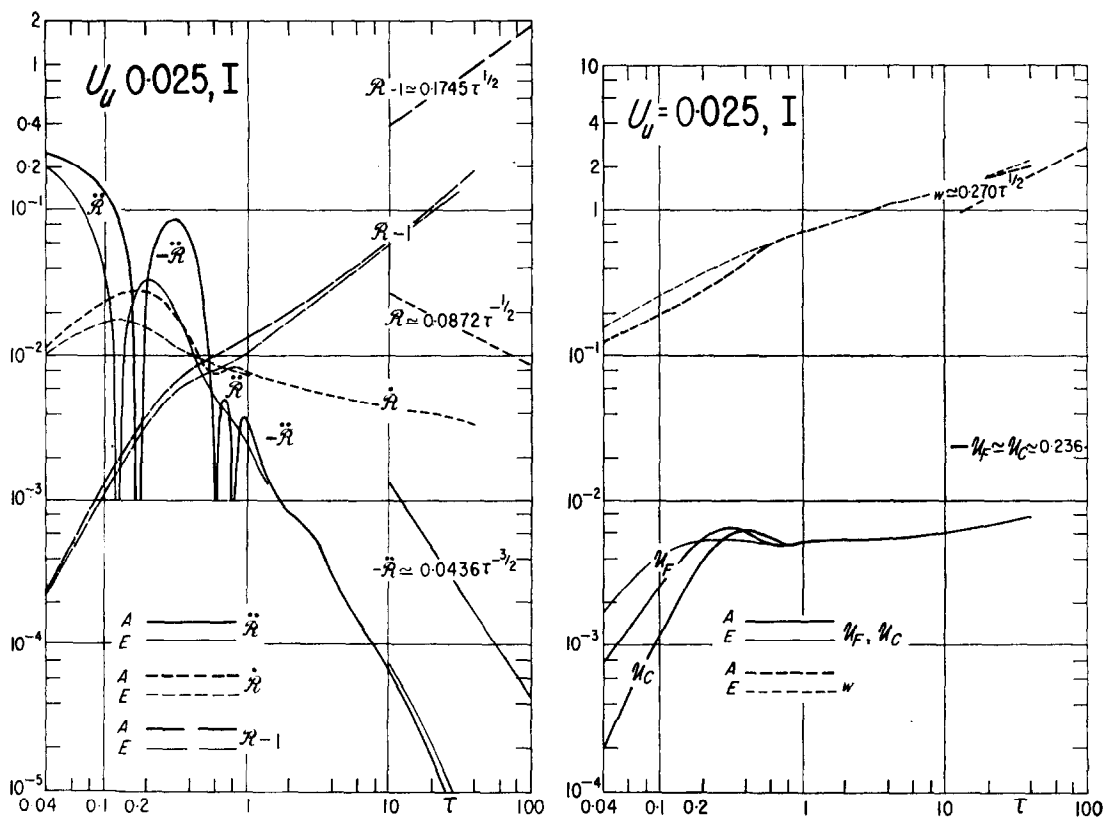


FIG. 8. Comparison of numerically integrated method I (curve A) and simplified method I (curve E; assumption of isothermal nucleus) solutions for the case of nickel, $R_n = 0.794$, $T_f - T_\infty = 17.5$ degC undercooling.

Table 2. Comparison of numerical integrations

τ	Method	$R - 1$	\dot{R}	\ddot{R}	w	U_F	U_C
10^{-6}	A, B, D	0.01214630680	0.029261360	0.29261360	0.0370663310		0.01410664890
	E	0.01214630682	0.029261363	0.29261362	0.0370663743		
10^{-1}	A	0.02126694	0.0226028	0.136364	0.190011	0.02259370	0.02120870
	B	0.02126800	0.0226094	0.136270	0.190056	0.02259526	0.02120978
	D	0.02105275	0.0164497	0.0379543	0.257511	0.02423597	
	E	0.02105276	0.0164497	0.0379542	0.257511	0.02423597	
10	A	0.0596445	0.02440567	-0.04683999	1.35005	0.02591294	0.02590172
	B	0.0596645	0.02440518	-0.04683883	1.35028	0.02591327	0.02590206
	C	0.0597611	0.02427862	-0.04763372	1.38247	0.02591507	
	D	0.0555399	0.02422323	-0.04737602	1.38386	0.02584437	
	E	0.0555399	0.02422323	-0.04737603	1.38386	0.02584437	
30.01	A	0.141538	0.02395638	-0.0467874	1.82470	0.02717979	0.02716887
	C	0.137920	0.02372120	-0.04880931	1.91545	0.02712778	
	D	0.132852	0.02368642	-0.04831342	1.91356	0.02705416	
	E	0.132852	0.02368642	-0.04831649	1.91356	0.02705417	
30.1	B	-4.1×10^{23}	-2.8×10^{22}	2.1×10^{14}	-3.3×10^7	1.4×10^{22}	3.9×10^{20}

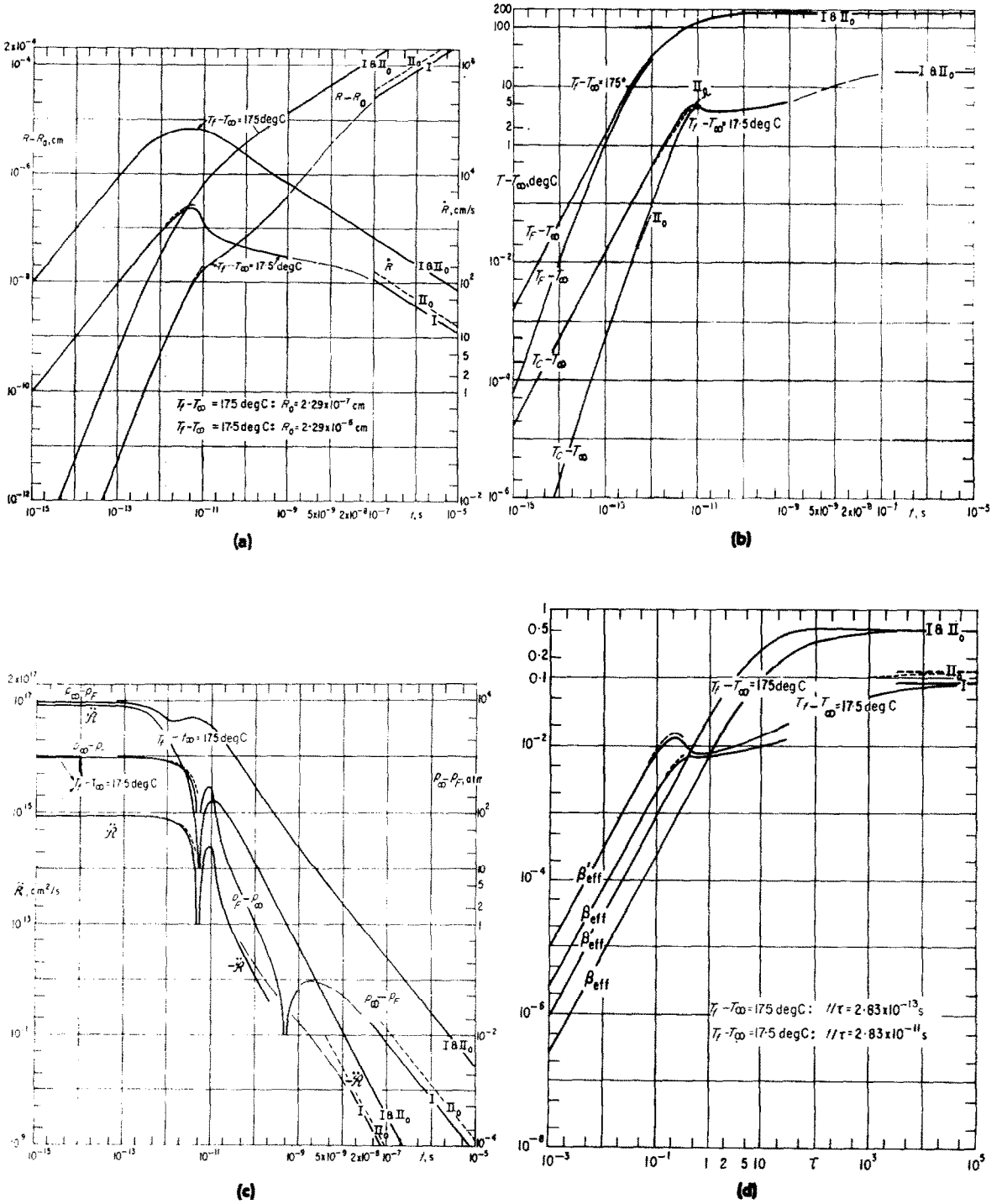


FIG. 9. Dimensional curves, vs time t , of radius, velocity, front temperature, nucleus center temperature, acceleration, front pressure, and effective solidification parameter of nickel, for $\mathcal{R}_n = 0.794$, at 175 and 17.5°C undercoolings.

$\tau = 30$ is reached. To go beyond, it would be necessary to use (from the beginning) a more accurate integration scheme (e.g. modified Adams method, or the like), in conjunction with double precision, which allows one to carry 16 significant digits, instead of eight in the integrations. In retrospect, a more accurate integration scheme would have been desirable. However, since—for the task on hand—our computed curves gave valid results in the most important τ region, the vicinity of τ_v and slightly beyond, we did not undertake the task of repeating the calculations by such a much more expensive computational scheme.

From Fig. 8 it is noted that, past τ_v , \mathcal{U}_F has a slight dip (because of the dynamic effect of large deceleration on freezing temperature); but when the surface temperature \mathcal{U}_F declines, heat may flow out from the hotter nucleus; thus \mathcal{U}_C may exceed \mathcal{U}_F over a small time interval. (The same is true also at $U_u = 0.25$; but here the time interval of heat outflow is so small that no dip is seen in the plotted curve of \mathcal{U}_F , nor can there be distinguished any crossover by \mathcal{U}_C .) The fluctuation in \mathcal{U}_F , Fig. 8(b), brings forth a corresponding fluctuation of \mathcal{R} about 0 [Fig. 8(a)]; this fluctuation does not arise when the simplified method I is used.

Although Table 2 reveals a difference between entries according to A and according to B , the differences are too small to show up on the graph paper; the error due to the larger integration step manifests itself mainly in an earlier breakdown of the calculations. (See the meaningless entries in Table 2 that were printed out for B at $\tau = 30.1$).[‡] Comparison of the entries for D and E indicates that the inaccuracy past the sixth digit of the initial data is of minor importance compared to step size and roundoff errors.

One might have endeavored to avoid the difficulty of canceling significant digits in (7.12) by backward integration of equations (7.11), say from $\tau = 10^8$, using the descending power series expressions for initial value determination. This was tried, but it was found that the cancellation of significant digits in (7.12) is even more serious in this case.

On the basis of Figs. 4–8 we plot in Fig. 9, vs dimensional t , the dimensional curves R , \dot{R} , \ddot{R} , $T_F - T_\infty$, $T_C - T_\infty$, $p_\infty - p_F$, as well as an effective β , using the alternate definitions

$$\beta_{\text{eff}} = (\mathcal{R} - 1)/2(\sqrt{\tau}) = (R - R_0)/2\sqrt{\kappa t}, \quad \beta'_{\text{eff}} = \dot{\mathcal{R}}(\sqrt{\tau}) = \dot{R}\sqrt{t/\kappa} \quad (7.14)$$

Thin long-dashed lines are used to indicate our guess for the missing connections between the I computations and the descending power series representations in the $U_u = 0.025$ case.

In (7.15) below we verify for the case $U_u = 0.025$ and in (7.16), (7.17) for the case $U_u = 0.25$, that the approximate formulas of section 6, based on chopped-off ascending or descending power series solutions in $\tau^{1/2}$, provide acceptable agreement with the values read off the numerically integrated curves of Figs. 4–9. This is the most important conclusion drawn from these figures; it obviates the necessity of investigating other cases by means of numerical integration, but assures us that the results based on the section 6 formulas and the corresponding Fig. 10 provide quantitatively acceptable estimates.

By formulas (6.8), (7.5) the tension maximum at the front, at time $\tau = 0$, is

$$\text{I, II}_0: -p_M = -p_\infty + 2\epsilon b_2 = -1.84 \times 10^{-5} + 0.01756 = 0.01754, \quad -p_M = 951 \text{ atm} \quad (7.15a)$$

The corresponding pressure on the solid phase [see (6.16a)] is

$$\text{I, II}_0: p_S(0) = p_M + 2\sigma' = -0.01754 + 0.00406 = -0.01348, \quad p_S(0) = -730 \text{ atm} \quad (7.15b)$$

and the extent at this instant of the negative pressure region in the liquid [see (6.14)] is

$$\text{I, II}_0: r_M/R_0 = \xi_M = 1 - p_M/p_\infty = 1 + 951 = 952 \quad (7.15c)$$

[‡] The large powers of 10 that multiply the various entries may be attributed to the fact that the computer cannot carry numbers larger than 10^{38} , and once this is reached for any one variable, everything gets garbled.

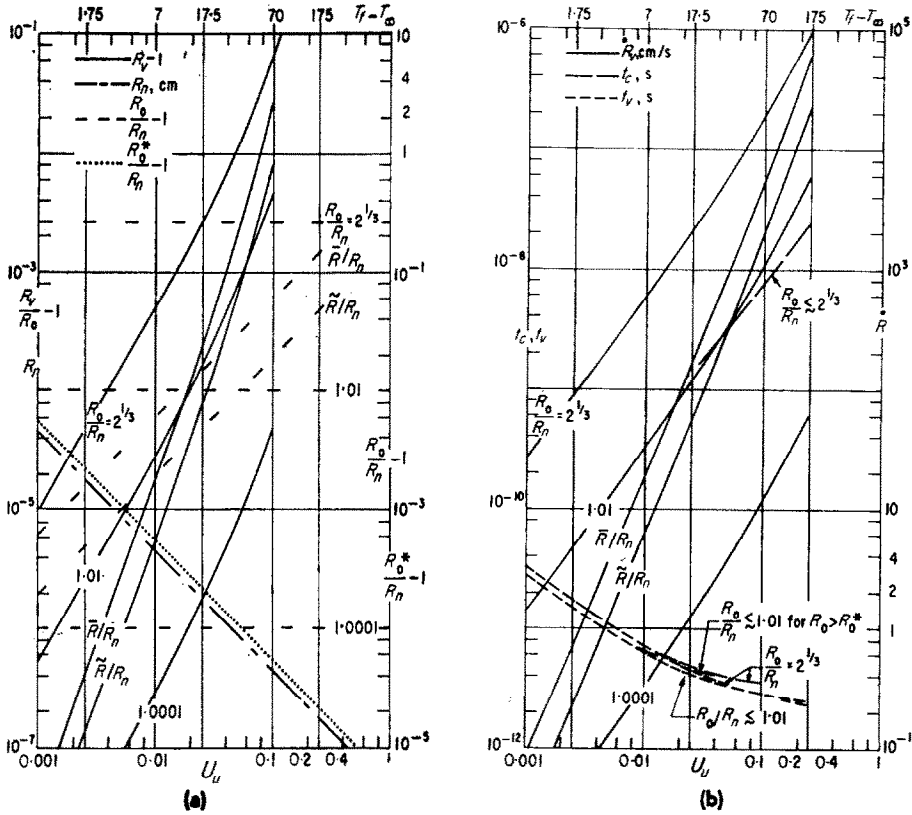


FIG. 10. Dependence on undercooling for, the case of nickel, of $R_n, R_0^*, \bar{R}, \tilde{R}, R_v, t_v, t_c, p_M, r_M, p_v, p_s(0), p_s(t_v)$, as determined by the formulas of section 6.

In these initial values no approximations are involved.

Maximum velocity is reached, by (6.4b), at time

$$\left. \begin{aligned} \text{I: } \tau_v &= 0.1300 [1 + 10.9\tau_v^2]^{2/3} = 0.150, t_v = 4.26 \times 10^{-12} \text{ s} \\ \text{II}_0: \tau_v &= 0.1324 [1 + 10.5\tau_v^2]^{2/3} = 0.153, t_v = 4.34 \times 10^{-12} \text{ s} \end{aligned} \right\} (7.15d)$$

whereas curve A of Fig. 8(a) shows

$$\text{I: } \tau_v = 0.18 \tag{7.15d'}$$

Velocity maximum and corresponding radius [see (6.1)] are ‡

$$\left. \begin{aligned} \text{I: } \dot{R}_v &= 0.2926\tau_v \left[1 - 8.52\tau_v^{3/2} + \frac{7.29}{2} \tau_v^2 \right] = 0.0440 \times 0.585 = 0.0257, \dot{R}_v = 2080 \text{ cm/s} \\ \text{II}_0: \dot{R}_v &= 0.2926\tau_v \left[1 - 8.30\tau_v^{3/2} + \frac{7.00}{2} \tau_v^2 \right] = 0.0448 \times 0.587 = 0.0263, \dot{R}_v = 2120 \text{ cm/s} \end{aligned} \right\} (7.15e)$$

‡ As in (6.4c) we append factor $\frac{1}{2}$ to the last (smallest) term in the bracket.

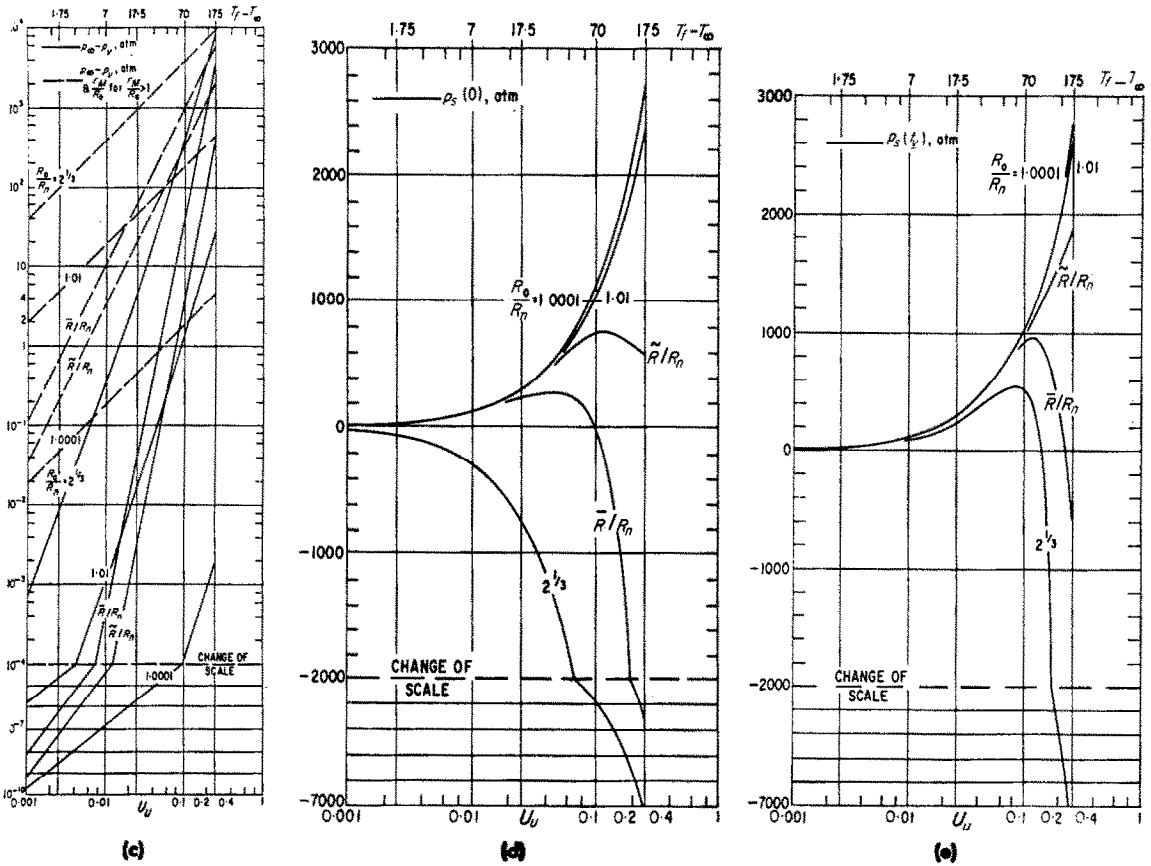


Fig. 10 (continued)

$$\begin{aligned}
 \text{I: } \mathcal{R}_v &= 1 + 0.1463 \tau_v^2 \left[1 - 4.87 \tau_v^{3/2} + \frac{3.64}{2} \tau_v^2 \right] = \\
 & \quad 1 + 0.0033 \times 0.758 = 1.0025, \quad R_v = 2.30 \times 10^{-6} \text{ cm} \\
 \text{II}_0: \mathcal{R}_v &= 1 + 0.1463 \tau_v^2 \left[1 - 4.72 \tau_v^{3/2} + \frac{3.49}{2} \tau_v^2 \right] = \\
 & \quad 1 + 0.0034 \times 0.758 = 1.0026, \quad R_v = 2.30 \times 10^{-6} \text{ cm}
 \end{aligned}
 \tag{7.15e}$$

Figure 8(a) shows

$$\text{I: } \mathcal{R}_v = 2.8 \times 10^{-2}, \quad \mathcal{R}_v = 1.0030 \tag{7.15e'}$$

By time τ_v the front tension has dropped, according to (6.7b), to

$$\begin{aligned}
 \text{I: } -\mu_v &= -1.84 \times 10^{-5} + 0.122 \times 0.0257^2 = (-1.84 + 8.08) \times 10^{-5}, \\
 & \quad p_v = 1 - 4.38 = -3.38 \text{ atm} \\
 \text{II}_0: -\mu_v &= -1.84 \times 10^{-5} + 0.122 \times 0.0263^2 = (-1.84 + 8.40) \times 10^{-5}, \\
 & \quad p_v = 1 - 4.56 = -3.56 \text{ atm}
 \end{aligned}
 \tag{7.15f}$$

as compared with

$$\text{I: } p_v = -4 \text{ atm} \quad (7.15f')$$

in Fig. 9(c).[‡] The pressure on the frozen nucleus has risen by this time [see (6.16b)] to

$$\begin{aligned} \text{I: } p_S(\tau_v) &= 1.84 \times 10^{-5} - 0.12 \times 0.0257^2 + \frac{0.00406}{1.0025} = (2 + 396) \times 10^{-5} \\ p_S(t_v) &= 1 + 215 = 216 \text{ atm} \\ \text{II}_0: p_S(\tau_v) &= 1.84 \times 10^{-5} - 0.12 \times 0.0263^2 + \frac{0.00405}{1.0026} = (2 + 396) \times 10^{-5} \end{aligned} \quad (7.15g)$$

As the nucleus grows the liquid tension at the front continues to decline (and the surrounding negative pressure region continues to contract), while the positive pressure on the solid nucleus also relaxes. The front pressure passes through the zero value, by (6.11), at the time and radius

$$\begin{aligned} \text{I: } \tau_c &= 0.1300 \left[1 - 0.001 + \frac{22.5}{2} \tau_c^2 \right]^{2/3} = 0.152, \quad t_c = 4.31 \times 10^{-12} \text{ s} \\ \text{II}_0: \tau_c &= 0.1324 \left[1 - 0.001 + \frac{21.7}{2} \tau_c^2 \right]^{2/3} = 0.155, \quad t_c = 4.40 \times 10^{-12} \text{ s} \\ \text{I: } \mathcal{R}_c &= 1.0025, \quad R_c = 2.30 \times 10^{-6} \text{ cm} \\ \text{II}_0: \mathcal{R}_c &= 1.0026, \quad R_c = 2.30 \times 10^{-6} \text{ cm} \end{aligned} \quad (7.15h)$$

i.e. τ_c practically coincides with τ_v : we have the case of Fig. 3 curve *c* on hand. The curve in Fig. 9(c) [or rather, the data on which the curve is based] shows

$$\text{I: } \tau_c^* = 0.182, \mathcal{R}_c = 1.003 \quad (7.15h')$$

Corresponding results for $U_u = 0.25$ are [the units for (7.16b, 17b) are listed in (7.7b)], by formulas I:

$$\begin{aligned} -\mu_M &= 0.001756, \quad \mu_S(0) = -0.00135, \quad \tau_v = 7.5, \quad \dot{R}_v = 0.110, \quad R_v = 1.41 \\ -\mu_v &= 0.00148, \quad \mu_S = -0.00117, \quad \tau_c = 8.74 \times 10^4, \quad \mathcal{R}_c = 300 \end{aligned} \quad (7.16a)$$

$$\begin{aligned} -p_M^* &= 9520, \quad p_S(0) = -7310, \quad t_v = 2.1 \times 10^{-12}, \quad \dot{R}_v = 89000, \quad R_v = 3.23 \times 10^{-7} \\ -p_v &= 8000, \quad p_S(t_v) = -6300, \quad t_c = 2.5 \times 10^{-8}, \quad R_c = 6.9 \times 10^{-5} \end{aligned} \quad (7.16b)$$

and by formulas II₀:

$$\begin{aligned} -\mu_M &= 0.001756, \quad \mu_S(0) = -0.00135, \quad \tau_v = 8.0, \quad \dot{R}_v = 0.117, \quad R_v = 1.47 \\ -\mu_v &= 0.00167, \quad \mu_S(\tau_v) = -0.00136, \quad \tau_c = 8.95 \times 10^4, \quad \mathcal{R}_c = 308 \end{aligned} \quad (7.17a)$$

$$\begin{aligned} -p_M &= 9520, \quad p_S(0) = -7310, \quad t_v = 2.3 \times 10^{-12}, \quad \dot{R}_v = 94000, \quad R_v = 3.38 \times 10^{-7} \\ -p_v &= 9040, \quad p_S(t_v) = -7400, \quad t_c = 2.5 \times 10^{-8}, \quad R_c = 7.1 \times 10^{-5} \end{aligned} \quad (7.17b)$$

[‡] This really is not visible from Fig. 9(c), but is provided by the computed data from which Fig. 9(c) was plotted.

as compared with the values in Figs. 6 and 9:

$$\text{I: } \tau_v = 18.8, \bar{\mathcal{R}}_v = 0.0844, \mathcal{R}_v = 2.27, t_c = 2.4 \times 10^{-8}, R_c = 6.6 \times 10^{-5} \quad (7.16')$$

Two changes are noted in calculations (7.16), (7.17), as compared with the calculations leading to (7.15). One is a computational change. The iterative formula (6.4c) must now be used in a re-interpreted fashion. On calculating method I estimates of τ_v by iteration in accordance with (6.4b), one obtains successively $\tau_0 = 2.80$, $\tau_1 = 4.00$, $\tau_2 = 5.18$, $\tau_3 = 6.52$, $\tau_4 = 8.22$, $\tau_5 = 10.52$; with ratios $\tau_n/\tau_{n-1} = 1.43, 1.30, 1.260, 1.260, 1.292$. After a certain convergence the ratios diverge again. The least inconsistent ratio, 1.25, is obtained when $\tau = 7.5$. This we now adopt as the appropriate estimate of τ_v . [It may be added that when the ratios do converge to 1, as in (7.15d), but poorly, then it is most expeditious to plot τ_n vs $1/n$ and extrapolate to $1/n = 0$.]

The second change is more fundamental. The pressure variation is now represented by curve *b* of Fig. 3, and τ_c, \mathcal{R}_c are calculated in accordance with (6.13):

$$\left. \begin{aligned} \text{I: } \tau_c &= \frac{1.03 \times 0.509^2}{3.06 \times 10^{-6} - 1.12 \times 10^5 \tau_c^{-3/2}} = 8.74 \times 10^4, t_c = 2.48 \times 10^{-8} \text{ s} \\ \text{II}_0: \tau_c &= \frac{1.03 \times 0.516^2}{3.06 \times 10^{-6} - 0.91 \times 10^5 \tau_c^{-3/2}} = 8.95 \times 10^4, t_c = 2.54 \times 10^{-8} \text{ s} \\ \text{I: } \mathcal{R}_c &= 1.018 \tau_c^{1/2} [1 - 1.327 \tau_c^{-1/2}] = 300, R_c = 6.88 \times 10^{-5} \text{ cm} \\ \text{II}_0: \mathcal{R}_c &= 1.032 \tau_c^{1/2} [1 - 1.056 \tau_c^{-1/2}] = 308, R_c = 7.06 \times 10^{-5} \text{ cm} \end{aligned} \right\} \quad (7.18)$$

We plot in Fig. 10(a) vs undercooling, for the nickel nucleus, on the basis of similar, method II₀ calculations, $R_n, R_v - 1, (R_0/R_n) - 1$, as well as $(R_0^*/R_n) - 1$. [Recall (6.10) that R_0^* represents the least initial radius that is required so that a negative pressure region may develop in the liquid surrounding the nucleus.] The quantities t_v, \bar{R}_v, t_c are plotted in Fig. 10(b). The curve t_c has a high undercooling branch and a low undercooling branch [formulas (6.13) and (6.11)]. The discontinuous transition from one branch to the other occurs at a U_u value intermediate to 0.25 and 0.025; its precise location would have to be determined by plots of type Fig. 9(c) obtained from numerical integration for a host of U_u values; this task we did not undertake. $(p_\infty - p_M)_{\text{atm}} = r_M/R_0$ and $p_\infty - p_v$ are plotted in Fig. 10(c); $p_S(0)$ in Fig. 10(d); $p_S(t_v)$ in Fig. 10(e). All plots are made for the cases $R_0/R_n = 2^{1/3}, 1.01, 1.0001$, as well as for the cases \bar{R}/R_n and \bar{R}/R_n where

$$\left. \begin{aligned} \frac{\bar{R}}{R_n} &= 1 + \frac{U_u}{cT_f^a/\lambda} \frac{\Gamma\lambda'}{4\sigma'} \left[\frac{\kappa T_f^a}{\pi\sigma'} \right]^{1/2} = 1 + 0.190 U_u \\ \bar{R}/R_n &= 1 + 0.190 \times 10^{1/2} U_u \end{aligned} \right\} \quad (7.19a, b)$$

Formula (7.19a) of *J. W. Cahn* is obtained by selecting $R_0 - R_n$ as the radius increase $\bar{R} - R_n$ that produces a departure of κT_f^a from the maximum W_{max} of the free energy W at R_n [see, e.g. p. 238 of reference [4] for the expression of W]:

$$\left. \begin{aligned} -\kappa T_f^a &= W - W_{\text{max}} = \frac{1}{2} \frac{\partial^2 W(R_n)}{\partial R^2} (\bar{R}_0 - R_n)^2 \\ W &= 4\pi\sigma' R^2 - \frac{4\pi}{3} R^3 \Gamma\lambda' \frac{T_f - T_\infty}{T_f^a} \end{aligned} \right\} \quad (7.20a, b)$$

Formula (7.19b) assumes a departure of $10\kappa T_f^a$. In other words, it is assumed that thermal fluctuations may produce nuclei of size \bar{R} , or perhaps size \bar{R} .

8. THE SPECIAL CASE $\epsilon = 0$

In what has preceded it was tacitly assumed that $\epsilon \neq 0$, $\epsilon \neq -1$, and division by ϵ and $1 + \epsilon$ was freely undertaken. The important special case $\epsilon = -1$ (which closely represents the nucleation of vapor bubbles) will be relegated to a later study; here we summarize the modifications demanded by the special case $\epsilon = 0$. We may conceive of the metal as existing in various physical forms, distinguished only by the value of ϵ . We want to investigate the dependence of the pressure field, in particular of p_M , on ϵ , all other properties of the metal being held constant. This curve [see (6.8b), (2.16a)]

$$p_M - p_\infty = - (1 - \mathcal{R}_n) \gamma \lambda' \frac{T_f - T_\infty}{T_f^\alpha} \frac{1 + \epsilon}{\epsilon} \tag{8.1a}$$

is plotted for the case of nickel at 175°C undercooling and initial radius $R_0 = 2^{1/3} R_n$ in Fig. 11, solid lines.

On the other hand, when $\epsilon = 0$, then by (2.7b), (2.9a) also

$$u(r) = u_F = 0, \quad p(r) = p_F = p_\infty \quad (r \geq R_0) \tag{8.2a, b}$$

Thus there is no flow in the liquid, no accompanying pressure change; in particular, the pressure at the freezing front is the ambient pressure p_∞ . The pressure on the solid phase is given by (6.15); the stagnation term $\epsilon^2 \mathcal{R}^2 / 2$ is now absent. Furthermore, by (2.11, 18) the interface temperature (the freezing temperature) is now given by

$$T_F - T_\infty = \frac{2\sigma'}{\Gamma \lambda' R_n} T_f^\alpha \left(1 - \frac{R_n}{R}\right), \quad U_F = U_u \left(1 - \frac{R_n}{R}\right) \tag{8.2c}$$

The dynamic terms associated with U_d are absent. Supplementing relation (8.1a) which indicates

$$\epsilon \rightarrow 0^+: \quad p_M \rightarrow -\infty; \quad \epsilon \rightarrow 0^-: \quad p_M \rightarrow +\infty \tag{8.1b, c}$$

we now have

$$\epsilon = 0: \quad p_M = p_\infty \tag{8.1d}$$

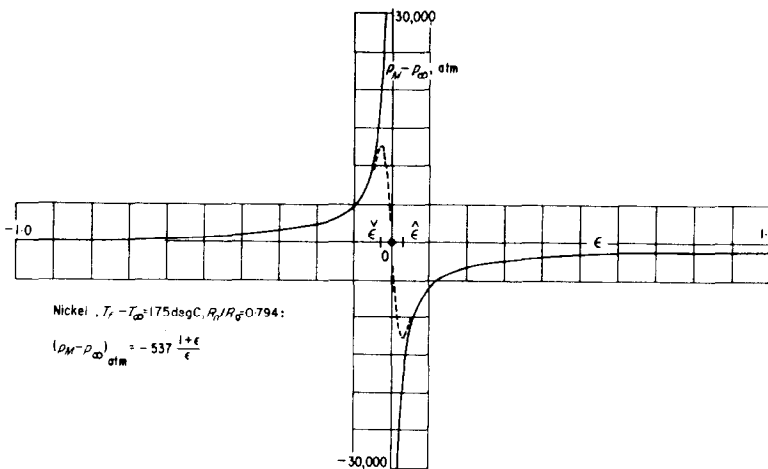


FIG. 11. Solid line and dot at origin indicates variation of maximum pressure p_M with density parameter ϵ by present theory; dashed line shows expected behavior in a more refined theory.

It seems that in a more refined description of the phenomenon, by utilizing more elaborate differential equations than those employed in section 2, the transition in $p_M - p_\infty$ from $-\infty$ through 0 to $+\infty$ as ϵ changes from positive to negative values would have to take place somewhat in the fashion indicated by dashed lines in Fig. 11. Within the range $\hat{\epsilon}$ to $\check{\epsilon}$ (where $\hat{\epsilon} < 0.06$, since nickel, $\epsilon = 0.06$, fits the present analysis) the behavior would have to depart from (8.1a). Determination of $\hat{\epsilon}$, $\check{\epsilon}$ for which peak $|p_M|$ occurs constitutes an interesting problem, outside the scope of the present study.

When ϵ is neither 0^+ or 0^- but is *precisely* zero, then the interface condition (8.2c) in conjunction with the initial values

$$U(r) = U_F = 0, \quad \mathcal{R}(0) = 1, \quad \dot{\mathcal{R}}(0) = 0 \tag{8.3a, b, c}$$

imposes the requirement

$$\mathcal{R}_n = \mathcal{R}_0 = 1, \quad R_0 = R_n \tag{8.4}$$

Replacement of relations (5.11) by

$$\begin{aligned} \mathcal{R} &= 1 + b_{3/2} \tau^{3/2} + b_2 \tau^2 + \dots, \quad \mathcal{U}_F = f_1 \tau + f_{3/2} \tau^{3/2} + \dots, \quad \mathcal{U}_C = c_{3/2} \tau^{3/2} + c_2 \tau^2 + \dots, \\ w &= d_{1/2} \tau^{1/2} + d_1 \tau + \dots, \quad l = l_{1/2} \tau^{1/2} = \sqrt{(\mathcal{K}/2)} \tau^{1/2}, \quad \mathcal{E} = 1 \end{aligned} \tag{8.5}$$

[equation (4.3) can no longer demand that $n_1 > 2$, since now $\mathcal{U}_d = 0$ and the \mathcal{R} term is absent in (8.2c); for the sake of simplicity we henceforth restrict ourselves to the I approximation] leads to equations for the coefficients analogous to (5.12⁰, 12_B, 12₀) which we do not write out. (8.2c) now gives rise, in place of (5.13), to the relation

$$f_1 \tau + f_{3/2} \tau^{3/2} + \dots = U_u [1 - \{1 - b_{3/2} \tau^{3/2} - b_2 \tau^2 + \dots\}] \tag{8.6}$$

It follows, in conjunction with the analog of (5.12_B), that

$$f_1 = f_{3/2} = \dots = b_{3/2} = b_2 = \dots = 0 \tag{8.7}$$

\mathcal{R}_n is again found to be a radius of neutral equilibrium.

Thus, in order that the process of freezing may get under way, it is necessary to relinquish (8.4) and the condition (8.3c) of zero initial velocity that prompted it. Writing

$$\begin{aligned} \mathcal{R} &= 1 + b_{1/2} \tau^{1/2} + b_1 \tau + b_{3/2} \tau^{3/2} + \dots, \quad U_F = f_0 + f_{1/2} \tau^{1/2} + f_1 \tau + \dots, \\ U_C &= c_{1/2} \tau^{1/2} + c_1 \tau + \dots, \quad w = d_{1/2} \tau^{1/2} + d_1 \tau + \dots, \quad l = l_{1/2} \tau^{1/2} = \sqrt{(\mathcal{K}/2)} \tau^{1/2}, \quad \mathcal{E} = 1 \end{aligned} \tag{8.8}$$

we find, in place of (5.12_I, 12_B, 12₀, 13) the relations

$$\begin{aligned} f_0 \tau^{-1/2} \left\langle \frac{c_{1/2}}{\frac{1}{6} f_0} - \frac{1}{2} b_{1/2} + \frac{1}{2} l_{1/2} - \frac{\mathcal{K}}{l_{1/2}} \right\rangle + f_0 \tau^0 \left\langle \left(\frac{1}{8} b_{1/2} - \frac{1}{2} l_{1/2} \right) \frac{c_{1/2}}{f_0} + \frac{1}{8} \frac{c_1}{f_0} + \frac{l_{1/2} f_{1/2}}{2 f_0} \right. \\ \left. + \left(\frac{1}{8} b_{1/2} - \frac{1}{2} l_{1/2} + \frac{\mathcal{K}}{l_{1/2}} \right) \frac{c_{1/2} - f_{1/2}}{f_0} - b_1 - \frac{1}{2} b_{1/2}^2 + \frac{5}{2} b_{1/2} l_{1/2} - 5 l_{1/2}^2 - 2 \mathcal{K} \right\rangle + \dots = 0 \end{aligned} \tag{8.9_I}$$

$$\begin{aligned} \tau^{-1/2} \left\langle \frac{K}{\frac{1}{2} b_{1/2} - \left(\frac{K}{l_{1/2}} + \frac{1}{d_{1/2}} \right) f_0} \right\rangle + \tau^0 \left\langle b_1 + \frac{1}{2} b_{1/2}^2 + (c_{1/2} - f_{1/2}) \frac{K}{l_{1/2}} + \left(\frac{d_1}{d_{1/2}^2} - 2 K \right) f_0 \right. \\ \left. - \frac{f_{1/2} + b_{1/2} f_0}{d_{1/2}} \right\rangle + \dots = 0 \end{aligned} \tag{8.9_B}$$

$$f_0 \tau^{-1/2} \left\langle \frac{1}{2} b_{1/2} + \frac{1}{2} d_{1/2} - \frac{1}{d_{1/2}} \right\rangle + f_0 \tau^0 \left\langle b_1 + b_{1/2}^2 + 2b_{1/2} d_{1/2} + 2d_{1/2}^2 + d_1 - 2 \frac{b_{1/2}}{d_{1/2}} + \frac{d_1}{d_{1/2}^2} + \frac{f_{1/2}}{f_0} \left(\frac{1}{2} b_{1/2} + d_{1/2} - \frac{1}{d_{1/2}} \right) \right\rangle + \dots = 0 \quad (8.9a)$$

$$\tau^0 \langle -f_0 + U_u(1 - \mathcal{R}_n) \rangle + \tau^{1/2} \langle -f_{1/2} + U_u \mathcal{R}_n b_{1/2} \rangle + \tau \langle -f_1 + U_u \mathcal{R}_n (b_1 - b_{1/2}^2) \rangle + \dots = 0 \quad (8.9b)$$

They lead to

$$\left. \begin{aligned} f_0 &= U_u(1 - \mathcal{R}_n), \quad d_{1/2} = -\frac{\mathcal{K}f_0}{l_{1/2}} + \left[\left(\frac{\mathcal{K}f_0}{l_{1/2}} \right)^2 + 2(1 - f_0) \right]^{1/2} \\ b_{1/2} &= 2 \left(\frac{\mathcal{K}}{l_{1/2}} + \frac{1}{d_{1/2}} \right) f_0, \quad c_{1/2} = \left(3b_{1/2} - 3l_{1/2} + 6 \frac{\mathcal{K}}{l_{1/2}} \right) f_0 \\ f_{1/2} &= U_u \mathcal{R}_n b_{1/2}, \dots \end{aligned} \right\} \quad (8.10)$$

For example, when

$$\mathcal{K} = \mathcal{K} = 1, \quad U_u = 0.25, \quad \mathcal{R}_n = 0.794 \quad (8.11a)$$

then

$$f_0 = 0.05150, \quad d_{1/2} = 1.3064, \quad b_{1/2} = 0.2245, \quad c_{1/2} = 0.3624, \quad f_{1/2} = 0.0446 \quad (8.11b)$$

In order that growth may start, a radius fluctuation to a value $R_0 > R_n$ is necessary. The surface temperature of the nucleus then *jumps* (instantaneously) from T_∞ to $T_\infty + (T_f - T_\infty)(1 - \mathcal{R}_n)$, and freezing ensues with *infinite initial velocity*. Since both liquid and solid phases have the same density, no physical motion occurs, no inertia effects are involved, and compressibility plays no role. The freezing process for $\epsilon = 0$ is thus seen to be totally different from that of case $|\epsilon| \ll 1$, and the question—as mentioned before—then arises how the transition from $|\epsilon| \ll 1$ to $\epsilon = 0$ takes place.

ACKNOWLEDGEMENT

The present investigation was proposed by R. L. Fullman. To him, J. W. Cahn, B. Chalmers, and J. L. Walker, I wish to express my appreciation for many useful discussions and suggestions. I thank Miss M. DaCosta for patient checking of derivations and for programming the computations. But I want particularly to record my indebtedness to J. W. Cahn for providing me with the vital formulas (A1, 2) and (7.19).

Zusammenfassung—Wenn Nickel in seiner weniger dichten Schmelze erstarrt, die um mehr als 175°C unter ihre Gleichgewichtserstarrungstemperatur abgekühlt ist, zeigt das verfestigte Material—wie es zuerst von J. L. Walker beobachtet wurde—eine aufgelockerte Feinkonstruktur (vermutlich als Ergebnis einer von den riesigen, negativen Drücken um die wachsenden Kerne verursachten Kavitation), wohingegen bei geringerer Unterkühlung als 175°C die beobachtete Struktur grobkörnig ist. Zweck der vorliegenden Analyse war, numerische (theoretische) Schätzungen für die Drücke, Strömungsgeschwindigkeiten und für die damit verbundenen Zeitmassstäbe festzulegen. Dies bedingte eine Studie über Erstarren, das sich aus einem endlichen Ursprungskeim entwickelt. Unter Verwendung einer "verallgemeinerten Orthogonalisations-Lösungsmethode" wird der Erstarrungsprozess weiter auf der Basis der inkompressiblen, nicht zähigkeitsbehafteten Hydrodynamik verfolgt, wobei die Druckabhängigkeit der Erstarrungstemperatur ebenfalls mit einbezogen wird. Die Lösung des Hauptsystems der Differentialgleichungen wird als eine Summe $\sum_0^{K-1} F_k$ von [Vektor] Funktionen $F_k(\xi)$ (ξ ist die dimensionslose Radialkoordinate) angeführt, deren Zeitabhängigkeit (τ ist die dimensionslose Zeit) von den Orthogonalitätsbedingungen (Grenzschichtintegralgleichungen) bestimmt wird, worin die Integranden-Gewichtsfunktionen vom Typ ξ^{km} verwendet werden.

$k = 0, 1, \dots, K - 1$. Wir beziehen auf Näherungen I, II, III, ... wenn $K = 1, 2, 3, \dots$ ($K = 1$ entspricht der konventionellen Grenzschichtlösung vom Typ Karman-Pohlhausen-Goodman-Veynik) und auf die Näherungen $\Pi_1, \Pi_{\frac{1}{2}}, \Pi_0$, wenn $k = 2$ und $m = 1, \frac{1}{2}, 0$. Wenn für $\sum F_k(\xi)$ eine Reihe von in τ gestörten und in ξ abklingenden Exponenten verwendet wird, unterscheidet sich das Diagramm für die Lösung Π_0 in seinem asymptotischen Verhalten ($\tau \rightarrow \infty$) nicht von der genau bekannten strengen Lösung des Problems, wo der Kern vom Radius 0 aus wächst und die Druckabhängigkeit der Erstarrungstemperatur nicht beachtet wird. Dieser asymptotische Bereich wird jedoch erst erreicht, wenn ungefähr 10^{-7} s vom Wachstumsbeginn an vergangen sind, während der maximale Flüssigkeitsstrom zum wachsenden Kern (bei einer 100 m/s übersteigenden Geschwindigkeit) in den ersten 10^{-11} s erfolgt und von Spannungen von mehreren tausend Atmosphären begleitet wird. Dieser erste Teil des Phänomens (bis 10^{-11} s) kann durch in $\tau^{1/2}$ in den Störfaktoren ansteigende Potenzreihen, der letzte (nach 10^{-7} s) durch in $\tau^{1/2}$ abfallende Potenzreihen dargestellt werden. Der riesige dazwischenliegende Zeitanteil muss durch numerische Integration des zugehörigen Differentialgleichungssystem überbrückt werden. Ausser der Bestätigung der erwarteten Druckverteilung ergab die Analyse auch ein unerwartetes Ergebnis. Der Erstarrungsvorgang, wie er jetzt beschrieben wurde, unterscheidet sich für den Fall der genauen Null-Dichteänderung völlig von dem für infinitesimale Dichteänderung. Letztere beginnt von einem endlichen Anfangsradius ausgehend mit der Geschwindigkeit 0, die erstere mit unbegrenzter Geschwindigkeit. Diese Unstetigkeit (mit der Dichteänderung) in der Lösung zeigt, dass weitere Studien nötig sind.

Аннотация—Когда никель замерзает в своем менее плотном расплаве, охлажденном более чем на 175° ниже своей равновесной температуры замерзания, затвердевающий материал представляет собой, как впервые наблюдал Дж. Л. Уолкер, мелкозернистую дисперсную структуру (повидимому, как результат кавитации, вызванной большими отрицательными давлениями, окружающими растущие ядра), в то время как при охлаждении менее глубоко, чем указанное, наблюдаемая структура будет крупнозернистой. Цель настоящей работы состоит в нахождении численных (теоретических) оценок давлений скоростей потока и соответствующих масштабов времени. Это вынуждает рассматривать замерзание как процесс, развивающийся от начальных ядер (зародышей) конечных размеров. Процесс замерзания описывается на основе динамики несжимаемой невязкой жидкости с использованием решений, полученных «методом обобщенной ортогонализации» и с учетом зависимости температуры замерзания от давления. Решение основной системы дифференциальных уравнений представляется как сумма вида $\sum_0^{K-1} F_k$ векторных функций $F_k(\xi)$ (ξ есть безразмерная радиальная координата), чья зависимость от времени (τ —безразмерное время) определяется из условий ортогональности (интегральные уравнения для пограничного слоя) с использованием в подинтегральных выражениях весовых функций типа ξ^{km} ; $k = 0, 1, \dots, K - 1$.

Мы используем приближения I, II, III ... когда $K = 1, 2, 3, \dots$ ($K = 1$ соответствует обычному решению пограничного слоя типа Кармана-Польгаузена-Гудмена-Вейника) и приближения $\Pi_1, \Pi_{\frac{1}{2}}, \Pi_0$ при $K = 2$ и $m = 1, \frac{1}{2}, 0$. Используя для $\sum F_k(\xi)$ последовательность возмущенных (по τ) затухающих (по ξ) показательных функций, было найдено, что график решения Π_0 по своему асимптотическому поведению (при $\tau \rightarrow \infty$) не отличается от хорошо известного точного решения задачи, когда ядро растёт от нулевого радиуса, а зависимость температуры замерзания от давления не учитывается. Однако этот асимптотический период не наступает раньше чем приблизительно 10^{-7} сек после начала роста, тогда как максимальный напор жидкости на растущее ядро (со скоростью выше 100 м/сек) происходит в течении первых 10^{-11} сек и сопровождается напряжениями в несколько тысяч атмосфер. Эту первую часть процесса (до 10^{-11} сек) можно выразить возрастающим степенным рядом по $\tau^{1/2}$ последний участок (после 10^{-7} сек)—убывающий степенным рядом по $\tau^{1/2}$; а поведение в большой промежуточной области можно определить при помощи численного интегрирования соответствующей системы дифференциальных уравнений. Кроме подтверждения ожидаемого распределения давления анализ дал неожиданный результат. Как теперь очевидно, процесс замерзания для случая нулевого изменения плотности совершенно отличен от процесса замерзания для бесконечно малого изменения плотности. Последний начинается с начальных ядер конечных размеров при нулевой скорости, а первый—при бесконечной скорости. Этот разрыв (с изменением плотности) в решениях указывает на необходимость дальнейшего изучения.